# Functional analyses of Mushroom body miniature (Mbm) in growth and proliferation of neural progenitor cells in the central brain of *Drosophila melanogaster*


**Dissertation zur Erlangung des naturwissenschaftlichen Doktorgrades der Julius-Maximilians-Universität Würzburg**

**vorgelegt von**

**Anna Hovhanyan**

**aus Eriwan, Armenien**

**Würzburg, Februar 2014**

Eingereicht am: ……..

Mitglieder der Promotionskommission:

Vorsitzender: …….. Prof. Dr. Markus Engstler
Gutachter: ……... Prof. Dr. Thomas Raabe
Gutachter: ……... Prof. Dr. Charlotte Förster

Tag des Promotionskolloquiums: ……
Doktorurkunde ausgehändigt am: ……....

**Erklärung**

Erklärung gemäß §4 Abs.3.S. 3, 5 und 8 der Promotionsordnung der Fakultät für Biologie der Julius-Maximilians-Universität Würzburg vom 15.März 1999 in der Fassung vom 12.August 2009.

Hiermit erkläre ich ehrenwörtlich, dass ich die vorliegende Dissertation selbstständig angefertigt und keine anderen als die angegebenen Quellen und Hilfsmittel benutzt habe. Ich erkläre, dass die vorliegende Dissertation weder in gleicher noch in ähnlicher Form bereits in einem Prüfungsverfahren vorgelegen hat.
Ich erkläre, dass ich außer den mit dem Zulassungsantrag urkundlich belegten Graden keine weiteren akademischen Grade erworben oder zu erwerben versucht habe.

Würzburg, 10. Februar 2014

Anna Hovhanyan

**List of contents**

# 1 Introduction

## 1.1 Neurogenesis in Drosophila melanogaster

*Drosophila* is a holometabolous insect, which during development undergoes complete metamorphosis, including the larval, pupal and adult forms. This process is powered by environmental, systemic and local signals. The central nervous system (CNS) of *Drosophila* is generated during embryonic and postembryonic phases of neurogenesis, which are separated by quiescence, a known pause in proliferation of the neural progenitor cells (neuroblasts) (Figure 1).

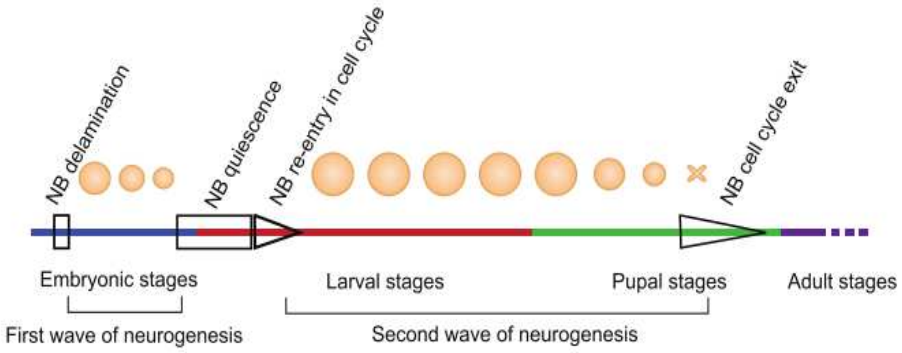


Homem & Knoblich, 2012

**Figure 1. Two waves of neurogenesis during *Drosophila* development.**
Neuroblasts (NBs) are presented above the line. Embryonic NBs delaminate from the neuroectoderm. Embryonic NBs do not re-grow after each division. They enter to the quiescence state at late embryogenesis. NBs reactivate after larval hatching to start postembryonic neurogenesis. In contrast to embryonic NBs, larval NBs re-grow after each division and can divide more often. At late larval and pupal stages, NBs terminate proliferation.

The larval CNS develops during embryonic neurogenesis, whereas for building the adult CNS, both phases are responsible. The CNS of *D. melanogaster* comprises the optic lobes, the central brain and the ventral nerve cord (VNC). Particularly, the central brain consists of the proto-, deuto- and tritocerebrum, which in the adult brain built up the supraesophageal ganglion. The VNC includes 3 gnathal (=subesophageal ganglion), 3 thoracic, and 9 abdominal neuromeres. The central brain and the VNC arise from the neuroectodermal cells placed at the ventral region of the early embryo, in contrast to optic lobe neuroblasts (NBs), which develop from neuroepithelial placodes during larval stage (Egger et *al*. 2008, Skeath & Thor 2003, Technau et al, 2006). Consequently, the brain derives from the anterior region of neuroectoderm called procephalic neuroectoderm,

whereas the VNC develops from the posterior ventral neuroectoderm. Development of the CNS is best studied in the VNC, because it consists of a sequence of repetitive segmental units called neuromeres. In general, the body of *Drosophila* is divided into metameric segments. Each segment consists of bilaterally arranged hemisegments (right and left part of the embryo), which are the developmental units of the developing CNS. Onset of neurogenesis is the delamination of multipotent stem cells, neuroblasts (NBs), from the neuroectoderm, each of which has a specific identity. The unique fate of NBs is determined by the time and positional information in the neuroectoderm, which is provided by anterior-posterior (AP) and dorso-ventral (DV) patterning genes (Urbach & Technau 2003; Skeath 1999, Baht 1999). The segment polarity genes within each hemisegment subdivide the neuroectoderm along the AP axis into transverse rows and are responsible for different fate of the NBs, which are arising in different rows. Respectively, DV patterning genes subdivide the neuroectoderm along the DV axis into longitudinal columns and ensure that each delaminated NB in different columns acquires an unique identity (Bhat 1999, Skeath 1999). Due to overlapping activities of AP and DV patterning genes, a Cartesian coordinate system is formed in each hemisegment, where each proneural cluster or neural equivalence group consists of 6-8 cells (Figure 2 A), and is responsible for the specific NB to be formed (Skeath 1999). However, besides prepatterning genes, expression of proneural and neurogenic genes are needed for singling out a NB from a proneural cluster. Initially, combinations of the three proneural genes, *achaete* (*ac*), *scute* (*sc*) and *lethal of scute* (*l'sc*), which together form the *achaete-scute-complex* (AS-C), are expressed in all cells of a proneural cluster and each cell acquires neural potential (Campos-Ortega 1993, Skeath & Thor 2003, Egger et al. 2008, Hartenstein &Wodarz 2013). However, only a single cell, which expresses the highest level of AS-C will gain the NB fate. This selection process is regulated by lateral inhibition mediated by the Notch signaling pathway. Lateral inhibition restricts the expression of proneural genes to the presumptive NB. In the case of loss of function of any of the neurogenic genes encoding Notch signaling components, most of the cells in proneural clusters adopt the NB fate (Lehmann et *al.* 1981, Lehmann et *al.* 1983, Jimenez & Campos-Ortega, 1990). The Notch (N) signaling cascade is activated by binding of the transmembrane ligand Delta (D) to the Notch receptor of the neighboring cell. This initiates a proteolytic cleavage cascade of Notch and translocation of the Notch intracellular domain ($N^{ICD}$) to the nucleus. $N^{ICD}$ interacts with Suppressor of hairless (Su(H)), triggering the expression of *Enhancer of Split E(spl)*genes, which, in part, encode transcriptional repressors for proneural genes (Figure 2 B). Concurrently, there is a positive

feedback loop between AS-C and N signaling, as D activation depends on the AS-C (Heitzler et *al.* 1996, Skeath & Thor, 2003). This means that the activation of N signaling leads to repression of AS-C in the cell. Respectively, the cell with less expression of proneural genes has reduced D activity, which results in lowering the capacity of this cell to activate N in neighboring cells. Relying on this, the cell in the proneural cluster, which initially has higher levels of AS-C or D will obtain the NB fate and downregulates through N signaling the expression of proneural genes in the neighboring cells. Although each cell of a proneuronal cluster expresses AS-C and N pathway components it is thought that subtle differences causes an imbalance, which leads to the selection and later the delamination of a single cell with the NB fate from the neuroectoderm (Figure 2 A).

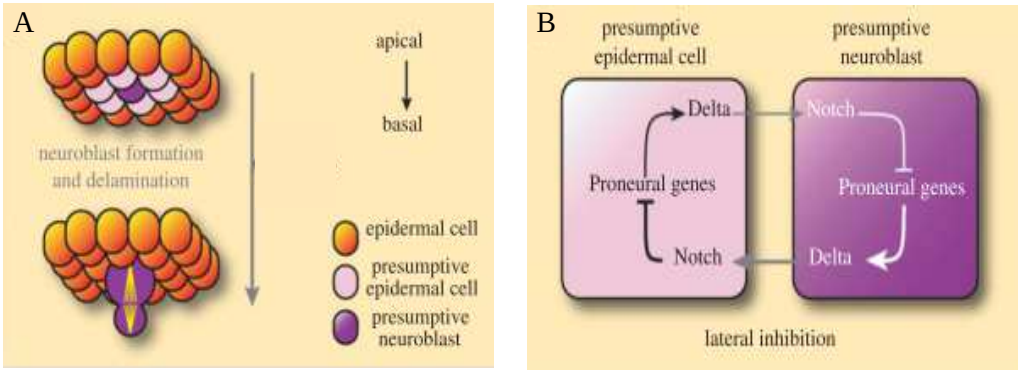


Egger et *al.* 2008

**Figure 2. Neuroblast formation during embryogenesis.**
A) Only a single neuroblast delaminates from a proneural cluster. The selected neuroblast delaminates basally into the embryo, enlarges and starts to divide asymmetrically. The remaining cells of the proneural cluster acquire epidermal fate. B) Simplified scheme of lateral inhibition, which regulates neuroblast selection via Notch, Delta and proneural genes (for details see text).

However, it is important to mention that other proneural genes also are involved in neurogenesis, since half of the NBs formed during embryonic neurogenesis lack AS-C function. NB delamination begins between embryonic stage 8 and 11 (Campos-Ortega & Hartenstein, 1985) and consists of five waves (S1-S5) of NBs segregation. Three longitudinal columns of NBs (medial, intermediate and lateral) are generated during S1-S3 phases (Campos-Ortega & Hartenstein, 1985), whereas NBs derived from S4 and S5 phase are scattered between existing columns of NBs. An invariant pattern of about 30 NBs is formed in each thoracic and abdominal hemisegment. Moreover, NBs in different segments, which become specified in an analogous spatio-temporal pattern, are homologous NBs and acquire similar fate. As it was described by Bossing et *al.* 1996 and Schmidt et *al.* 1997, 17 embryonic NBs are derived from ventral half of the neuroectoderm

and form the medial and intermediate columns of NBs, while the other 13 NBs are derived from the dorsal neuroectoderm and form the lateral column of NBs. After delamination, NBs enter mitosis and divide in a stem-cell like manner to generate ~500 and ~400 neurons/glia cells in thorax and in abdomen, respectively. However, the size of NB lineages generated during embryonic phase of neurogenesis within each hemisegment varies. In addition, thoracic NBs generate larger clones in comparison to the corresponding NBs in abdominal segments (Bossing et *al.* 1996, Schmid et *al.* 1999).

The situation is more complex in case of brain development. The insect brain is traditionally subdivided into tritocerebrum, deutocerebrum and protocerebrum (Bullock and Horridge, 1965). Like in case of the VNC, segment polarity and DV patterning genes are providing spatiotemporal information to the NBs arising in the procephalic neuroectoderm. With regard to the expression of these genes it was shown that the pregnathal neuroectoderm give rise to four segments or neuromeres in each hemisphere of brain: the tritocerebrum or intercalary segment, the deutocerebrum or antennal segment, and the most prominent part of brain or the protocerebrum, which consist of ocular and labral neuromers (Schmidt-Ott et *al.* 1994, Schmidt-Ott & Technau 1992, Urbach & Technau 2003b). As it was shown by Urbach & Technau 2003b, segment polarity and DV patterning genes are clearly demarcating segmental boundaries in the developing brain. The brain NBs are generated between embryonic stages 8 and late 11 and originate from ectodermal domains with distinct mitotic behaviors. Already in 1989, Foe (1989) subdivided the procephalic neuroectoderm into several mitotic domains, where all cells within a discrete domain are synchronously entering the mitotic cycle but do not have synchrony with cells of other domains. Essentially, the brain NBs develop from 4 or 5 mitotic domains, named B, 1, 5, 9 and possibly 2 (Figure 3 A). Urbach et *al.* (2003) showed a correlation between the brain NBs subpopulations and mitotic domains. Correspondingly, mitotic domain B generates about 25 NBs, and all NBs contribute to the central part of the protocerebrum. 10 posterior protocerebral, most deutocerebral and some anterior tritocerebral NBs arise from mitotic domain 9. Anterior population of about 15 protocerebral NBs derive from domain 1, whereas in the dorsoposterior part of the protocerebrum about 15 NBs originate from mitotic domain 5. Relying on the fact that the relative position of mitotic domains are invariant during embryonic stages 8-11, mitotic domain 2 gives rise to part of the tritocerebral NBs (Urbach et *al*. 2003). It was also shown that there are distinct modes of brain NB formation, which are conditioned by mitotic domain origin (Figure 3 B). For example, neuroectodermal cells in mitotic domain B do

not divide prior to NBs delamination, whereas cells in mitotic domain 1, 5 and 2 divide parallel to the ectodermal layer and as a result one of the daughter cells delaminates as a NB. In the case of domain 9, NB formation can be achieved in 2 ways: delamination and directed mitosis (Figure 3 B (a1, a2)) (Urbach & Technau 2004, Urbach et *al.* 2003).

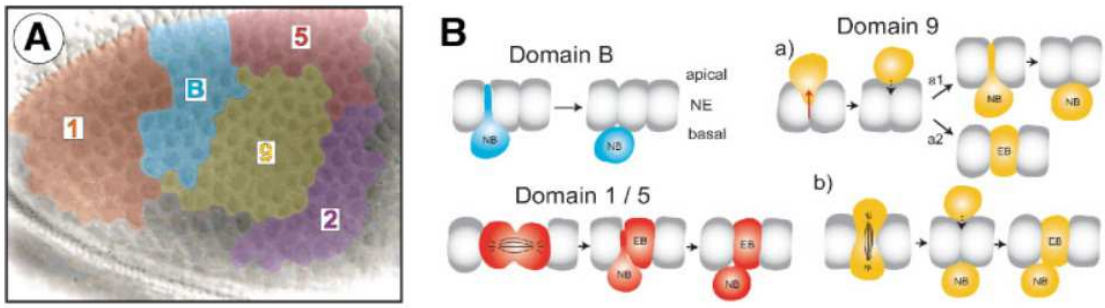


Urbach & Technau, 2004

**Figure 3. Neuroblast formation in the brain.**
A) Blastodermal head region (lateral view), where different colors represent positions of mitotic domains 1, 2, 5, 9 and B. B) In mitotic domain B, neuroblasts delaminate basally from neuroectoderm. In mitotic domain 1 and 5, neuroectodermal progenitors divide parallel to ectoderm, where one of the daughter cells stay in ectoderm as an epidermoblast, whereas the second delaminates as a neuroblast. In mitotic domain 9, neuroblasts form in two distinct ways. In one case, the neuroectodermal cell moves apically (Ba), reintegrates and delaminates as a neuroblast (Ba1) or remains in ectoderm as an epidermoblast (Ba2). In the other case, cells divide perpendicular to the ectoderm (Bb), where one of the cells moves apically, then reintegrates into the ectoderm as an epidermoblast, whereas the other delaminates basally to become a neuroblast.

Like in the VNC, proneural genes are also expressed within the procephalic neuroectoderm. However, they are expressed in small proneural clusters and in larger ectodermal domains. Behavior of proneural genes in small proneural clusters is similar to the VNC. The procephalic neuroectoderm region, which broadly expresses proneural *l'sc*, generates more than one NB. This fact can be explained by lower efficiency of lateral inhibition, which is essential for controlling the process of single NB formation from proneural clusters in the VNC (Younossi-Harteinstein et *al.* 1996). Experimental data indicated that in all mitotic domains more than one of neighboring cells in proneural cluster are becoming NBs, especially within mitotic domain B where many of adjacent cells gain NB fate, due to less efficient lateral inhibition (Urbach et *al.* 2003). By the end of embryonic neurogenesis about 100 brain NBs are generated, which presumably represent the complete population of embryonic brain NBs (Urbach et *al.* 2003, Urbach & Technau 2003). In principal, most of the NBs stop to divide at embryonic stage 14, besides 4 mushroom body NBs, which continuously divide until pupal stages (Ito & Hotta 1992). Generally, the NB is always in the superficial layer of the CNS, whereas each newly born

ganglion mother cell (GMC) pushes the older once and neurons to the deeper layer of the embryo CNS. During embryogenesis, the NBs generate neuronal diversity in an invariant temporal sequence due to a temporal transcription-factor (TTF) cascade (Person & Doe 2003, Schmidt et *al.* 1999, Petson & Doe 2004, Brody & Odenwald 2000). So far, 4 members of TTF cascade have identified, which are expressed in NBs in a sequential manner: Hunchback (Hb) →Kruppel (Kr) → Pdm→ Castor (Cas) (Isshiki et *al.* 2001, Grosskortenhaus et *al.* 2005, Brody & Odenwald 2000, Grosskortenhaus et *al.*2006). GMCs and their lineages retain the transcription factor, which is expressed in NB at the time of GMC's birth. Therefore, Hb is found in the deepest and consequently Cas in the most superficial layers of neurons (Figure 4) (Isshiki et *al.* 2001, Brody & Odenwald 2000). There is a cross-regulatory interaction between TTFs, where each gene can activate the next one in the pathway and simultaneously repress the 'next plus one' gene (Isshiki et *al.* 2001).

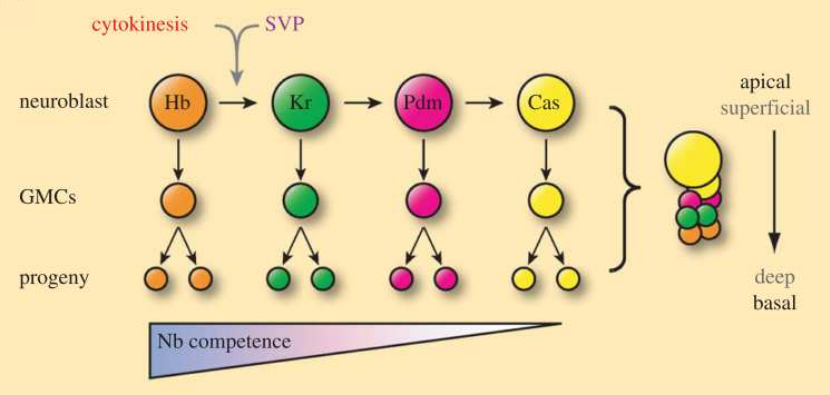


Egger et *al.* 2007

**Figure 4. Temporal neuroblast progression.**
Hb, Kr, Pdm, Cas are expressed sequentially in the neuroblast. Each GMC and its lineage are carrying the transcription factor, which is present at the time of GMC birth. Cytokinesis and Svp are required for Hb to Kr transition.

Indeed, there are two timing mechanisms, which regulate transition of temporal identity in NBs: a cytokinesis-dependent timing of Hb → Kr transition and cell-cycle independent timing of Kr → Pdm → Cas transition (Grosskortenhaus et *al.* 2005). In addition, the nuclear receptor Seven-up (Svp) is also required for this transition via downregulation of Hb (Figure 4) (Kanai et *al.* 2005). The first phase of neurogenesis ends when the embryonic lineages of nervous system are generated. This is a crucial moment, when each NB has to choose whether to enter a quiescent state or to undergo apoptosis. As it was mentioned above, NB segregation in abdominal and thoracic segments are identical. However, only 3 from 30 abdominal NBs persist to first instar larvae compared with 20

from 30 thoracic NBs per hemisegment (Truman & Bate 1988, Prokop & Technau 1991). This correlates with a burst of NB apoptosis in the abdominal segment of the embryo, which is regulated by pro-apoptotic genes (Peterson et *al.* 2002, White et *al.* 1994). The rest of the CNS NBs, except the mushroom body NBs, enter a mitotic quiescence state and reactivate cell division during early larval stage. Embryonic NBs reduce in size with each division (Figure 1), which may act as a triggering signal for entering quiescence (Harteinstein et *al.* 1987). Segment-specific characteristics during development are regulated by homeotic genes (Morata 1993). *Anntenopodia* (*Anp*) controls segment identities in the head and anterior thorax, while *Ultrabithorax* (*Ubx*) and *abdominal-A* (*abd-A*) control those of the posterior thorax and abdomen. In addition it was shown that in the larval and adult CNS *abd-A* and *Ubx* coordinate the cell number differences in the abdomen and thorax due to programming proliferation in embryo and larva, as well as the number of persisting NBs in post-embryonic stage (Prokop et *al.* 1998).

Postembryonic neurogenesis begins during first larval instar and continues into the pupal stage (Figure 1). This second wave of neurogenesis generates 90% neurons of the adult CNS (Truman & Bate 1988, Prokop & Technau 1991). Most NBs are quiescent during larval hatching and start to divide at specific time points after hatching. About 8-10 hours are needed for activation of central brain, 10-12 h for optic lobe and 28 h for thoracic NB division (Truman & Bate 1988, Prokop & Technau 1991, Ebens et *al.* 1993, Green et *al.* 1993, Datta 1995). NB reactivation is regulated by 2 kinds of extrinsic signals: humoral signals and signals received from microenvironment surrounding the stem cells. NBs in the larval brain are separated from each other by glial cells, which form a stem cell niche. It was demonstrated that signals needed for NB reactivation are derived from the surrounding glia cells (Ebens et *al.* 1993, Park et *al.* 2003, Dumstrei et *al.* 2003, Datta 1999, Truman et *al.* 1994). To be able to reenter mitosis, at first the NB has to enlarge, which depends on nutrition, especially on the presence of amino acids (Figure 5) (Truman & Bate 1988, Britton & Edgar 1998). One of the humoral signals required for cell-cycle reentry is a fat body derived mitogen (FBDM) provided by the fat body in response of nutritional amino acids (Britton & Edgar 1998, Colombani et *al.* 2003).

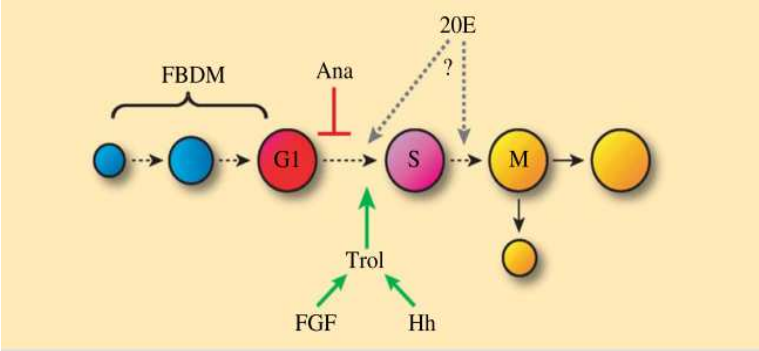


Egger et *al.* 2007

**Figure 5. Schematic representation of neuroblast reactivation.**
Fat-body derived mitogen (FBDM) triggers neuroblast enlargement. Anachronism (Ana) arrests neuroblasts in G1 phase until repression is relieved by fibroblast growth factor (FGF) and Hedgehog (Hh) signaling mediated control of terribly reduced optic lobe (Trol). As a result, neuroblasts enter S phase. The role of ecdysone (20E) in this process is not clear.

Under starvation conditions, larvae do not produce the FBDM and consequently NBs are not able to enlarge. Even overexpression of regulators for G1 to S phase transition is not able to reactivate NBs. In contrast, nutrition deprivation after NB reactivation does not affect cell division (Britton & Edgar 1998). The second stage of reactivation is entry into S phase, which is governed by several factors. The *anachronism* (*ana*) gene plays an important role in timing of postembryonic NB proliferation. The product of *ana* is a glycoprotein secreted by glia cells, which represses premature proliferation of postembryonic NBs and maintains them in a quiescence phase. NBs precociously enter S phase in *ana* mutants (Ebens et *al.* 1993). Seemingly, prior to release of NBs from G1 stage, *ana* expression has to be downregulated. Mutation of *terribly reduced optic lobes* (*trol*) strongly retards NB reactivation. Particularly, NBs enlarge, but never enter S phase. However this phenotype could be rescued by overexpression of *Cyclin E*. In *trol* mutants *cyclin E* is less expressed, assuming that for reactivation of *trol* mutant NBs, Cyclin E is required (Caldwell & Datta 1998). In double mutants for *ana*/*trol*, precocious NB reactivation was observed demonstrating that Trol acts downstream of Ana (Datta 1995). *Trol* codes for the proteoglycan Perlecan, which through binding to other factors regulates cellular signaling (Voigt et *al.* 2002, Park et *al.* 2003). Trol is expressed in first instar larval brains most likely in glia cells (Voigt et *al* 2002), which are placed in close vicinity to the superficially located NBs. Trol, due to the interplay with fibroblast growth factor (FGF) and *hedgehog* (Hh) signaling, might regulate the reactivation of NB proliferation by suppressing or bypassing the repressive effect of Ana (Figure 5) (Voigt et *al.* 2002, Park et

*al.* 2003, Datta 1995). Moreover, the steroid hormone Ecdysone (20E – 20-hydroxyecdysone) might affect NB reactivation. In explant culture of larval CNS, Ecdysone is maintaining *in vivo* levels of NB reactivation (Datta 1999). However, expression of the Ecdysone receptor in NBs is detectable in the middle of second larval instar, when many NBs are already dividing (Truman et *al.* 1994). Therefore, it is unclear how Ecdysone is influencing NB reactivation. Alternatively, Ecdysone could have an effect on NBs, which reenter mitosis later in development (Egger et *al.* 2008).

After entering mitosis, NBs divide asymmetrically to give rise to a larger self-renewing NB and smaller differentiating progeny. In contrast to embryonic NBs, larval NBs re-grow after each division and are able to divide many times. Four types of NBs in the brain lobes and 2 types in the ventral nerve cord can be distinguished: type I, type II, mushroom body and optic lobe NBs in the brain lobes and abdominal and thoracic NBs in the ventral nerve cord, which are presenting type I NBs (Figure 6) (Sousa-Nunes et *al.* 2010, Bayraktar et *al.* 2010, Homem & Knoblich 2012). Optic lobe NBs arise only during larval stage from the optic lobe neuroepithelium, starting with symmetric division to segregate neuroepithelial cells which form two proliferating centers: Inner Proliferation Center (IPC) and Outer Proliferation Center (OPC). Most of the neurons of the optic lobe derive from these centers via neurogenesis, which involves an early larval phase of symmetric divisions and late larval asymmetric NB division (Egger et *al.* 2007).

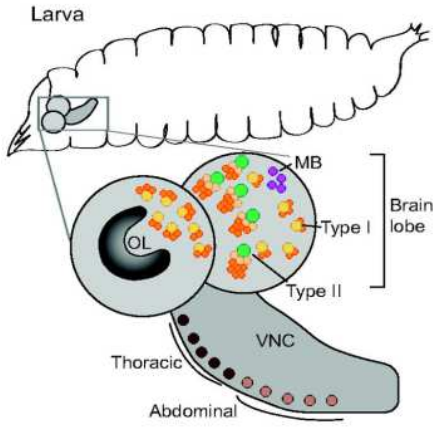


**Figure 6. The 3rd instar larval brain.**
Ventral nerve cord (VNC) with thoracic and abdominal neuroblasts, brain lobes and associated optic lobes (OL). Mushroom body (MB), Type I and Type II neuroblasts are indicated.

Homem & Knoblich 2012

Mushroom body (MB) NBs are a notable exception because they divide continuously through both phases of neurogenesis and generate about 5-fold more neurons compared to the other Type 1 NBs. There are approximately 90 type I NBs in each brain lobe, which represent most of the central brain NBs. They express the transcription factors Deadpan (Dpn) and Asense (Ase), which are regulating NB self-renewal (Wallace et *al.* 2000). In

addition, cytoplasmic Prospero (Pros) becomes segregated into the ganglion mother cell (GMC) and enters the nucleus to control GMC fate. Type I NBs are dividing asymmetrically to give rise to a self-renewing NB and a GMC, which divides one more time to generate two neurons or glia cells (Figure 7 A). There are only eight Type II NBs in each brain lobe, which express Dpn but not Ase and Pros. These NBs divide asymmetrically to generate a self-renewing NB and a transient amplifying cell called immature intermediate neural progenitor (INP), which by transcriptional changes becomes a mature INP (Figure 7 B). Mature INPs are expressing the transcription factors Ase and Pros. Each mature INP divides asymmetrically three to five times to form another INP and a GMC. Like in Type I NB lineages, GMCs derived from INPs localize Pros in the nucleus, which restricts GMC to generate two post-mitotic neurons or glia cells.

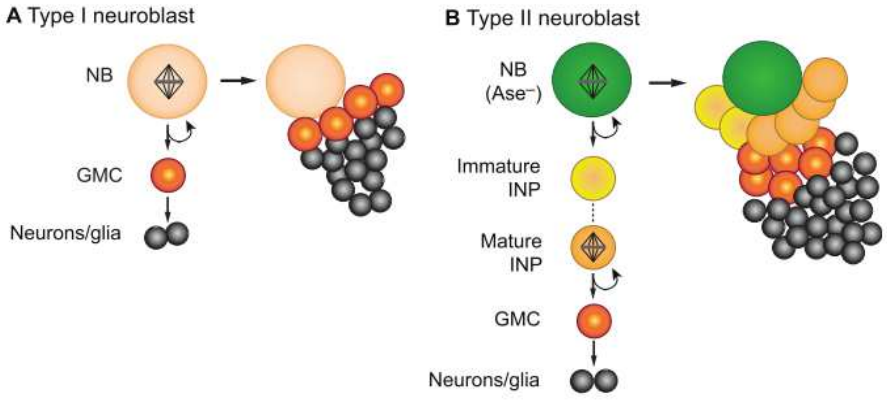


Homem & Knoblich 2012

**Figure 7. Asymmetric cell division of Type I and Type II neuroblasts.**
A) Type I neuroblasts divide asymmetrically to give rise to a self-renewing neuroblast and a GMC, which in its turn divides one more time to produce a pair of neurons or glia cells. B) Type II neuroblasts divide asymmetrically to generate a self-renewing neuroblast and an immature intermediate precursor (INP), which after maturation also divides asymmetrically to form a self-renewing INP and a GMC.

Owing to INPs, Type II neuroblasts generate larger cell lineages compared to Type I neuroblasts. In general, NBs in the CB and thorax continue to divide until pupal stage and each generates about 100 progeny in case of type 1 and more than 500 cells in case of type 2 NBs. Abdominal NBs stop to divide at larval stage, 2 days before pupation, and each generates about 12 progeny (Bello et *al.* 2003, Truman & Bate 1988). Also during postembryonic neurogenesis, a single NB sequentially generates different types of neurons. This was first demonstrated in the case of the 4 equipotent mushroom body NBs, each of which sequentially generates all types of Kenyon cells (Ito et *al.* 1997, Lee et *al.* 1999). Very recently it was shown that Type II NBs and INPs sequentially express a series of

transcription factors, which are required for the production of distinct neural subtypes (Bayraktar & Doe 2013). This mechanism corresponds to the TTF cascade for embryonic NBs as described before.

In principal, neurogenesis in all regions of the CNS ceases prior to fly hatching (Ito & Hotta 1992). NB termination is highly region specific and progresses through different mechanisms: cell cycle exit and apoptosis. In the abdominal region, Type I NBs terminate via apoptosis, where they stop to divide after upregulating homeotic gene *abd-A*, which in turn activates the proapoptotic genes *grim, hid* and *reaper* (*RHG*) and thus triggers NB death (Bello et *al.* 2003). However, it is important to mention that the transcription factor Grainyhead (Grh), which is expressed at late embryonic stage, is essential for terminating neural proliferation in the abdomen. Grh has segment specific activity. In the thorax, loss of Grh leads to reduction of mitotic activity of NBs followed by their apoptosis, whereas in the abdomen it leads to the failure of NBs to undergo apoptosis (Cenci & Gould 2005). Type I NBs in the central brain and thorax terminate proliferation via Pros-dependent cell cycle exit. TTFs are essential for this process. Cas regulates Grh activation, which is responsible for preventing premature cell cycle exit of Type I NBs, whereas Svp is essential for a Pros burst in the nucleus, which leads to induction of cell cycle exit (Maurange et *al.* 2008). Hence, Grh is regulating the timing of NB termination. Mushroom body NBs terminate proliferation last at pupal stage. They first reduce growth and proliferation due to decreased Insulin/PI3K signaling (see below). This results in localization of the transcriptional regulator Foxo in the nucleus, which finally leads to an autophagic cell death response (Siegrist et *al.* 2010). The time when NBs irreversibly stop to divide is very crucial for determining the final size of the CNS. Although different NBs terminate proliferation at different time points, it is completed by the end of metamorphosis and no mitotic active NBs can be identified in the adult *Drosophila* CNS.

## 1.2 Neuroblast asymmetric division

The diverse cell types in the nervous system, as in the other systems, are derived from asymmetric cell division of stem cells. In general, there are 2 mechanisms to regulate asymmetric cell division: asymmetry can be achieved via intrinsic mechanisms, where cell-fate determinants localize asymmetrically during mitosis and are inherited by only one of the daughter cells, and alternatively, when asymmetry depends on external polarity cues

provided by surrounding cells forming a stem cell niche (Horvitz & Herskowitz 1992, Yu et *al.* 2006, Lu et *al.* 2001). Niche-controlled stem cell division is highly flexible. Mitotic spindle orientation perpendicular to the niche surface ensures that the cell, which maintains contact with the niche, will keep the ability to self-renew. On the other hand, stem cells can divide parallel to the niche surface and generate two stem cells. The main purpose of this division is expansion of the stem cell population or compensation of stem cell loss (Li & Xie 2005).

Asymmetric division of neuroblasts largely depends on a cell-intrinsic mechanism. In prophase, Par proteins establish a polarity axis; in prometaphase, the mitotic spindle orientates along the polarity axis and cell fate determinants become asymmetrically localized; and finally, in telophase, cell fate determinants become differentially segregated into two unequal sized daughter cells (Figure 8).

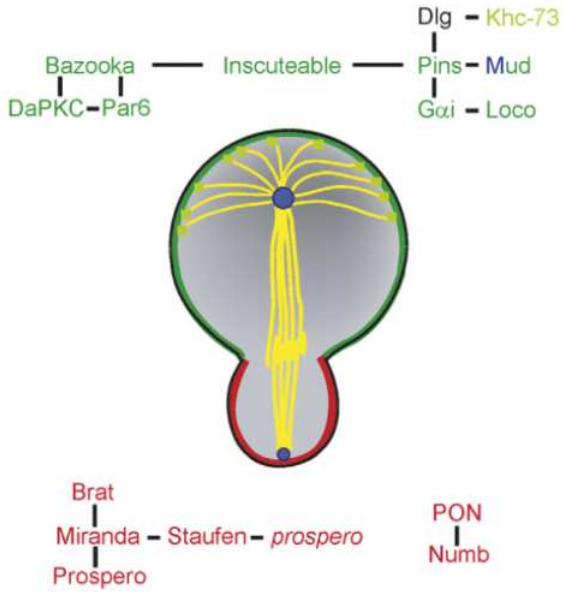


**Figure 8. Neuroblast asymmetric cell division.** Two evolutionary conserved protein complexes, (Bazooka/Par6/aPKC) and Gαi/Pins/Loco linked by Inscutable, localize apically. The Par complex is required for localization of two cell fate determinant protein complexes, Numb/Pon and Miranda/Brat/Pros, to the basal cortex, whereas Gαi/Pins/Dlg ensures mitotic spindle alignment and spindle asymmetry via binding to Mud, Khc-73 and Loco proteins. As a result of asymmetric cell division, cell fate determinants inherited by GMCs act to promote differentiation and suppress self-renewal.

Zhong & Chia 2008

An evolutionary conserved protein complex, called Par protein complex, accumulates at the apical cortex before mitosis. It consists of the proteins Bazooka (Par3), Par-6 and atypical protein kinase C (aPKC). Bazooka and Par-6 are PDZ domain-containing proteins, through which they can be bound to aPKC. Initially, the apical localization of the Par complex is inherited from the neurogenic ectoderm after neuroblast delamination, where they are localized apically and essential for establishing apico-basal polarity (Wodorz et *al.* 2000, Rolls et *al.* 2003). Orientation of the mitotic spindle, as well as unequal distribution of cell fate determinants follows the polarity axis establishment. The different cell fates are induced via unequal segregation of determinants in the daughter

cells. For GMCs, these are the proteins Numb, Prospero (Pros) and Brain tumor (Brat) (Spana et *al.* 1995, Hirata et *al.* 1995, Bello et *al.* 2006).

Numb is dispersed uniformly around the plasma membrane during interphase. With the onset of mitosis, it is accumulated around one of the spindle poles, which leads to the segregation of Numb in one of the daughter cells after cytokinesis (Rhyu et *al.* 1994), where it controls signal transduction of the Notch/Delta pathway through binding to the endocytic protein α-Adaptin (Berdnik et *al.* 2002, Schweisguth 2004). Numb mutation in larval neuroblasts causes overproliferation, which results in a tumor-like phenotype (Lee et *al.* 2006a, Wang et *al.* 2006). Similar phenotypes could also be observed in case of mutation of other determinants.

The transcription factor Prospero (Pros) is present in neuroblasts, however it enters the nucleus only in GMCs after asymmetric localization (Hirata et *al.* 1995, Knoblich et *al.* 1995). Pros regulates expression of about 700 target genes including cell cycle regulators, neuroblast self-renewing genes, as well as genes required for neuronal differentiation (Choksi et *al.* 2006), which indicates that Pros controls GMC exit from cell cycle and its entry into the differentiation pathway. Like for Numb, loss of Pros function in larval neuroblasts also causes stem-cell derived tumors (Lee et *al.* 2006c, Bello et *al.* 2006). The third segregating determinant Brat acts as an inhibitor of ribosome biogenesis and cell growth (Frank et *al.* 2002). *Brat* mutation in larval neuroblasts causes overproliferation. It is important to mention that the most pronounced effect of Brat is indicated in type II neuroblasts, which are lacking Pros, which explains why these cells are more sensible to loss of other tumor suppressors. However, in *brat* mutants, overexpression of Pros is able to rescue tumor formation (Lee et *al.* 2006c, Bello et *al.* 2006).

The asymmetric localization of cell fate determinants is governed by the adaptor proteins Miranda (Mir) and Partner of Numb (Pon) (Betschinger & Knoblich 2004). Miranda is a coiled-coil protein, which binds to Pros and Brat, and becomes segregated into the GMC. In case of *pros* and *brat* mutations, Mir localization is not affected, whereas in *mir* mutants protein determinants distribute homogeneously in the cytoplasm and segregate equally into both daughter cells. Like Mir, Pon is also coiled-coil protein, which binds to Numb, however it is not mandatory for its asymmetric localization. Mutation of *pon* causes delayed localization of Numb in metaphase, which is recovered during anaphase and telophase (Wang et *al.* 2007). Hence, Pon contributes to Numb asymmetric localization, but it is not needed at late stages of mitosis.

The mechanism through which the Par complex drives localization of cell fate determinants has been recently revealed. Numb is attached to the plasma membrane through positively charged amino acids in its N terminus, which also contains three aPKC phosphorylation sites (Knoblich et *al.* 1997). These positive charges are neutralized by aPKC-mediated phosphorylation, which inhibits apical Numb membrane association and leads to its accumulation at the basal membrane (Wirtz-Peitz et *al.* 2008). In interphase neuroblasts, aPKC forms a complex with Par6 and Lethal (2) giant larvae (Lgl) (Betschinger et *al.* 2003). This complex cannot phosphorylate Numb. However, by onset of mitosis, Par6 is phosphorylated by the cell cycle dependent protein kinase Aurora-A, which leads to the activation of aPKC, which in turn phosphorylates Lgl (Figure 9). Due to phosphorylation, Lgl is released from the complex allowing Par3 to associate with it. Only the form of the Par complex, which contains Par3 is active, since Par3 can bind to Numb and aPKC. Hence, the role of Lgl is to ensure substrate specificity and not recruitment of determinants to the cortex (Wirtz-Peitz et *al.* 2008). A similar aPKC phosphorylation dependent exclusion mechanism has been shown for Miranda (Atwood & Prehoda, 2009). In spite of the fact that Pon can also be phosphorylated by aPKC, it can be phosphorylated by mitotic kinase Polo as well (Wang et *al.* 2007), which may provide another regulatory signal for determinant localization.

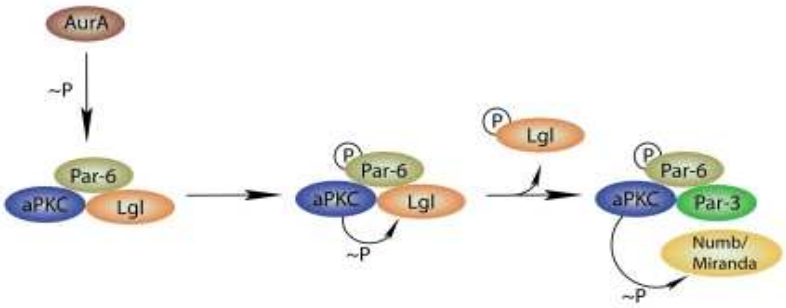


Neumüller & Knoblich 2009

**Figure 9. The Par complex is required for cell fate determinants localization.**
A cascade of phosphorylations triggers the replacement of Lgl protein by Par3, which in turn is responsible for change in substrate specificity of aPKC towards Numb and Miranda, thereby excluding them from the apical cortex.

The final step to ensure asymmetric cell division is orientation of the mitotic spindle along the apico-basal axis and its asymmetric organization to specify different daughter cell sizes. Localization and organization of mitotic spindle is achieved by linking the Par complex via Inscutable (Insc) to Partner of Inscutable (Pins), which in turn

associates through three GoLoco domains with the heterotrimeric G protein subunit Gαi. In addition, Pins binds to Mushroom body defect (Mud) via its tetratricopeptide repeats (TPRs). Intramolecular interaction of Pins GoLoco and TPRs domains leads to differential Gαi binding, which is important for correct spindle alignment (Nipper et *al.* 2007). Particularly, binding of Gαi to GoLoco domain 1 ensures Pins localization to the apical cortex and establishment of cortical polarity. Further binding of Gαi to the 2 and 3 GoLoco domains destabilizes intramolecular interactions, thus allowing association of Mud with Pins and localization to the apical cortex, which is important for aligning the mitotic spindle with the cortical polarity axis. Recently was shown that the PDZ protein Canoe also associates with Pins and has a regulatory effect on cell polarity and apico-basal orientation of the mitotic spindle (Speicher et *al.* 2008). It is known that the Mud orthologous NuMa (vertebrates) and LIN-5 (*C. elegans*) associate with the Dynein/Dynactin protein complex to regulate spindle assembly (Nguyen-Ngoc et *al.* 2007, Merdes et *al.* 2000). Recently, the dynein light-chain protein Cut up (Ctp) was identified as a Mud interaction partner (Wang et *al.* 2011). This suggests that Gαi/Pins/Mud also recruit the Dynein/Dynactin complex to the apical cortex, which exerts minus-end directed motor activity, thus aligning the mitotic spindle with the apico-basal axis (Figure 9) (Siller & Doe 2009).

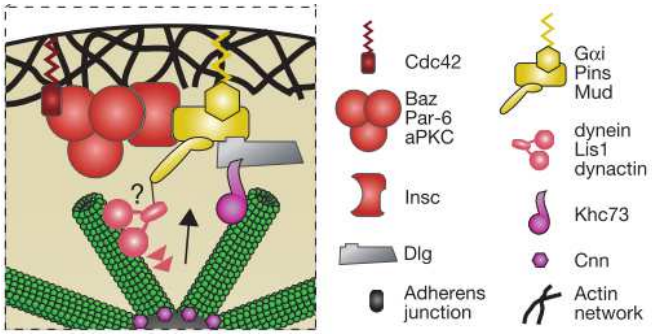


Siller & Doe, 2009

**Figure 10. Mitotic spindle orientation.** Microtubules are anchored to the apical cortex through Dlg and Khc73, where Dlg associates with Pins and Khc73 locolizes to the microtubule plus-end, respectively. Spindle positioning is mediated by Gαi/Pins/Mud. Mud associates with dynein, which moves towards the minus-end of the microtubules thereby generating pulling force to recruit the spindle to the cortex.

Cells have a second spindle orientation pathway, which consists of Pins, Discs large (Dlg) and kinesin heavy chain 73 (Khc73) to ensure asymmetric spindle orientation. It induces the formation of a Dlg/Pins/ Gαi crescent through binding astral microtubules to Dlg via Khc73, which is localized at the plus ends of astral microtubules (Sigrist & Doe 2005).

## 1.3 Nutrient-sensing mechanisms regulating cell growth

Development of multicellular organisms is determined by many genetic and environmental factors. The main environmental factor, which influences the growth rate, is the availability of nutrients controlling both cell and organismal growth. This process is regulated via cooperation of cell-autonomous and systemic response to nutrients and involves two pathways. Cell-autonomous control of growth is responsible for the ability of cells to assess their nutritional status via the protein kinase TOR (target of rapamycin) pathway. The systemic control mechanism is responsible for coordination of growth in whole animals and is governed by the insulin/insulin like peptide (ILP) pathway (in vertebrates insulin growth factor (IGF)), which in turn regulates the phosphatidylinositol 3-kinase (PI3K (in *Drosophila* p110))/AKT protein kinase signaling pathway (Hietakangas & Cohen 2009, Colombani et *al.* 2003, Britton & Edgar 1998). These two pathways interact at multiple levels to assure the normal development of the organisms.

*Drosophila* neuroblasts exit mitotic quiescence with beginning of larval development, which is accompanied by cell growth and re-entry of mitotic activity. In response to nutrition, an unknown fat body derived signal (FDS or fat body derived mitogen (FBDM)) acts on the larval CNS and triggers neuroblast enlargement and entry into the cell-cycle (Figure 11). After activation of mitosis, neuroblasts continue to proliferate independent of nutrient stimulus (Britton and Edgar 1998). In general, the fat body of insects is the storing tissue for proteins, lipids and glycogen. It shows dramatic response to nutrient starvation, accompanied by loss of texture and change in opacity. This could be explained by the mobilization of the stored metabolites to support proliferation of mitotic tissues in case of starvation.

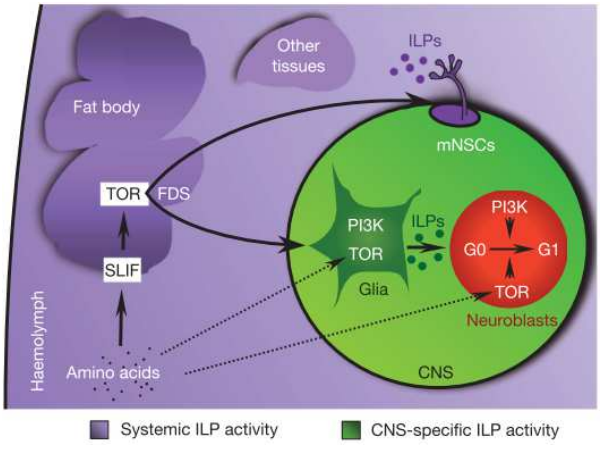


**Figure 11. Fat body dependent regulation of CNS and body growth.**
The fat body takes up amino acids by the amino acid transporter Slimfast (SLIF), which results in release of the FDS. In response to the FDS, glia cells and mNSCs secrete ILPs. Glial ILP signaling links the amino-acid/TOR dependent FDS with InR/PI3K/TOR signaling in neuroblasts. Direct sensing of amino acids may also contribute to reactivation of neuroblasts.

Sousa-Nunes et *al.* 2011

In *Drosophila,* seven ILPs (ILP1-7) and a single insulin-like receptor (InR) were identified. Neuroblasts are surrounded by glia cells, which receive the nutrition dependent FDS and in turn produce ILPs. ILP2 and ILP6 are the most prominent peptides, which drive neuroblast activation through the InR/PI3K/Akt pathway (Chell & Brand 2010, Sousa-Nunes et *al.* 2011). Besides glia cells, brain median neurosecretory cells (mNSC) also produce ILPs in response to the FDS signal (Figure 11Figure 11). However, glia cell derived ILPs are required for the activation of neuroblasts, whereas mNSC produced ILPs are essential for organismal growth regulation (Sousa-Nunes et *al.* 2011). In summary, InR/PI3K/TOR pathway mediated neuroblast reactivation is induced by ILP signaling received from glia cells which are activated by amino acid/TOR mediated FDS (model is proposed by Sousa-Nunes et *al.* 2011).

Activation of InR by ILPs triggers activation of PI3K, which in its turn mediates phosphorylation and activation of AKT by PDK1. AKT is a protein kinase that further triggers the TOR pathway (Figure 12 A). TOR kinase exists in two complexes and both are important in growth regulation, although they act in different ways (Loewith et *al.* 2002): TOR complex 1 (TORC1) is the main component for nutrient and energy sensing to control growth, whereas TOR complex 2 (TORC2) has modulatory role in insulin signaling by phosphorylation of AKT. At the same time, the TORC1 complex can be activated by circulating amino acids through the small GTPase Rag (Kim et *al.* 2008). Two key substrates phosphorylated by TORC1 complex are protein kinase S6K and initiation factor 4E binding protein (4E-BP) (Montagne et *al.* 1999, Tettweiler et *al.* 2005). Most of the TORC1 regulated genes are involved in ribosome biogenesis and consequently, the combined activities of the PI3K/AKT and TOR pathways mediate cellular protein synthesis and simultaneously inhibit the transcription factor Forkhead box class O (FoxO) function, which limits growth rate in response to lower nutritional status, to regulate tissue growth and proliferation (Guertin et *al.* 2006, Matsuzaki et *al.* 2003). Moreover, most of the TORC1 regulated genes are targets of the transcription factor Myc and its expression is regulated by TOR. In addition, Myc is regulated by PI3K/AKT via FoxO, where FoxO directly binds to the Myc promoter. However, this process is tissue specific or depends on metabolic state of the cell (Li et *al.* 2010, Parici et *al.* 2011, Teleman et *al.* 2008).

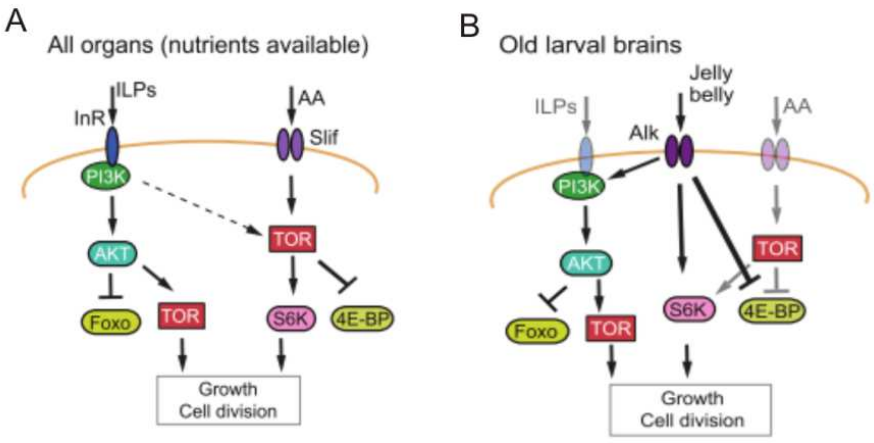


Homem & Knoblich 2012

**Figure 12. Schematic presentation of neuroblast growth control.**
A) Amino acid mediated signaling pathways. PI3K/AKT activates by ILPs, which inhibits FoxO and activates TOR. Slif mediates TOR activation by amino acids, which activates S6K and inhibits 4E-BP. In combination, these two pathways regulate protein biosynthesis, cell growth and proliferation. B) Nutrient independent regulation of growth after reactivation of neuroblasts. Alk kinase is expressed in neuroblasts during late developmental age and activated by its ligand Jeb (Jelly Belly). Activated AKT directly phosphorylates S6K and 4E-BP resulting in cell growth and proliferation.

Although neuroblast reactivation and proliferation requires convergence of InR/PI3K/AKT and TOR pathways stimulated by nutrition, neuroblasts have a brain-sparing mechanism, which allows maintaining the growth at late larval stages also under nutrient restriction. Under these conditions, Jelly Belly (Jeb)/anaplastic lymphoma kinase (Alk) signaling bypasses the requirement of ILP mediated InR activation (Figure 12 B) (Cheng et *al.* 2011). Alk is expressed in the developing CNS neuroblasts and becomes activated by the ligand Jeb expressed in glia cells. Both are strongly expressed during fed and fasting conditions. Alk promotes neuroblast growth by activation of the PI3K pathway in combination with a direct activation of TOR effector protein S6K, thus protecting CNS development against reductions in amino acids.

Nutrient availability is a key determinant of organismal growth and development. During development, animals face periods with food availability and restriction. To survive all unfavorable conditions, the organism has a high adaptive response to environmental conditions, which are triggered by several protective mechanisms, ensuring to overcome restrictions and finally to complete normal development.

## 1.4 Ribosome biogenesis: a major regulator of cell growth

Ribosome biogenesis highlights the growth capacity of cells, as protein synthesis is a crucial step in growing and dividing cells. It requires enormous number of functional ribosomes, which are molecular factories responsible for protein synthesis. Ribosome biogenesis takes place in the nucleolus, a subnuclear compartment, where the ribosome subunits generating transcription and processing machineries are localized. Before assembling the mature ribosome several major processes take place starting from 1) transcription of preribosomal RNA (pre-rRNA) from ribosomal DNA (rDNA), 2) association of non-ribosomal proteins and small nucleolar RNAs (snoRNAs) to control pre-rRNA modification and processing into the 18S, 28S (in lower eukaryotes 25S), and 5.8S ribosomal RNAs (rRNAs), 3) further incorporation of ribosomal proteins (RPs) and 5S rRNA into pre-ribosomal small (40S) and large (60S) subunits and 5) transport of maturing 40S and 60S subunits to the cytoplasm, completing the maturation and assembling the 80S ribosome. Generally, the nucleolus is intact during interphase and becomes disassembled during mitosis. Inherently, the nucleolus is a dynamic organelle, since its size and structure is directly related to ribosome production (Melese & Xue, 1995). The structure of the nucleolus varies between different animal and plant species. Nevertheless, there are three structural compartments which built up the nucleolus: the fibrillar center (FC), the dense fibrillar component (DFC), and the granular component (GC), which is surrounding the FC and DFC (Figure 13). In contrast to higher eukaryotes, *Drosophila* nucleoli comprise only two subcompartments: fibrillar and granular components (F and GC), which are intermingled. Each nucleolar compartment has a distinct role in ribosome biogenesis.

Ribosome assembly is a highly controlled stepwise process, which requires all three nuclear RNA polymerases (RNA pol I, II and III). The initiation of ribosomal subunits synthesis starts with transcription of rDNA by RNA pol I to generate the pre-rRNA, which takes place at the border between the FC and DFC in higher eukaryotes or in the fibrillar compartment in lower eukaryotes. Further processing of the pre-rRNA into the 28S, 18S and 5.8S rRNAs takes place in the DFC and assembling of 5S rRNA and RPs occur in the GC (Figure 13) 5S rRNA is separately synthesized by RNA pol III. RP synthesis is mediated by RNA pol II and is regulated by the Myc transcription factor (Schlosser et *al.* 2003). RPs are synthesized in the cytoplasm and then become imported to the nucleus (Schlosser et *al.* 2003).

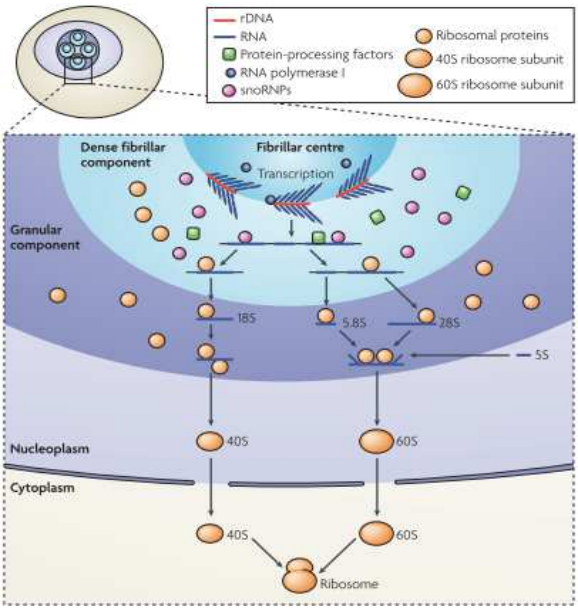


**Figure 13. Structural organization of the nucleolus and major steps of ribosome biogenesis.**
Generation of 40S and 60S ribosomal subunits and their assembly to 80S mature ribosomes in the cytoplasm (see detailed explanation in the text).

Boisvert et *al.* 2007

The control of regulation of pre-rRNA synthesis is the key step in ribosome biogenesis. It is sensitive to nutrient starvation or inhibition of protein synthesis, which is again reactivated by addition of nutrients, growth or other stimuli. In response to nutritional signals, the TOR pathway mediates phosphorylation of several co-factors of RNA pol I, such as TIF-IA (transcription initiation factor IA) and UBF (upstream binding factor), directing RNA pol I recruitment to rDNA and further initiates transcription (Mayer et *al.* 2004, Lempiäinen & Shore 2009). On the other hand, the UBF encoding gene *UBTF* is a transcription target of Myc, which is one of the downstream targets of the PI3K/TOR pathway (Grandori et *al.* 2005, Arabi et *al.* 2005, Poortinga et *al.* 2004).

The earliest pre-ribosomal particle is the 90S particle, which contains the 47S pre-rRNA (in lower eukaryotes 35S pre-rRNA) and many ribosomal and non-ribosomal proteins (Trapman et *al.* 1975). To form the functional ribosome, the processing machineries are coupled with the transcription machinery to drive pre-rRNA processing and modification, as well as RPs assembly. The U3 snoRNA and its associated factors, called small subunit (SSU) processome, are binding to 35S pre-rRNA and are responsible for the early cleavage of pre-rRNA and 40S assembly (Dragon et *al.* 2002). It has been also shown that 90S pre-rRNA is nearly completely lacking 60S subunit components, except for some factors (Nop1 and Rrp5), which are involved in assembly of both particles (Grandi et *al.* 2002). The SSU processome mediates 35S pre-rRNA modification and cleavage into 20S and 27S (28S in higher eukaryotes) rRNAs (Figure 13), which are the characteristic intermediates for pre-40S and pre-60S subunits, respectively (Henras et *al.*

2008). Most of non-ribosomal factors dissociate from the pre-40S particle and essential biogenesis factors and RPs are recruited to the 20S rRNA. In general, pre-40S subunit has a proper structure, besides the characteristic “beak” structure, which is essential for association with the 60S subunit. The formation of “beak” takes place in the cytoplasm after transport of pre-40S due to phosphorylation/dephosphorylation events (Schäfer et *al.* 2006). The final maturation of 40S subunit proceeds in the cytoplasm and depends on cleavage of the 20S rRNA to generate the mature 18S rRNA. This processing step completes 40S assembly. The final 40S small ribosomal subunit consists of 18S rRNA and 32 RPs.

An important step in assembly of pre-60S is the incorporation of 5S rRNA (Figure 13) which is synthesized in the nucleoplasm, followed by transport to the cytoplasm, where it is associated with RpL5 and afterwards imported back to the nucleus, where incorporation takes place (Steitz et *al.* 1988). Transcription of the 5S rRNA is mediated by RNA pol III, which is regulated by direct interaction of Myc with TFIIIB (Gomez-Roman et *al.* 2003, Grandori et *al.* 2005). Within the pre-60S particle, cleavage and further processing of 27S pre-rRNA yield the mature 5.8S and 25S rRNAs (Kressler et *al.* 2010). The large ribosomal subunit associates with many non-ribosomal and ribosomal factors, as well as RPs to assure its further maturation and transport to the cytoplasm. In summary, ~ 50 non-ribosomal proteins are associated with the pre-60S subunit, whereas only 5 are remaining in the mature 60S subunit (Kressler et *al.* 2010). The mature 60S subunit is composed of 5.8S, 25S (28S in higher eukaryotes) and 5S rRNAs and 47 RPs. The final step to generate the functional 80S ribosome is the assembly of 40S and 60S subunits with mRNA in the cytoplasm.

## 1.5 The Mbm (mushroom body minature) protein is involved in *Drosophila* CNS development

The characterization of the *mushroom body miniature (mbm)* gene started nearly 30 years ago by isolation of the hypomorphic $mbm^{1}$ allele in a genetic screen for altered mushroom body (MB) structure. The MB is a bilaterally arranged structure in the protocerebrum of *Drosophila* and most other insect species, and it is responsible for olfactory learning, memory and decision making (Heisenberg et *al.* 1985, Heisenberg 2003). Each MB arises from a group of four apparently equipotent neuroblasts, which continuously divide from embryonic until pupal stages to sequentially generate several

types of intrinsic MB neurons (Kenyon cells, KCs) (Ito & Hotta 1992, Ito et *al.* 1997, Lee et *al.* 1999, Kunz et *al.* 2012). Approximately 2000 Kenyon cells build up the MB structure in each adult brain hemisphere (Aso et *al*. 2009). Dendrites of the Kenyon cells, which are located in the dorsal cortex, form the calyx together with the synaptic endings from projection neurons, whereas axons fasciculate in the anterior-ventral projecting peduncle, where most of them bifurcate to form a system of medial and dorsal projecting lobes. MB γ neurons are born before the mid-third-larval instar, then α´/β´neurons are born, and finally the α/β neurons are added at pupal stages (Lee et *al.* 1999). Furthermore, γ neuron axons undergo massive remodeling during metamorphosis to establish adult-specific branching patterns (Technau and Heisenberg 1982, Lee et *al*. 1999). *Mbm*$^{1}$ mutants show sexual dimorphism. MB development of female flies proceeds normally until the 3$^{rd}$ instar larva, followed by inappropriate remodeling of KCs axons. In addition, a reduction in Kenyon cell number was observed, resulting in a grossly reduced MB neuropile in the adult (Heisenberg et *al*. 1985, de Belle & Heisenberg 1996, Raabe et *al.* 2004). The phenotype caused by *mbm*$^{1}$ is variable ranging from moderate to strong reduction of the MB neuropile, however, the structural subdivision of the MBs is apparently maintained in all cases (Figure 14).

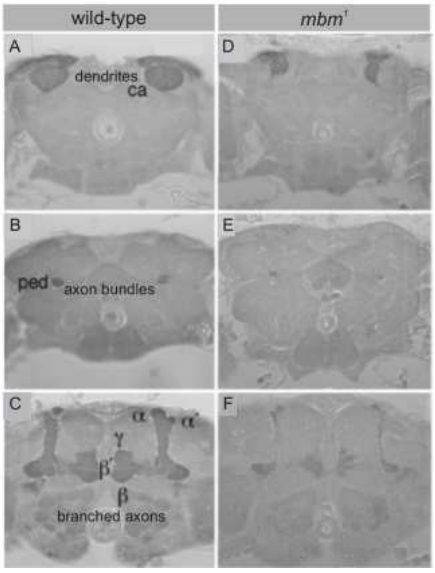


**Figure 14. Analysis of the *mbm1* phenotype.**
Frontal section of paraffin embedded heads of wt (A-C) and *mbm*$^{1}$ (D-F) females. Kenyon cell dendrites form the calyx (ca), axons form peduncle (ped) and then branch into the lobe system (γ, α´/β´, α/β). The structural subdivision is maintained in *mbm*$^{1}$ flies, though there is an overall size reduction.

Raabe et *al.* 2004

Cloning of the gene revealed that the predicted transcription unit CG11604 corresponds to the *mbm* gene (Raabe et *al.* 2004). It encodes a protein with characteristic structural features including several clusters enriched in certain amino acids. Particularly, two R/G rich regions, two stretches with basic amino acids and three clusters of acidic

amino acids are evident, but the most prominent structural feature of Mbm is a pair of CCHC zinc fingers located in the C-terminal half of the protein (Figure 15). Zinc finger structures and functions are extraordinarily diverse including DNA recognition, RNA packaging, transcriptional activation, regulation of apoptosis, protein folding and assembly (Krishna et *al.* 2003, Laity et *al.* 2001). Furthermore, Mbm was identified as a phosphoprotein (Bodenmiller et *al.* 2008, Zhai et *al.* 2008).


**Figure 15. Schematic presentation of the Mbm protein structure.**
Clusters of enriched amino acids are marked with different colors and symbolically marked with: arginine/glycine – R/G (red), basic amino acid clusters – BC-1 and BC-2 (green), acidic amino acid clusters – AC-1, AC-2 and AC-3 (blue) and two zinc fingers – ZF-1 and ZF-2 (yellow).

Mbm expression was detected in the MB neuropile. Particularly, Mbm shows a cell cycle dependent localization in neuroblasts. It was detected in the nucleus of interphase cells, followed by cytoplasmic distribution during the cell cycle (Raabe et *al.* 2004). Bromodesoxyuridine (BrdU) pulse labeling experiments indicated a function of Mbm in proliferation of neuroblasts. Moreover, recently was identified that Mbm is transcriptional target of *Drosophila* Myc transcription factor (Hulf et *al.* 2005).

## 1.6 Aim

Previous studies with the hypomorphic *mbm*$^{1}$ allele have revealed that in adult flies mushroom bodies (MB) are grossly reduced compared to wild-type (Heisenberg et *al.* 1985). Heteroallelic combinations of *mbm* also caused MB neuroblast proliferation defects (Raabe et *al.* 2004). However, at which step Mbm is required for neuroblast proliferation still remains elusive. Unfortunately, homology searches provided no hint about the molecular function of Mbm.

The aim of this work was to identify the role of Mbm in *Drosophila* brain development and for that the following issues were addressed:

1. Evaluation of the Mbm expression pattern in the brain by generation of a more specific anti-Mbm anitibody. In this respect, the subcellular localization of Mbm in neuroblasts was of particular interest.
2. All analyses so far were done with the hypomorphic *mbm*$^{1}$ mutant, which still expresses low amounts of Mbm protein. Thus, a detailed phenotypic analysis was necessary with a verified null allele of *mbm*. The major emphasis was the analysis of central brain neuroblasts with respect to proliferation capacity, asymmetric cell division and cell growth. These analyses should provide the basic information, which cellular process might be affected by loss of Mbm function. Based on these findings, further studies should be performed to get insights into the molecular function of Mbm.
3. Based on transcriptome analysis, Mbm is a transcription target of Myc (Hulf et *al.* 2005). Thus an important aim was to verify the function of Myc as a transcriptional regulator of *mbm* expression both *in vitro* and *in vivo*.
4. Relaying on the fact that Mbm is a phosphoprotein (Bodenmiller et *al.* 2008, Zhai et *al.* 2007), a major aim was to determine the relevant protein kinase, to identify phosphorylation sites followed by testing their functional relevance *in vivo*.

# 2 Materials and Methods

## 2.1 Materials

### 2.1.1 Chemicals, enzymes and equipment

All chemicals used during the study were from Applichem, Sigma, Roche and Roth companies. Restriction enzymes and polymerases were from NEB. Equipment used for experiments were from Biorad, Eppendorf, Biozym, Greiner, Sarstedt, Biotech and Biometra.

### 2.1.2 Reagents

| **Name** | **Usage** | **Manufacturer** | **Final concentration** |
|---|---|---|---|
| Pepstatin A | Protease inhibitor | Roche | 0,7 µg/ml |
| Leupeptin | Protease inhibitor | Applichem | 5 µg/ml |
| Antipatin | Protein inhibitor | Applichem | 5 µg/ml |
| Aprotinin | Protein inhibitor | Roth | 10 µg/ml |
| Complete, Mini | Protease inhibitor Cocktail | Roche | 1X |
| PMSF | Protease inhibitor | Sigma | 0,2 µg/ml |
| Protein G-Agarose | Immunoprecipitation | Roche | - |
| Glutathion Sephatose 4B | Protein purification | GE Healthcare | - |
| ATP | Kinase assay | Applichem | - |
| [$\gamma$-$^{32}$P] ATP | Kinase assay | PerkinElmer | 3000 Ci/mmol |
| Schneider´s *Drosophila* Medium | Cell culture | Gibco/BRL | - |
| Cellfectin | Cell transfection | Invitrogen | - |
| ECL Plus | Western blotting detection | GE Healthcare | - |
| Vectashield | Immunosteining | Vector Lab | - |

### 2.1.3 Special equipment

| **Apparatus** | **Model** | **Manufacturer** |
|---|---|---|
| Confocal laser microscope | TCS SP5 | Leica |
| Confocal laser microscope | FLUOVIEW 1000 IX 81 | Olympus |
| Fluorescent microscope | DM6000 | Leica |
| Luminometer | GloMax® Microplate Luminometer | Promega |
| Flow Cytometer | BD FACSCanto™ II | Becton Dickinson |

### 2.1.4 Kits

| **Name** | **Producer** |
|---|---|
| QIAamp DNA Mini Kit | Qiagen |
| QIAamp DNA Midi Kit | Qiagen |
| NucleoSpin®Extract II | Macherey-Nagel |
| Dual-Luciferase Reporter Assay System | Promega |
| Click-iT® EdU Alexa Fluor® 488 Imaging Kit | Invitrogen |
| Click-iT® HPG Alexa Fluor® 488 Protein Synthesis Assay Kit | Invitrogen |
| MEGAscript® RNAi Kit | Ambion |
| CellTrace™ CFSE Cell Proliferation Kit - For Flow Cytometry | Molecular Probes |
| QuikChange site-directed Mutagenesis | Stratagene |

### 2.1.5 Cells

| **Name** | **Source** |
|---|---|
| *E. coli* cell strains: **DH5α™; Bl21** | Invitrogen, Novagen |
| *Drosophila* Schneider 2 (S2) cells | *Drosophila* Genomics Resource Center (DGRC) |

### 2.1.6 Buffers and solutions

**LB medium (1L)**
10g Sodium chloride (NaCl)
10g Bacto-Tryptone
5g Yeast extract

**Lysis buffer (TPE)**
1% Triton x 100
100 mM Ethylene diamine tetraacetic acid (EDTA)
1x Phosphate Buffered Saline

**Lysis buffer**
25 mM Tris
150 mM Sodium chloride
10% Glycerin
1% Triton X-100
1% Nonidet-P40
1x Protease Inhibitor Cocktail

**1x Phosphate Buffered Saline – PBS, pH 7.4**
137 mM Sodium chloride
2,7 mM Potassium chloride (KCl)
8,1 mM Disodium hydrogen phosphate-dihydrate ($Na_2HPO_4.2H_2O$)
1,8 mM Monopotassium phosphate ($KH_2PO_4$)

**Glutathione (GSH) Wash buffer**
50 mM Tris(hydroxymethyl)aminomethane (Tris) pH 7.5
100 mM Disodium ethylene diamine tetraacetic acid ($Na_2EDTA$) pH 7.5
0,1% Tween 20

**Glutathione Elution Buffer**
10 mM Reduced Glutathione
50 mM Tris-HCl (adjust pH 8.0)

**Laemmli sample buffer**
70 M Tris-HCl pH 6.8
3% SDS (Sodium dodecyl sulfate)
40% glycerol
0.5 ml 0.5 M EDTA
0,05% Bromophenol Blue
5% β-mercaptoethanol (14.3 M)

**1x Running Buffer**
25 mM Tris-base
200 mM Glycine
0,1% SDS

**Stacking buffer (SDS-PAGE)**
0,5 M Tris 0.5 M pH 6.8
0,4% SDS

**Separating buffer (SDS-PAGE)**
1.5 M Tris pH 8.8
0,4% SDS

**Coomassie staining solution**
Coomassie brilliant blue R-250
10% Acetic acid
50% Methanol

**Distaining solution I**
40% Methanol
10% Acetic acid

**Distaining solution II**
20% Methanol
10% Acetic acid

**1X Transfer Buffer (Western blot)**
25 mM Tris pH 8.3
192 mM glycine
20% Methanol

**1 x TBS-T**
10 mM Tris pH 7,5
150 mM NaCl
0.05% Tween 20

**TBE buffer**
0,89 M Tris
0,89 M Boric acid
4% EDTA pH 8.0

**Sodium phosphate buffer pH 6.8 (PLP)**
463 µl Disodium hydrogen phosphate (0,5M ($Na_2HPO_4$))
537 µl Sodium dihydrogen phosphate (0,5M ($NaH_2PO_4$))

**PLP**
720 µl 8% PFA (paraformaldehyde) freshly defrozed
1 ml 0,15 M DL-Lysin
200 µl 0,1 M Sodium periodate ($NaIO_4$)
120 µl Sodium phosphate buffer pH 6.8

**1x PBS-T pH 7.4**
137 mM Sodium chloride
2,7 mM Potassium chloride (KCl)
8,1 mM Disodium hydrogen phosphate-dihydrate ($Na_2HPO_4.2H_2O$)
1,8 mM Monopotassium phosphate ($KH_2PO_4$)
0,3% TritonX100

### 2.1.7 Primers

| Primer | Sequence 5´-3´ |
|---|---|
| E-box1-NcoI F. | CTG**CCATGG**CGTCGCAGTAGC |
| E-box1-NcoI R. | CCTCCACTGTTG**CCATGG**TGGAATTG |
| E-box1+2-NcoI F. | GGAA**CCATGG**CGCAGCGAGCGC |
| E-box1+2-NcoI R. | CCTCCACTGTTG**CCATGG**TGGAATTG |
| ΔE-box1- F. | CCCCAATCGGCTCAA**GAATTC**CGCCGCAACTAGGC |
| ΔE-box1- R. | GCCTAGTTGCGGCG**GAATTC**TTGAGCCGATTGGGG |
| AC-1 F. | CCGACTCCTCAACT**GCG**GAC**GCC**GAC**GCC**GATGATGAACAGAG |
| AC-1 R. | CTCTGTTCATCATC**GGC**GTC**GGC**GTC**CGC**AGTTGAGGAGTCGG |
| AC-2 F. | CCAGTTTACCATT**GCC**GATGAGGAGGAA**GCCGCC**GAACCTGAAGACG |
| AC-2 R. | CGTCTTCAGGTTC**GGCGGC**TTCCTCCTCATC**GGC**AATGGTAAACTGG |
| Mbm-RNAi-2 F | **TAATACGACTCACTATAGGGAGA**GAACCCGAACCAGGGGAAATGG |
| Mbm-RNAi-2 R | **TAATACGACTCACTATAGGGAGA**CGTCATGATCTTTCGGCTCCACC |

### 2.1.8 List of antibodies

## Primary antibodies

| Antigen | Animal | Clon | Dilution | Usage | Cat. Nr. | Origin |
|---|---|---|---|---|---|---|
| aPKC | rabbit | polyclonal | 1:1000 | IF | sc-216 | Santa Cruz,Boptechnology |
| Miranda | mouse | 81-0 | 1:20 | IF | - | F. Matsuzaki, Kobe, Japan |
| Pins | rat | polyclonal | 1:500 | IF | - | F. Matsuzaki |
| Phospho-histone H3 | rabbit | polyclonal | 1:2500 | IF | 06-570 | Millipore-Upstate |
| GFP | chicken | polyclonal | 1:1000 | IF | AB16901 | Millipore |
| Fibrillarin | mouse | 72B9 | 1:50 | IF | - | U. Scheer, Würzburg, Germany |
| Fibrillarin | mouse | P2G3 | 1:250 | IF | - | U. Scheer |
| Mbm | guinea pig | Syc-143 | 1:100 | IF | - | Eurogentec |
| Nop5 | rabbit | polyclonal | 1:600 | IF | - | G. Vorbrüggen, Göttingen, Germany |
| Lamine | mouse | ADL67.10 | 1:10 | IF | - | Developmental Studies Hybridoma Bank (DSHB) |
| Lamine | mouse | ADL195 | 1:10 | IF | - | DSHB |
| Armadillo | mouse | N2.7A1 | 1:100 | IF | - | DSHB |
| CK2α | rabbit | polyclonal | 1:400 | IF | KAP-ST010 | Stressgen |
| Numb | guinea pig | polyclonal | 1:1000 | IF | - | J. Skeath, St.Louis, MO, USA |
| γ-Tubulin | mouse | GTU-88 | 1:100 | IF | T 6557 | Sigma |
| Mbm | rabbit | EP031195 (mbm-95) | 1:166 | WB | - | T. Raabe, Würzburg, Germany |
| α-Tubulin | mouse | NDM1A | 1:2500 | WB | TT9026 | Sigma |

## Secondary antibodies

| **Specificity** | **Conjugate** | **Animal** | **Dilution** | **Usage** | **Cat.Nr.** | **Origin** |
|---|---|---|---|---|---|---|
| Rat | Cy3 | rat | 1:100 | IF | 012-160-003 | Dianova |
| Guinea pig | Cy3 | goat | 1:100 | IF | 106-166-003 | Dianova |
| Guinea pig | Cy2 | goat | 1:100 | IF | 106-225-003 | Dianova |
| Rabbit | Alexa488 | goat | 1:250 | IF | A-11034 | Molecular probes |
| Mouse | Alexa488 | gout | 1:250 | IF | A-11001 | Molecular probes |
| Chicken | DyLight488 | goat | 1:200 | IF | 103-485-155 | Dianova |
| Rabbit | Cy5 | goat | 1:100 | IF | 111-175-144 | Dianova |
| Mouse | Cy5 | donkey | 1:100 | IF | 715-175-151 | Dianova |
| Rabbit | HRP | donkey | 1:5000 | WB | NA9340V | Amersham GE Healtcare |
| Mouse | HRP | sheep | 1:5000 | WB | NA931 | Amersham GE Healtcare |

### 2.1.9 Fly stocks

| **Stock label** | **Reference** |
|---|---|
| $w^{1118}$ | T. Raabe, Würzburg, Germany |

| **Gal4- Driver Lines** | |
|---|---|
| **Stock label** | **Reference** |
| *worniu-Gal4*/SM6, CyO | Albertson and Doe, 2003 |
| *Mz1060-Gal4* | J. Urban, Mainz, Germany |

| **Transgenes** | |
|---|---|
| **Stock label** | **Reference** |
| $w^{*}$*; P{lacW}mbm*$^{SH1819}$/Cyo, Ubi-GFP, (*mbm*$^{SH1819}$/Cyo, Ubi-GFP) *mbm*$^{SH1819}$, P{neoFRT}40A/CyO, Ubi-GFP | S.W. Oh et *al.* (2003) |
| *w*;mbm*$^{pTW115}$(*P[mbm*$^{wt}$*]*) | T. Raabe (2004)/ |
| *w*, CK2β*$^{mbuΔA26\text{-}2L}$/FM7a, Act-GFP (*CK2β*$^{Δ26}$) | E. Jauch/ T. Raabe |
| *w*, CK2β*$^{mbuΔA26\text{-}2L}$*; CK2β*$^{gDNA}$ | E. Jauch/ T. Raabe |
| *UAS-GFP::NS1* | R. Rosby et *al.* (2009) |
| *UAS-mRFP::RpS6* (3rd chromosome) | R. Rosby et *al.* (2009) |
| *UAS-GFP::RpL11* (2nd chromosome) | R. Rosby et *al.* (2009) |
| *UAS-GFP::Nol12* (3rd chromosome) | J. Marinho et *al.* (2011) |
| *mbm*$^{SH1819}$/Cyo, Ubi-GFP; *UAS-GFP::NS1*/ TM6B, Tb | T. Raabe (combined for this study) |
| *mbm*$^{SH1819}$*, UAS-GFP::RpL11*/Cyo, Ubi-GFP | T. Raabe (combined for this study) |
| *mbm*$^{SH1819}$/Cyo, Ubi-GFP; *UAS-mRFP::RpS6*/ TM6B, Tb | T. Raabe (combined for this study) |
| *mbm*$^{SH1819}$/Cyo, Ubi-GFP; *UAS-GFP::Nol12*/ TM6B, Tb | T. Raabe (combined for this study) |
| *UAS-CK2α-RNAi* (2nd chromosome) | R. Jackson, Boston, USA |
| *UAS-CK2α-RNAi* (3rd chromosome) | Bloomington stock center #35136 |
| *UAS-CK2α*$^{Tik}$ (3rd chromosome) | Meissner et *al.* (2008) |
| *mbm*$^{SH1819}$/Cyo, Ubi-GFP; *P[mbm*$^{wt}$*]*/ TM6B, Tb | produced for this work |
| *mbm*$^{SH1819}$/Cyo, Ubi-GFP; *P[mbm*$^{AC\text{-}1ΔP}$*]*/ TM6B, Tb | produced for this work |
| *mbm*$^{SH1819}$/Cyo, Ubi-GFP; *P[mbm*$^{AC\text{-}2ΔP}$*]*/ TM6B, Tb | produced for this work |
| *mbm*$^{SH1819}$/Cyo, Ubi-GFP; *P[mbm*$^{AC\text{-}1+2ΔP}$*]*/ TM6B, Tb | produced for this work |

## 2.2 Methods

### 2.2.1 Generation of transgenic flies

The previously described 4.3kb HindIII genomic rescue construct *P[TW115]* (Raabe et *al.* 2004) served as a template to simultaneously replace codons in acidic cluster AC-1 (S288A, S290A, T292A) and in acidic cluster AC-2 (T327A, S332A, T333A) to alanine by *in vitro* mutagenesis. Prior to mutagenesis this construct was cut out with NotI/KpnI and subcloned to pBluescript II SK (-) vector. Afterwards mutagenesis was done using QuikChange site-directed Mutagenesis kit. Primers used for mutagenesis are mentioned in the primer list. The sequences indicated in bold show the mutated codons for phosphorylation sites. All constructs were verified by sequencing and were cut out again with the same restriction enzymes to clone them into the pattB transformation vector to allow for PhiC31 mediated transgenesis at the *attP* site located at chromosomal position 62B2 on the 3$^{rd}$ chromosome (BestGene Inc.). For each construct, several independent transgenic lines.

### 2.2.2 Bacterial protein expression and purification

Because of complication to express a full-length Mbm protein, cloning into the EcoRI/XhoI cut bacterial expression vector pGEX-KG was carried out to separately express the N-terminal (amino acids 1-268, GST::Mbm1) and the C-terminal (amino acids 266-539, GST::Mbm2) half of the Mbm protein. The GST::Mbm2 construct was used as a template for *in vitro* mutagenesis to replace codons for the identified CK2 phosphorylation sites (S288A, S290A, T292A in the AC-1 cluster and T327A, S332A, T333A for AC-2). Primers used for mutagenesis were the same as in case of the transgenic constructs. Correspondingly, the complete open reading frame of CK2α was amplified by linker PCR and cloned into the pGEX-5X-1 vector digested with EcoRI/SalI. All constructs were verified by sequencing. Plasmids were transformed into *E.coli* BL21 (DE3) and expressed proteins were purified according to "Isolation of GST-fusion proteins from IPTG-induced *Escherichia coli*" protocol (Feller Lab protocols, 2001). Proteins were dialyzed in 20 mM HEPES (pH 7.5) for 48 hours. Similar purifications of both parts of the Mbm protein were done for antibody generation and 30 μg from each GST::Mbm fusion protein were used for immunization of guinea pigs (Eurogentec).

### 2.2.3 *In vitro* kinase assay

Kinase assays were done using 6 μg of recombinant GST::CK2α. Reactions were set up with 30 μg of the corresponding GST::Mbm protein, 20mM $MgCl_2$ and ATP (10μC [$\gamma$-$^{32}$P] ATP (3000 Ci/mmol) in case of radioactive kinase assay 40 nMol ATP for mass spectrometry analysis. To exclude phosphorylation of GST by CK2, GST protein also was included in the kinase assay as a control. The reaction was carried out in kinase buffer (20mM HEPES, pH 7.5, in a total volume of 50 μl) at 30$^{o}$C for 30 min and stopped by adding Laemmli buffer. Afterward, samples were incubated at 95$^{o}$C for 2 min and separated by 9% SDS-polyacrylamide gel electrophoresis (SDS-PAGE) and analyzed by autoradiography. For mass spectrometry analysis, the SDS-PAGE gel was stained with Colloidal coomassie staining and protein bands corresponding in size to GST::Mbm were cut out.

### 2.2.4 Immunoblot

For immunoblot analysis, protein lysates from 80 brains from 3$^{rd}$ instar larvae of the indicated genotypes were prepared in lysis buffer separated by 9% SDS-PAGE and transferred on nitrocellulose membrane for 2 hours using a semidry system (Bio-Rad Laboraories, Hercules, CA). The blots were blocked with 5% nonfat dry milk in 1 x TBS-T for 1 hour and incubated overnight at 4 $^{o}$C with rabbit anti-mbm95 and mouse anti-α-tubulin antibodies. Afterwards, the blots were probed with secondary antibodies diluted in 1xTBS-T and detected using the ECL Plus detection reagents.

### 2.2.5 Immunohistochemical analysis

3$^{rd}$ instar larval brains of the indicated genotypes were fixed for 30 min on ice in PLP, washed in 1x PBS (phosphate-buffered saline) and permeabilized for 10 min in 1x PBS containing 0,3% Triton X-100 (PBS-T). Brains were blocked in PBS-T containing 3% normal goat serum (NGS) for 2 hours at room temperature and probed overnight at 4$^{o}$C with the corresponding primary antibodies diluted in PBS-T/3% NGS. Afterwards, brains were washed 3 times for 1 hour in PBS-T and reprobed overnight at 4$^{o}$C with the corresponding secondary antibodies. Tissues were then washed for 1-2 days at 4$^{o}$C in 1x PBS, 0,3% TritonX-100 and mounted in Vectashield mounting media. Images were

recorded with a 0,5 µm step size with a Leica SP5 or an Olympus FLUOVIEW 1000 IX 81 confocal microscope and processed with ImageJ 1.46r software.

### 2.2.6 Neuroblast proliferation assay

Neuroblast proliferation was detected by using the Click-iT® Alexa Fluor 488 EdU imaging kit. In this assay, the modified thymidine analogue 5-ethynyl-2´-deoxyuridine (EdU) is incorporated into newly synthesized DNA. Detection is based on a copper-catalyzed covalent reaction between an azide and an alkyne. EdU contains the alkyne and the Alexa Fluor® 488 contains the azide. For EdU labeling, larval brains were dissected in PBS and incubated with 20 µM EdU in PBS for 2 hour at room temperature. After fixation in 4% paraformaldehyde for 15 min, brains were briefly washed in PBS-T and blocked in the same solution supplemented with 1% BSA for 30 min. EdU incorporation was detected according to the instruction manual (Invitrogen). After EdU labeling, brains were co-stained with an anti- Miranda antibody according to the standard protocol (see 1.2.5). Confocal images were collected with a Leica SP5 microscope and processed with ImageJ 1.46r software.

### 2.2.7 Metabolic labeling assay

Metabolic labeling of proteins was done using the Click-iT® HPG Alexa Fluor 488 protein synthesis assay kit (Invitrogen). The idea is that L-homopropargylglycine (HPG), an amino acid analog of methionine, penetrates into the cells and becomes incorporated into proteins during active protein synthesis. HPG incorporation is then detected by the Alexa Fluor 488® azide. Protein synthesis within a 1 hour interval was analyzed by incubation of dissected 3$^{rd}$ instar larval brains with HPG (50 µM f.c. in PBS) at room temerature, followed by fixation in 4% paraformaldehyde for 15 min. Signal was detected according to the instruction manual (Invitrogen). Afterwards, neuroblasts were co-stained for Miranda and Nop5 according to the standard protocol (see 1.2.5). Confocal images were collected with a Leica SP5 confocal microscope and processed with ImageJ 1.46r software.

### 2.2.8 Luciferase reporter assay

***Luciferase reporters*** – Sequences relative to Mbm translation start site containing two E-boxes (-1265 to -3: E-box1 at -47 to -42 and E-box2 at -516 to -511 positions) and correspondingly, only E-box1 (at -47 to -42 position) were amplified by NcoI linker PCR and fused to the firefly luciferase (FLuc) ORF. In the ΔE-box1 mutant, the sequence "CACGTG" was replaced by "GAATTC". The oligonucleotides used for *in vitro* mutagenesis are listed in 1.1.7. The sequences indicated in bold show the mutated E-box.

***Expression plasmids*** – Amplified sequences were cloned into the pGL3-basic vector (Promega) to perform luciferase reporter assays. In total 4 constructs were made: E-box1-FLuc, ΔE- box1-FLuc ; E-box1 placed in reverse direction (revE-box1-FLuc) and E-box 1+2-FLuc containing both E-boxes. Myc-dsRNA (Hulf et *al.* 2005), pBSattB-UAS-HA-Myc (Myc overexpression in S2 cells, Schwinkendorf, D., and Gallant, P.,2009) has been described (Hulf et *al.* 2005, Furrer et *al.* 2010); tub-GAL4 was used to drive expression of UAS-HA-Myc in transiently transfected S2 cell. As a control, constructs with the E-box containing promotor sequences of the verified Myc target gene CG5033 (E-box-CG5033) respectively an E-box mutated version (ΔE-box-CG5033) were included (Hulf et *al.* 2005).

***Culture of Drosophila S2 cells*** - *Drosophila* S2 cells were cultured at 24°C in 1x Schneider‘s Drosophila medium (Gibco/BRL), supplemented with 10% fetal bovine serum (heat-inactivated) and 1% Penicillin/Streptomycin (Invitrogen).

For luciferase assays, 1.3 x $10^6$ cells per well (in 0.65 ml) were plated in 24-well plates. Cellfectin was diluted 1:5 in serum-free medium to a final volume of 21 µl and incubated for 45 min at room temperature, then mixed with 21 µl of serum-free medium containing the appropriate plasmids (0,5 µg for the different E-box-mbm-FLuc and the E-box-CG5033-FLuc constructs, 2 µg ΔE-box-CG5033-FLuc, 0,5 µg ΔE-box-CG5033-RLuc, 50 ng UAS-HA::Myc, 0,1 µg tub-Gal4) and 30 ng Myc dsRNA, incubated for another 15 min at room temperature and finally diluted with 178 µl serum-free medium (SFM) and added to the cells previously washed with 1x 500 µl SFM. 16 hours later, the transfection mix was replaced by adding 650 µl complete medium and the incubation was continued for the indicated duration of time (typically 48 hours).

***Luciferase assay*** - Cells were harvested typically 48 h after transfection, washed in 1x PBS and lysed for 15 min in 100 µl 1x Passive Lysis Buffer (Dual Luciferase Reporter Assay System, Promega). 10 µl of each lysate was transferred to luminometric 96 well plates (Greiner) and relative reporter gene expression was determined with a Glomax

luminometer. The luminometer protocol was adjusted to disperse 50 µl luciferase substrates per measurement (Luciferase Assay Reagent II (LAR II) and Stop & Glo® Reagent, both provided with the Dual Luciferase Reporter Assay System). Each transfection was performed in duplicate, and all values are indicated as averages of duplicates with standard deviations. The experiment was repeated three times.

### 2.2.9 Neuroblast and wing imaginal disc cell size measurement and statistic

Neuroblasts areas were calculated considering only neuroblasts at metaphase stage because at this stage the apico-basal axis of cell is clearly distinguished. The apico-basal axis was determined by aPKC and Miranda staining. The "length" and "width" of neuroblasts were measured using the Straight Line tool of ImageJ 1.46r software (NIH, Bethesda, MA, USA) placed in the center of the apical aPKC and the basal Miranda crescents and the corresponding orthogonal axis. For each genotype 110-160 neuroblasts were measured. Furthermore, in order to calculate the nuclear to cytoplasmic ratio (equation NA/(CA-NA)), cell (CA) and nuclear areas (NA) of the irregularly shaped interphase neuroblasts were measured by the freehand selection tool of ImageJ. The same tool was used to measure the wing imaginal disc cell sizes placed in the pouch region. For this purpose wing imaginal discs from 3$^{rd}$ instar larvae were stained for Armadillo to outline cell junctions using the same staining protocol as for brain preparations**.**

**Data analysis**- Cell area was calculated by $\pi$ r1r2 where r1 and r2 are the semi "length" and semi width" axes. Distributions of variables did not deviate significantly from normality (Kolmogorov-Smirnov test, $P>0.2$). Hence, parametric statistics was applied, where the areas were calculated as dependent variables and the strain (wild-type vs. mutant) as independent variable. One-way ANOVA was performed to compare the size of neuroblasts between the wild-type and the mutant lines, whereas for NA/(CA-NA) and for wing imaginal cell size measurement t-test was done.

### 2.2.10 Quantitavie analysis of Mbm signal intensity in larval neuroblasts

The Mbm signal intensity measurment in different compartments of the neuroblast (nucleolus and cytoplasm) was done by ImageJ. To analyze Mbm signal separately in the nucleolus and in the cytoplasm between different genotypes, in one case the nucleolus and in the other the cytoplasm were removed from image by using ImageJ Freehand selection

and Fill tools. Afterwards, quantification was done according to the protocol from Andlauer & Sigrest, 2012 (Cold spring Harb Protoc; 2012; doi: 10.1101/pdb.prot068601).

### 2.2.11 S2 cell staining and flow cytometry

#### S2 cell staining

S2 cell stainings were done on cover slips, which were placed in 6-well plates. Before seeding, each cover slip was coated with 100 µl poly-L-lysine (Sigma) to generate adherence. After 20 min incubation, poly-L-lysine was removed and cover slips were washed with 1x PBS. 1 x $10^6$ cells were seeded on each cover slip and incubated for 2 hours at 24°C. Afterwards, the medium was removed and cells were fixed with 4% paraformaldehyde for 20 min. Cells were washed 3x with PBS and 1x with PBS-T, then blocked in PBS-T containing 1% NGS for 1 hour, washed again with PBS and applied with the primary antibodies diluted in PBS. Incubation was done for 1.5 hour at room temperature with gently mixing. Then, cells were washed with 1x PBS and the corresponding secondary antibodies (in PBS) were applied. After incubation for 1 hour in the dark, cells were washed 3x with PBS, mounted in Vectashield and analyzed by fluorescence microscopy (Leica).

#### Flow cytometry (FACS)

S2 cells proliferation assay was done according to the protocol provided with the CellTrace™ CFSE cell proliferation Kit (Molecular Probes). The idea of the method is that CFSE (carboxyfluorescein diacetate succinimidyl ester) passively diffuses into cells. The dye is retained by the cells throughout proliferation and therefore can be used for *in vivo* tracing. To compare whether loss of Mbm affects S2 cell proliferation, 4 x $10^6$ cells were transfected with 2 µg *mbm* dsRNA. Tamplate DNA was produced by linker PCR (primers are mentioned in 1.1.7) and was transcribed to RNA by The MEGAscript® RNAi Kit (Ambion) according to the protocol provoded with the kit. As a transfection reagent Cellfectin was used. S2 cell proliferation was measured by FACS (Becton Dickinson) after 3 and 7 days of transfection. As a null measurement CFSE fluorescence was measured at day 0.

### 2.2.12 Mass spectrometry (MS) analysis

Non-radioactive kinase assays of GST::CK2 and GST::Mbm proteins were performed as described in 2.2.3. Protein bands corresponding to Mbm size were cut out from the SDS-PAGE gel and sent for MS analysis to Dr. Jens Pfannstiel (Life Science Center of the University of Hohenheim). The MascotTM 2.3 (Matrix Science, UK) search engines were used for protein identification. Spectra were searched against the *Drosophila* subset of the NCBI protein sequence database downloaded as FASTA-formatted sequences from (ftp://ftp.ncbi.nih.gov/blast/db/FASTA/nr.gz). Proteome Discoverer 1.3 (Thermo Fisher Scientific) was used for data analysis. Phosphopeptide MS/MS spectra sequence assignments and phosphorylated residues were verified manually.

# 3 Results

## 3.1 Generation of a Mbm antibody

Despite the fact that in our laboratory an anti-Mbm antibody (rabbit anti-mbm95) was previously produced, it was necessary to generate a new ani-Mbm antibody. Although anti-mbm95 is nicely working on Western blots, there was a specificity problem in immunostainings. In order to generate a new anti-Mbm antibody, two previously established GST::Mbm constructs (GST::Mbm1 (amino acids 1-268) and GST::Mbm2 (amino acids 266-539), Anselm Ebert, Diploma thesis 2002) were expressed in bacteria and purified according to the "Isolation of GST-fusion proteins from IPTG-induced *Escherichia coli*" protocol (Feller Lab protocols, 2001). This strategy was chosen because of difficulties to produce the full length GST::Mbm protein. First, protein purification conditions were optimized according to "Quick check of GST-fusion expression" protocol (Feller Lab protocols, 2001) followed by large scale protein purification (Figure 16 A, B).

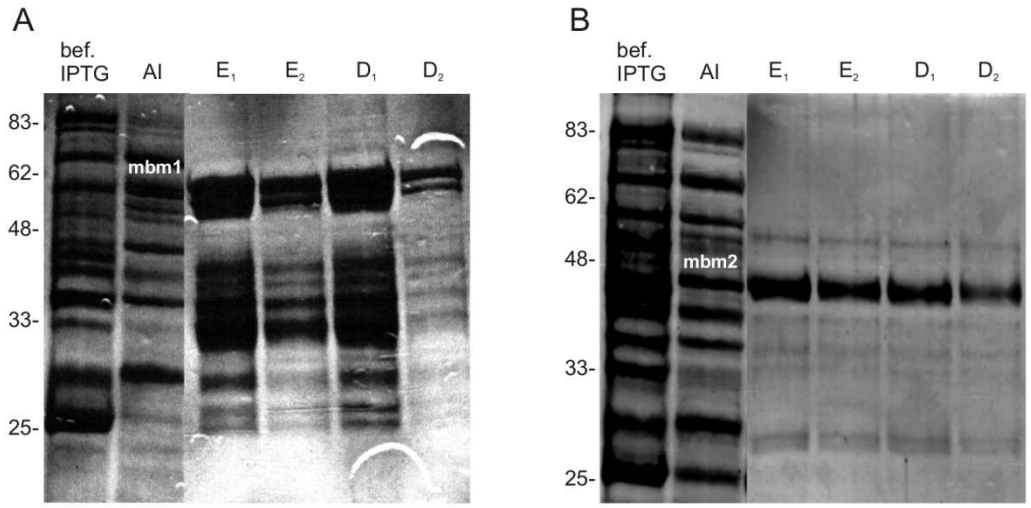


**Figure 16. Coomassie staining of purified GST::Mbm1 and GST::Mbm2 protein fragments after PAGE.**

A, B) In both pictures, the 1st line represents the crude sample before induction of GST::Mbm expression with IPTG (isopropyl β-D-thiogalactoside), the 2nd line is after induction (AI) with IPTG, lines 3 and 4 were loaded with samples from eluted fractions from gluthatione sepharose columns ($E_1$ and $E_2$), and lines 5 and 6 represent eluted proteins after dialyzing ($D_1$ and $D_2$).

Afterwards 30 µg from each purified fusion protein (samples were from $D_1$) were used for immunization of guinea pigs (Eurogentec). For each fusion protein, two independent animals were immunized and the corresponding anti-Mbm antisera were received (SYC142/143 for GST::Mbm1 and SYC144/145 for GST-Mbm2). All sera were

tested in different dilutions both in flies and S2 culture cells by Western blot and immunohistochemical analyses. The best results were obtained for SYC143 and therefore, all further experiments were carried out with this antiserum to detect Mbm.

## 3.2 Mbm is a new nucleolar protein

The previously characterized hypomorphic *mbm*$^{1}$ allele carries a single point mutation in the 5´ untranslated region, thereby introducing an additional start codon followed by a stop codon after 33 nucleotides, which creates a short open reading frame (ORF) upstream the *mbm* ORF (Figure 17 A). This resulted in reduced expression levels of the full length Mbm protein (Raabe et *al.* 2004). Relaying on this fact and also on the fact that homozygous *mbm*$^{1}$ flies are viable, all following experiments were performed with a recently isolated P-element insertion (SH1819), which localizes right after the beginning of the translation start site of the *mbm* gene and thus should behave as a null allele (Figure 17 A) (Oh et *al.* 2003). Homozygous *mbm*$^{SH1819}$ animals are lethal around pupal formation, although there are few escapers with a delayed eclosion time. Lethality can be rescued by a previously established genomic transgene *P[mbm*$^{wt}$*]* (Figure 17 A) (Raabe et al., 2004).

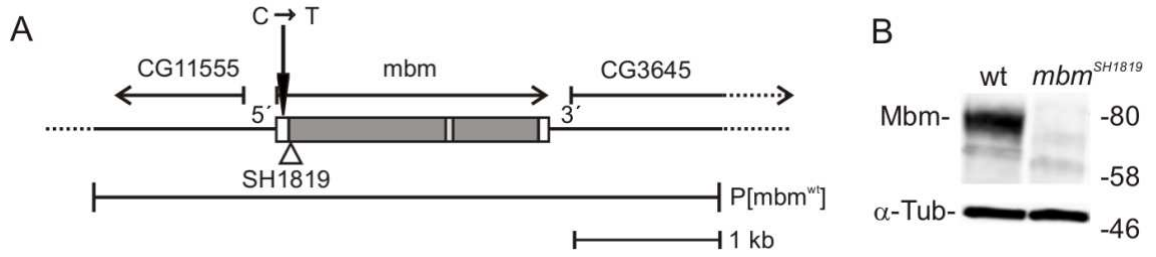


**Figure 17. Genomic organization of *mbm* and flanking transcription units.**
A) The coding sequence, the 5´ and 3´ untranslated regions and the single intron of the *mbm* transcription unit are represented by dark gray, white and light grey boxes, respectively. The rectangle represents the position of SH1819 P-element insertion. The C to T transition of *mbm*$^{1}$ in the 5´ untranslated region is indicated by an arrow. The genomic rescue construct *P[mbm*$^{wt}$*]* is shown below. B) Western blot of 3$^{rd}$ instar larval brain lysates from wild-type (wt) and *mbm*$^{SH1819}$ stained for Mbm. α-Tubulin was used as a loading control.

First, the lack of Mbm expression in homozygous *mbm*$^{SH1819}$ animals was verified by Western blot analyses using 3$^{rd}$ instar larval brain lysates from wild-type (wt) and *mbm*$^{SH1819}$. In the wild-type, a strong protein band, which often appears as a doublet of bands, was detected around 80 kDa, whereas in *mbm*$^{SH1819}$ this band was absent (Figure 17 B). This confirmed that *mbm*$^{SH1819}$ behaves as a null mutant.

### 3.2.1 Endogenous expression of Mbm

Immunohistochemical analyses of wild-type and *mbm*$^{SH1819}$ 3$^{rd}$ instar larval brains were performed to determine the exact localization pattern of Mbm protein. Stainings for Mbm and Lamine, a nuclear membrane protein, revealed that Mbm was strongly enriched in a subcompartment of the nucleus of neuroblasts. Mbm was completely absent in *mbm*$^{SH1819}$ neuroblasts (arrow in Figure 18 A) thus confirming the Western blot result.

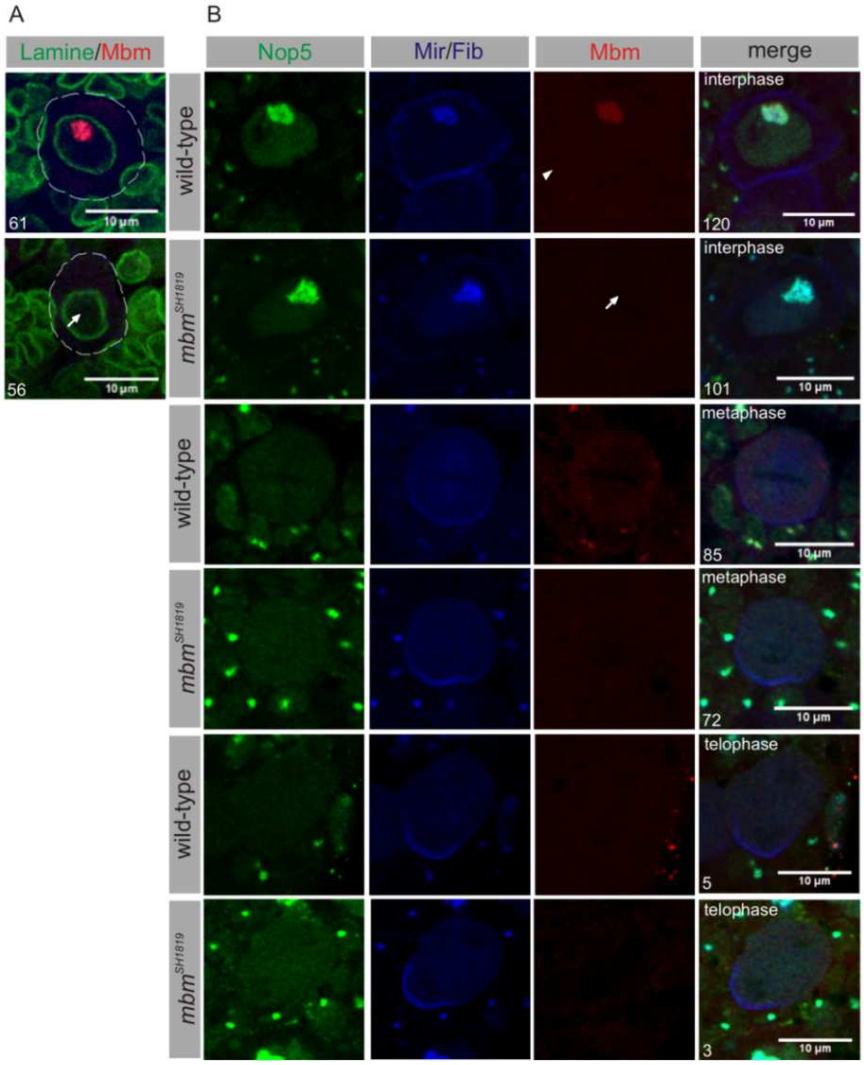


**Figure 18. Localization pattern of endogenous Mbm.**
A) Enrichment of Mbm within the nucleus of wild-type central brain neuroblasts. A single neuroblast is indicated by a dashed circle (Mbm (red) and Lamine (green) as a nuclear membrane marker). B) Mbm (red) and two nucleolar markers, Nop5 (green) and Fibrillarin (blue), colocalize in wild-type interphase neuroblast nucleoli. Weak homogenous signals are observed when neuroblasts enter mitosis. The localization patterns of Nop5 and Fibrillarin are not altered in *mbm*$^{SH1819}$. Representative wild-type metaphase and telophase neuroblasts in comparison with *mbm*$^{SH1819}$ neuroblasts are shown. Differential cortical localization of Miranda (blue) was used to distinguish cell cycle phases. The arrow indicates absence of Mbm in *mbm*$^{SH1819}$, whereas the arrowhead points to Mbm in a surrounding GMC. At least 10 brains were analyzed for each genotype. Numbers in confocal images indicate the number of analyzed neuroblasts in this and the following figures. Apical is upwards in mitotic neuroblasts.

To determine the subnuclear localization of Mbm, co-staining with the nucleolar markers Fibrillarin and Nop5 were done. The colocalization of all three proteins in wild-type interphase neuroblasts confirmed that Mbm is a new nucleolar protein (Figure 18 B). Because *Drosophila* nucleoli do not have the tripartite organization (fibrillar centre, dense fibrillar component, granular component) but instead intermingled fibrillar and granular components, the subnucleolar localization of Mbm could not be determined. However, the perfect colocalization with Nop5 and Fibrillarin suggests that Mbm is localized in the fibrillar component. Although Mbm is predominantly expressed in neuroblasts, ganglion mother cells, neurons and glia cells also showed a weak nucleolar Mbm signal (arrowhead in Figure 18 B). In addition, following Fibrillarin and Nop5 throughout the cell cycle revealed no difference between wild-type and $mbm^{SH1819}$ neuroblasts (Figure 18 B). Particularly, all three proteins have nucleolar accumulation in interphase neuroblasts. When cells enter mitosis, nucleolar proteins are released, while the nucleolus becomes disassembled. Accordingly, weak homogenous signals for Mbm, Nop5 and Fibrillarin were observed in wild-type meta- and telophase neuroblasts. The distribution of Nop5 and Fibrillarin was not altered in $mbm^{SH1819}$ (Figure 18 B).

## 3.3 Localization of other nucleolar proteins does not depend on Mbm

Further investigations were done to explore whether Mbm has an influence on other nucleolar components. One of the proteins of interest was Nucleostemin1 (NS1), which is indicated in the *Drosophila* protein interaction map (DPIM) as a direct or indirect interaction partner of Mbm. In this appraoch, protein-complexes were co-purified with FLAG-HA epitope-tagged proteins and further analyzed by mass spectrometry (Guruharsha et *al.* 2011). To evaluate a potential influence of Mbm on NS1, a *UAS-GFP::NS1* transgene was used (Rosby et *al.* 2009). Expression of *UAS-GFP::NS1* in either a wild-type or a $mbm^{SH1819}$ background was driven by the neuroblast specific driver line *Mz1060-Gal4*. Neuroblasts were stained for GFP, Mbm and Miranda as a neuroblast specific marker (Figure 19 A). Stainings revealed that NS1 expression levels or localization are not different between wild-type and $mbm^{SH1819}$ (Figure 19 A).

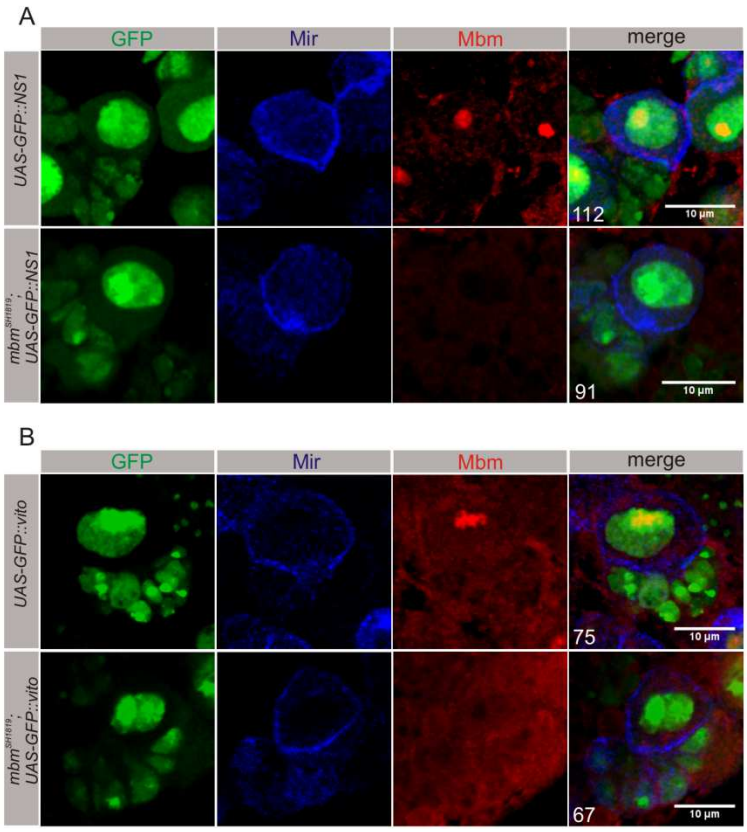


**Figure 19. Loss of Mbm does not affect behavior of other nucleolar proteins.**
A-B) Mbm (red) and two GFP-tagged nucleolar proteins (green), NS1 (A) and Vito (B), are localized in the nucleoli of wild-type neuroblasts. NS1 and Vito localization are not affected in *mbm*$^{SH1819}$ neuroblasts. Miranda (blue) was used as a marker for neuroblasts.

Moreover, relaying on the fact that the *Drosophila* Nol12 homologue Viriato (Vito) is a key determinant of nucleolar architecture (Marinho et *al.* 2011), immunostainings were done using a *UAS-GFP::vito* transgenic fly line (Marinho et *al.* 2011) expressed with *Mz1060-Gal4*. Loss of Mbm has no impact on localization of Vito and does not impair nucleolar integrity (Figure 19 B).

All experiments provided no evidence for localization defects of different nucleolar components in *mbm*$^{SH1819}$, which is in line with the assumption that Mbm does not have a function as a structural component of the nucleolus.

## 3.4 Mbm does not affect cell polarity, spindle orientation and asymmetry of cell division

During dissection it is clearly visible that *mbm*$^{SH1819}$ larvae have smaller brains compared to brains of wild-type animals of the same age, which could be due to a general proliferation defect of central brain neuroblasts. Direct evidence for a possible function of Mbm in cell proliferation was provided by 5-ethynyl-2´-deoxyuridine (EdU) pulse-labeling experiments. Dissected 3$^{rd}$ instar larval brains from wild-type and *mbm*$^{SH1819}$ were incubated for 2 hours in 20 µM EdU solution and then analyzed for incorporation of EdU into newly synthesized DNA (Figure 20).

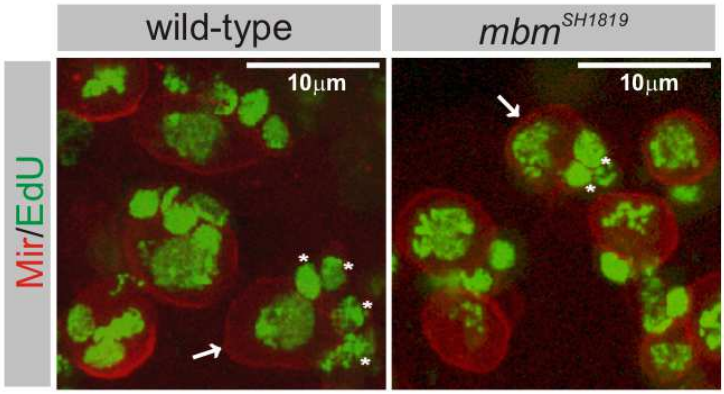


**Figure 20. Altered cell proliferation in *mbm*$^{SH1819}$.**
EdU incorporation (green) after 2h pulse labeling. 3-4 versus 1-2 EdU-positive GMCs or neurons (asterisks) are associated with single EdU-positive wild-type and *mbm*$^{SH1819}$ neuroblasts (arrows), respectively. Neuroblasts were stained for Miranda (red).

In the wild-type, up to four progeny cells (GMCs or neurons) were derived from a single neuroblast, whereas in case of *mbm*$^{SH1819}$ neuroblasts less cells were produced in the same time interval.

Although this experiment provided strong evidence that a proliferation defect is the major cause of the *mbm* small brain phenotype, it does not exclude the possibility of an additional requirement of Mbm in neuronal differentiation or survival (Raabe et al., 2004).

### 3.4.1 Mbm has no impact on asymmetric cell divition

The requirement of Mbm for neuroblast proliferation raised the question, whether Mbm is involved in the control of asymmetric cell division. It is well established that this process is mainly controlled by cell-intrinsic processes. Particularly, the apico-basal polarity axis is established by localization of the Par protein complex (Bazooka, Par6 and aPKC) to the apical cortex of the cell, which in turn controls cell fate determinant enrichment (Mir-Brat-Pros and Numb-Pon complexes) at the basal cortex. During cell division, the Par complex binds via Insc to Pins, which in turn associates with Mud/Dlg/ Gαi to control spindle orientation and asymmetry (see Figure 8 in introduction). Disturbances of these processes can lead to under- or overproliferation phenotypes (Sousa-Nunes & Somers 2013).

Immunohistochemical analyses for aPKC, Pins, Numb and Mir as representative members of each complex together with phospho-histone H3 (pH3) as a mitotic marker revealed no difference in the localization patterns of these proteins between wild-type and *mbm*$^{SH1819}$ metaphase neuroblasts (Figure 21). Furthermore, orientation of the mitotic spindle along the polarity axis was also not altered, as determined by centrosomal γ-Tubulin staining (Figure 21).

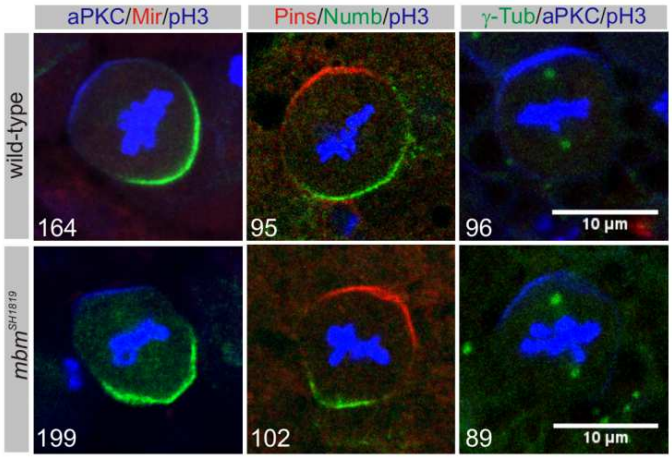


**Figure 21. Mbm does not affect neuroblast polarity and spindle orientation.**
Localization of apical proteins (aPKC and Pins) and basal cell fate determinants (Mir and Numb) are unaltered in *mbm*$^{SH1819}$ metaphase neuroblasts. Also orientation of the mitotic spindle is not disturbed in *mbm*$^{SH1819}$ neuroblasts as indicated by centrosomal γ-Tubulin relative to apical aPKC. Phospho-histone H3 (pH3) was used to mark chromatin during mitosis. 10 brains per staining and genotype were analyzed.

In addition, wild-type and *mbm*$^{SH1819}$ neuroblasts were analyzed throughout the complete cell cycle in order to look for possible alteration in asymmetry at different cell cycle stages (Figure 22).

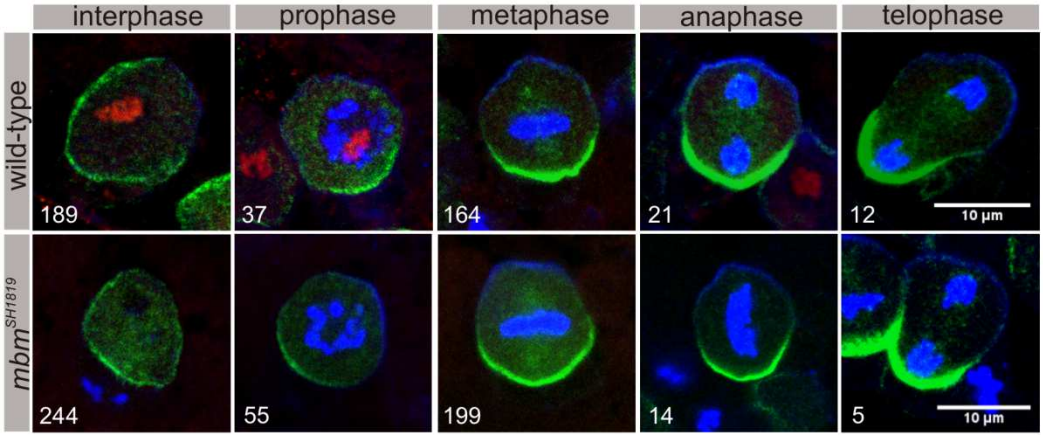


**Figure 22. Analysis of *mbm* neuroblasts during cell division.**
Neuroblasts at different cell cycle stages were stained for Mbm (red), Miranda (green), aPKC and phospho-histone H3 (both in blue). Miranda shows cortical localization in interphase neuroblasts, accumulates at the basal cortex in metaphase and becomes segregated into the future GMC in telophase. In $mbm^{SH1819}$, no Mbm protein can be detected but asymmetry of cell division and segregation of basal Miranda is not disturbed. 25 brains were analyzed for each genotype.

These results clearly showed that Mbm is not affecting apical and basal protein localization; consequently it is not required for establishment of cell polarity and also not for spindle orientation as central elements of asymmetric cell division. Moreover, asymmetry of cell division is not affected.

## 3.5 Mbm is required for cell size control

The involvement of the nucleolus in cell growth control allowed me to assume that Mbm as a new nucleolar protein might play a role in cell growth control. To investigate the addressed question, neuroblast size measurements were done. At first, only mitotic neuroblasts were analyzed because of their more globular shape and the distribution of apical and basal cell fate determinants, which allowed determining the apico-basal polarity axis of the cell. Neuroblasts were stained for the apico-basal markers aPKC and Miranda to measure the length of the apical-basal and the corresponding orthogonal axis to calculate cell area (Figure 23 A).

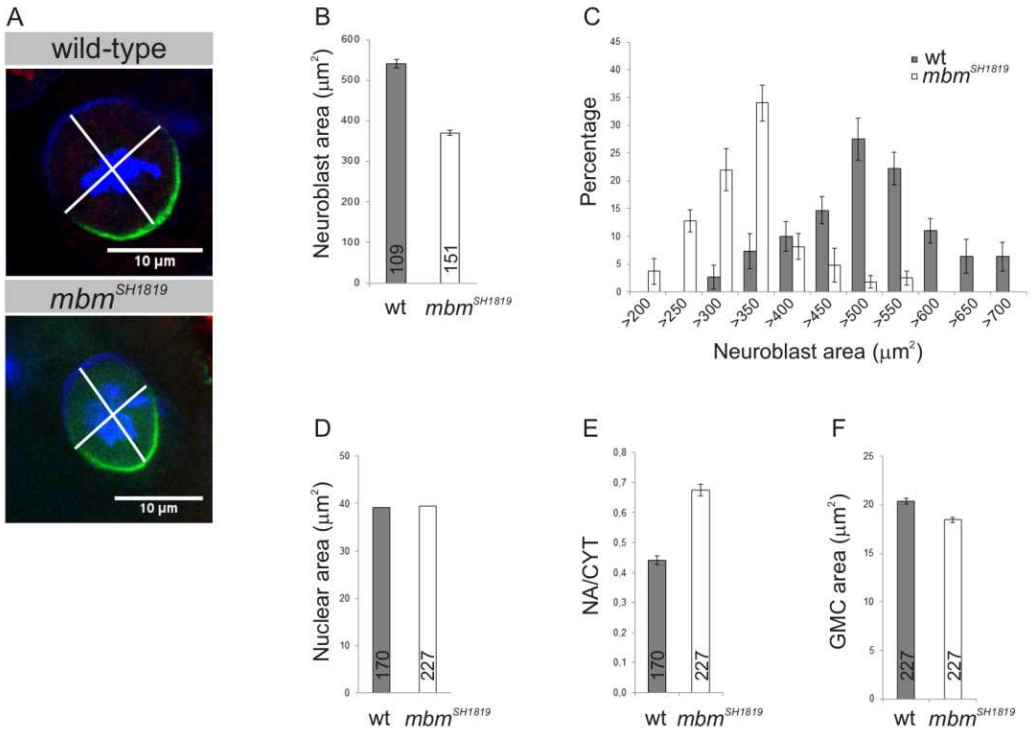


**Figure 23. Mbm affects neuroblast size.**
A) The apico-basal cortex is distinguished by aPKC (blue) and Miranda (green), respectively and phospho-histone H3 (pH3, blue) to reveal the mitotic stage. Apico-basal and orthogonal axes are indicated. B) The average cell size differs significantly between wild-type and *mbm*$^{SH1819}$ ($p<0.001$). C) Distribution of central brain neuroblast sizes in wild-type and *mbm*$^{SH1819}$ (wt: 109, *mbm*$^{SH1819}$:151 neuroblasts). (D, E) To determine nuclear areas and the nuclear to cytoplasmic ratio, interphase neuroblasts were analyzed. Nuclear area (NA) is identical between wild-type and *mbm*$^{SH1819}$ (D) but cell area (CA) and correspondingly the nuclear to cytoplasmic (CYT=CA-NA) ratio (E) differ significantly ($p<0.001$). (F) Also GMC size is slightly but significantly decreased in *mbm*$^{SH1819}$ ($p<0.001$).

The analysis revealed that the average neuroblast size in *mbm*$^{SH1819}$ is significantly smaller compared to wild-type (Figure 23 B). Because wild-type neuroblasts are not equal in size, the size distribution of wild-type and *mbm*$^{SH1819}$ neuroblasts was compared. There is a considerable shift towards smaller neuroblasts in *mbm*$^{SH1819}$ (Figure 23 C). Besides the effect on neuroblast size, a significant decrease of GMC size was also observed in *mbm*$^{SH1819}$ (Figure 23 F), which is in line with the previous finding that asymmetry of cell division is not affected (Figure 22Figure 22). In order to distinguish whether the smaller cell size in *mbm*$^{SH1819}$ is caused by a reduction of cytoplasmic and/or nuclear size, the relative cytoplasmic to nuclear areas of interphase neuroblasts were calculated. The results clearly indicated that there is no impact on nuclear size in *mbm*$^{SH1819}$, in contrast to the significant reduction of cytoplasmic area (Figure 23 D, E).

### 3.5.1 Effect of Mbm on cell size outside the neuroblast compartment

The finding, that *mbm* affects neuroblast size raised the question, whether Mbm has also an influence on cell size control in other tissues. For that purpose wing imaginal discs from wild-type and $mbm^{SH1819}$ were stained for Armadillo to mark cell membranes and Mbm. It is important to mention that Mbm is not expressed in the nucleolus of wing imaginal disc cells; instead it showed homogenous distribution in the entire cell. For cell size measurement, cells in the pouch region of wing imaginal discs were measured. The results indicated that there is no significant difference in cell size between wild-type and $mbm^{SH1819}$ (Figure 24).

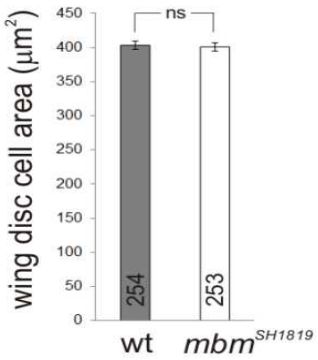


**Figure 24. Wing imaginal disc cell size measurement.**
Wing imaginal disc cell sizes do not differ significantly between wild-type and $mbm^{SH1819}$.

### 3.5.2 Mbm does not affect tissue culture S2 cells proliferation

*Drosophila* tissue culture S2 cells are a more accessible system than neuroblasts to perform cellular and biochemical assays, which require homogeneous cell populations. Indeed, Mbm is expressed in S2 cells. Stainings were done with anti-Mbm and phospho-histone H3 antibodies to reveal the expression of Mbm in interphase and mitotic cells (Figure 25).

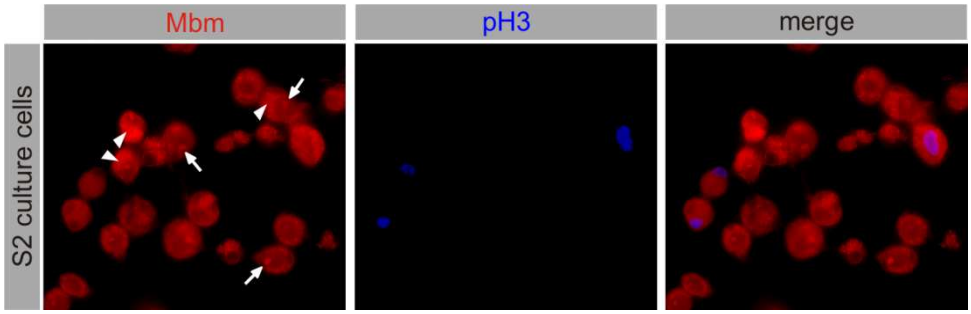


**Figure 25. Expression of Mbm in tissue culture S2 cells.**
Nucleolar and cytoplasmic localization of Mbm (red) are indicated by the arrows and arrowheads, respectively. Phospho-histone H3 antibody was used to mark mitotic cells.

In contrast to neuroblasts, expression of Mbm in interphase S2 culture cells is not restricted to the nucleolus (arrows in Figure 25), but is also clearly evident in the cytoplasm (arrowheads in Figure 25), whereas mitotic cells showed more homogenous cytoplasmic localization.

Because lack of Mbm impairs neuroblast proliferation, Mbm might also be required for S2 cell proliferation. To address this question, the proliferation rate of S2 cells was measured upon knock-down (kd) of Mbm by RNAi. Before starting the main experiments, efficiency of Mbm-kd was verified by incubation of S2 cells with different amounts of Mbm dsRNA synthesized *in vitro* for different time periods. Highest Mbm-kd was observed when cells were transfected with 2 µg of dsRNA and incubated for 3 days (data not shown). After this optimization step, S2 cells were transfected with dsRNAs targeting Mbm and cell proliferation rate was measured after 3 and 7 days of transfection by FACS analysis (Fluorescence-activated cell sorting). Efficiency of Mbm-kd at day 3 was checked by Western blot (Figure 26 A). In contrast to loss of function of Mbm in neuroblasts (Figure 20), both control and Mbm-kd S2 cells showed similar proliferation rates at both time points measured (B).

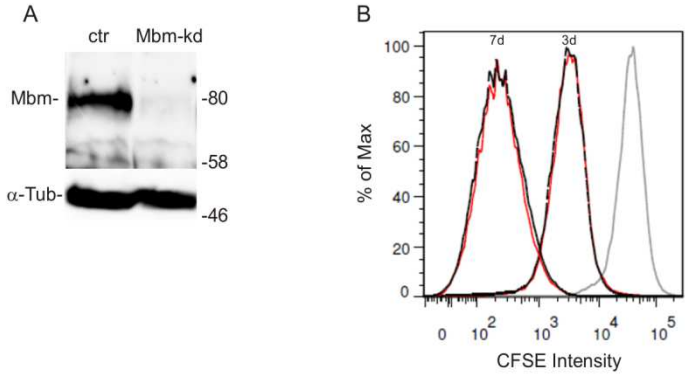


**Figure 26. Mbm has no effect on tissue culture S2 cell proliferation rate.**
A) Western blot of control (ctr) S2 cells and S2 cells that were transfected with dsRNA targeting Mbm. B) Proliferation of control (ctr: black-dashed graph) and Mbm knock-down (Mbm-kd: red graph) S2 cells grown for 3 and 7 days was measured by FACS analysis. There is no proliferation difference between ctr and Mbm-kd S2 cells after 3 or 7 days. The gray graph represents measurement of the Carboxyfluoresceinsuccinimidyl ester (CFSE) staining at day 0. This experiment was done in collaboration with Tanja Bedke and Benjamin Mentzel.

Moreover, using the same Mbm dsRNA, no impact on S2 cell size was observed (data from Eva Herter and Peter Gallant).

Overall, the results obtained from wing imaginal disc and S2 culture cell experiments indicated that Mbm has a more specific function in neuroblasts to maintain proper cell size and proliferation, despite its expression also in other cell types.

## 3.6 Role of Mbm in ribosome biogenesis

### 3.6.1 Loss of Mbm impairs nucleolar release of the small ribosomal subunit

Cell growth or increase in cell mass requires enormous number of ribosomes, prerequisites for protein synthesis. Thus, ribosome biogenesis emphasizes the growth capacity of cells. The nucleolar localization of Mbm and the cell size defect observed in *mbm*$^{SH1819}$ neuroblasts without affecting structural integrity of the nucleolus lead to the assumption that Mbm might be involved in ribosome biogenesis. The generation and assembly of large and small ribosomal subunits take place independently in the nucleolus, followed by their transport through the nucleoplasm to the cytoplasm where finally the mature and functional ribosome is (Tschochner and Hurt, 2003; Zemp and Kutay, 2007). Failure in the ribosome biogenesis machinery may result in retention of the impaired subunits in the nucleolus or nucleus. It was already shown by Rosby and coworkers (2009) that knock-down of *Drosophila* NS1 in salivary gland cells specifically blocks transport of large ribosomal subunit. This experiment was done by using a GFP-tagged variant of the RpL11 protein (GFP::RpL11), which is a ribosomal protein associated with large ribosomal subunit. Similar, transport of small ribosomal subunit was followed by a RFP-labeled RpS6 protein (mRFP::RpS6) as a component of the small ribosomal subunit, which was not affected by knock-down of NS1. The corresponding transgenic lines *UAS-GFP::RpL11* (on 2$^{nd}$ chromosome) and *UAS-mRFP::RpS6* (on 3$^{rd}$ chromosome) were obtained from Patrick diMario and combined with *mbm*$^{SH1819}$. In the case of the 2$^{nd}$ chromosomal *UAS-GFP::RpL11* line, it was necessary to recombine it onto the *mbm*$^{SH1819}$ chromosome. Neuroblast-specific expression of both reporters in either a wild-type or *mbm*$^{SH1819}$ background was achieved with the *Mz1060-Gal4* driver line. Analyses of larval brains revealed that GFP::RpL11 accumulated in the cytoplasm of all wild-type (n=122) and *mbm*$^{SH1819}$ (n=126) neuroblasts (Figure 28 A, B) indicating that Mbm has no effect on transport or assembly of large ribosomal subunits. Cytoplasmic localization of mRFP::RpS6 was also observed in most wild-type neuroblasts (Figure 28 C, 86% of neuroblasts showed predominantly cytoplasmic, 14% cytoplasmic and nucleolar localization, n=158). In contrast, mRFP::RpS6 localization in *mbm*$^{SH1819}$ neuroblasts was severely altered (Figure 28 D). mRFP::RpS6 was predominantly retained in the nucleolus (82%, n=123), although in some neuroblasts also homogenous cytoplasmic and nucleolar distribution was observed (18%, n=123 neuroblasts).

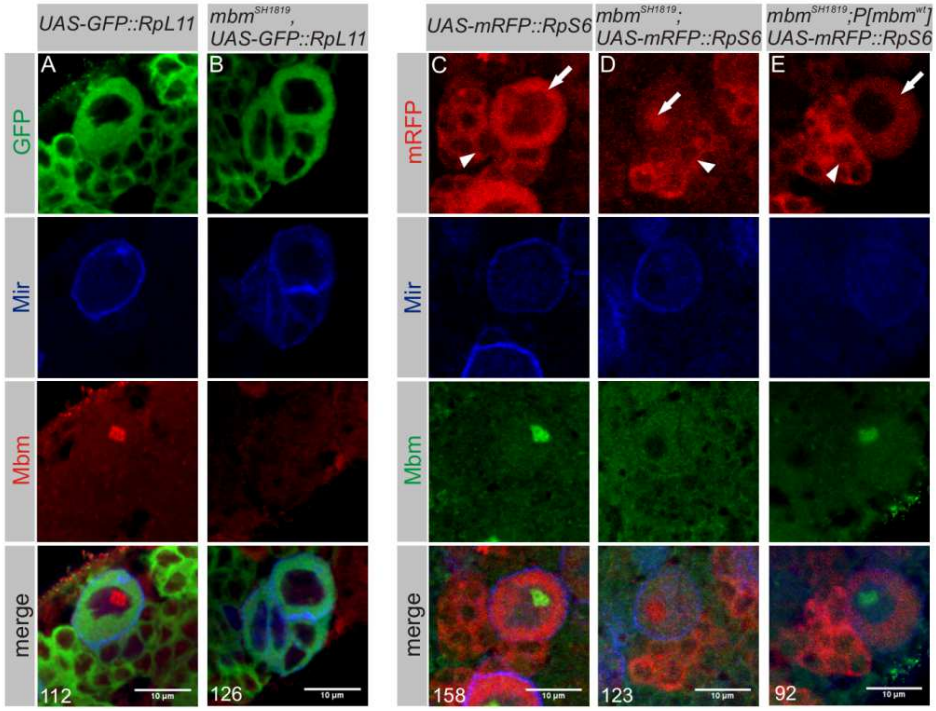


**Figure 27. Loss of Mbm affects small ribosomal subunit biogenesis.**
A, B) Expression of *UAS-GFP::RpL11* in neuroblasts with *Mz1060-Gal4* in an otherwise wild-type (A) or *mbm*$^{SH1819}$ (B) background. 3$^{rd}$ instar larval brains were stained for Mbm (red) and Miranda (blue), which was used as a neuroblast marker. Both genotypes show cytoplasmic accumulation of GFP::RpL11(green). C-E) Loss of Mbm affects cytoplasmic localization of mRFP::RpS6. Visualization of Mbm (green), Miranda (blue) and mRFP::RpS6 (red) expressed with *Mz1060-Gal4*. Wild-type neuroblasts show apparent cytoplasmic accumulation of mRFP::RpS6 (C), whereas *mbm*$^{SH1819}$ neuroblasts (D) retain mRFP::RpS6 in the nucleolus (arrows in C, D). Note that cytoplasmic localization is not affected in associated GMCs and neurons (arrowheads). (E) In *mbm*$^{SH1819}$*; P[mbm*$^{wt}$*]* neuroblasts, cytoplasmic localization of mRFP::RpS6 is restored (arrow). For each genotype, at least 12 brains were analyzed.

The mRFP::RpS6 localization defect could be completely reverted by introducing the genomic rescue construct *P[mbm*$^{wt}$*]* in a *mbm*$^{SH1819}$ background (Figure 28 E, 85% predominantly cytoplasmic, 15% cytoplasmic and nucleolar, n=92 neuroblasts). These observations indicate that Mbm is either required for maturation of the small ribosomal subunit or its release from the nucleolus to the nucleoplasm. The inheritance of mRFP::RpS6 and GFP::RpL11 expressed in neuroblasts into GMCs and neurons upon cell division also allowed monitoring their localization in these cells. Strikingly, cytoplasmic localization of mRFP::RpS6 in *mbm*$^{SH1819}$ GMCs or neurons was not affected (Figure 28 D, arrowhead) indicating a more specific requirement of Mbm for ribosome biogenesis in neuroblasts.

### 3.6.2 Loss of Mbm affects protein synthesis in neuroblasts

Failure to assemble the required number of functional ribosomes in the cytoplasm of neuroblasts could impair protein synthesis. To address this question, metabolic labeling experiments were done. Newly synthesized proteins in neuroblasts were labeled within a 1 h interval by incorporation of the methionine analog L-homopropargylglycine (HPG). Labeled proteins were detected in the cytoplasm and the nucleus of wild-type interphase neuroblasts. Strikingly, enhanced nuclear signal was evident in most neuroblasts (81% had enhanced nuclear signal, 19% showed equal cytoplasmic and nuclear staining, n=92 neuroblasts) (Figure 28 A). Once neuroblasts entered mitosis, the newly synthesized proteins equally distributed (Figure 28 A). In contrast, in *mbm*$^{SH1819}$ neuroblasts signal intensities appeared generally reduced, although in most cases they were still slightly higher than in the surrounding tissue. In addition, compared to wild-type neuroblasts, enhanced nuclear signal was observed only in 10% of the analyzed neuroblasts (n= 148) (Figure 28 B).

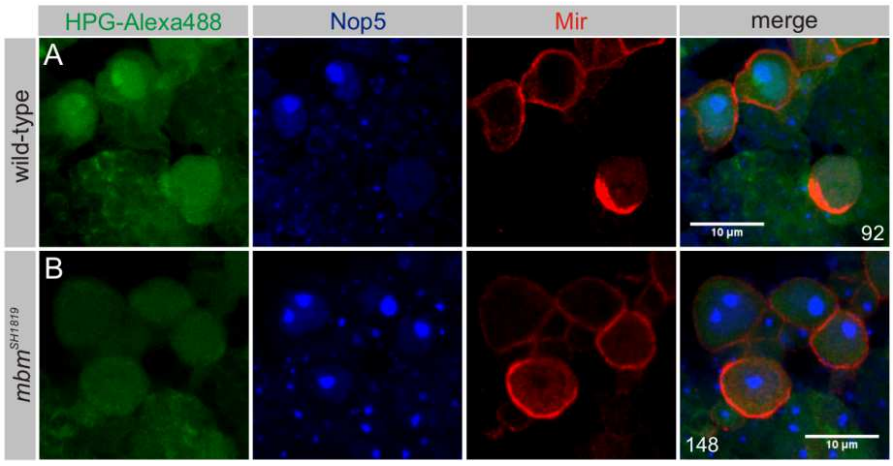


**Figure 28. Loss of Mbm reduced protein synthesis.**
A,B) Protein translation, as determined by metabolic labeling and detection of HPG-Alexa488 (green) is reduced in *mbm*$^{SH1819}$ neuroblasts, which were marked by Miranda (red) and Nop5 (blue). The stronger nuclear HPG-Alexa488 signal in wild-type neuroblasts (A) is no longer visible in *mbm*$^{SH1819}$ (B). The single metaphase neuroblast in (A) shows homogenous HPG-Alexa488 distribution. For each genotype, at least 20 brains were analyzed.

Even though it was not possible to compare absolute intensity levels between different preparations, the main loss of enhanced nuclear signal in *mbm*$^{SH1819}$ neuroblasts is the first evidence that the capability of these cells to synthesize proteins is impaired, which could finally lead to the observed cell growth defects.

## 3.7 Mbm transcription is regulated by Myc

Myc is a transcription factor that targets a large number of genes required for different cellular processes, including proliferation, growth, metabolism and apoptosis (Dang 1999, Dang 2013). A recent comprehensive transcriptome analysis in *Drosophila* S2 cells after downregulation of Myc has identified 544 regulated genes including *mbm* (Hulf et *al.* 2005), which provides a potential link between growth input signals and the growth regulatory function of Mbm in neuroblasts. One intriguing finding was that these genes also fall into functional classes with many of them playing a role in nucleolar function and ribosome biogenesis. Myc regulates multiple stages of ribosome biogenesis starting from regulation of rRNA transcription by RNA polymerase I and III and by RNA polymerase II driven expression of ribosomal components and modifying enzymes (Riggelen et *al.* 2010, Schlosser et *al.* 2003). In addition it plays role in the export of mature ribosomal subunits from the nucleus into the cytoplasm by direct regulation of Nucleophosmin (B23) expression, which associates with both ribosomal subunits and directs the nuclear export of them (Maggi et *al.* 2008, Zeller et *al.* 2001). Similar functions were established for *Drosophila* Myc (the corresponding gene is named *diminutive (dm)*) (Gallant 2013). The promoter regions of Myc target genes are characterized by the presence of E-box sequences (CACGTG and variations thereof), the known Myc binding site, which is commonly located within the first 100 nucleotides downstream the transcription start site. Frequently, the E-box motif is embedded in the extended consensus sequence AACACGTGCG (Hulf et al 2005, Furrer et al 2010). The transcriptional start site of *mbm* is predicted around position -82 relative to the translational start codon. Two E-box sequences are found upstream of the translational start codon. One canonical E-box is placed within the 5´-untranslated sequence from position -42 to -47 of *mbm* (E-box1) conforming also the extended E-box consensus sequence. A second, non-canonical E-box (E-box2) is positioned at -511 to -516 (CACATG) (Figure 29 A). Both E-boxes are present in the genomic construct *P[mbm$^{wt}$]*, which is able to rescue all known *mbm* phenotypes indicating the presence of all essential regulatory elements for *mbm* expression (Figure 17A and (Raabe et *al.* 2004)).

Chromatin immunopercipitation (ChIP) analyses verified direct binding of Myc to the *mbm* E-box1 element, which suggests that *mbm* expression might be directly controlled by Myc via E-box1 (Eva Herter and Peter Gallant).

In order to evaluate whether the identified E-boxes are functional and are required for *mbm* transcription, genomic fragments encompassing one or both E-box sequences or mutated variants were fused to the luciferase gene in order to perform gene reporter assays (collaboration with Eva Herter and Peter Gallant). E-box1-mbm consists of a 500bp genomic fragment upstream of the translational start of Mbm and includes only E-box1, in ΔE-box1-mbm, the E-box1 sequence was mutated to GAATTC and in rev-E-box1-mbm, the 500bp fragment was cloned in opposite orientation to control for directionality of E-box-mediated transcription. E-box1+2-mbm contains a 1260bp fragment and includes both E-box sequences (Figure 29 A). All constructs were fused to the firefly luciferase coding region such that the translation start of the luciferase corresponds to the ATG codon of Mbm.

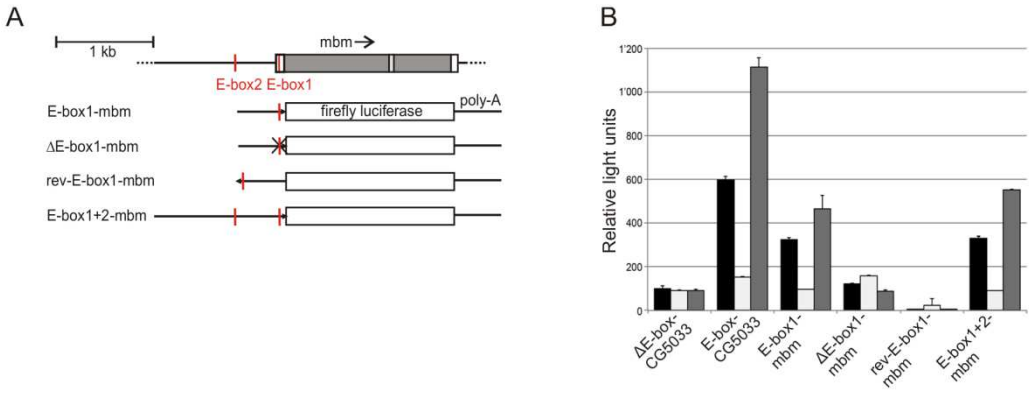


**Figure 29. Myc directly controls Mbm expression.**
A) *Mbm* gene locus with consensus E-box (E-box1) located in the 5´-untranslated sequence (white box) and the degenerate E-box (E-box2) further upstream. The dark grey boxes represent the *mbm* open reading frame. Below, the different *mbm*-promotor constructs fused to firefly luciferase are shown. B) Reporter constructs expressing firefly luciferase under the control of the indicated promoter regions were transfected into S2 cells together with a plasmid driving constitutive expression of Renilla luciferase. Shown are relative luciferase activities under control conditions (black bars), upon depletion of Myc by dsRNA (light grey bars), and Myc-overexpression conditions (dark grey bars). E-box-CG5033 and ΔE-box-CG5033 served as positive and negative controls, respectively (Hulf et *al.* 2005). A representative experiment is shown. Error bars indicate standard deviations from duplicate transfections.

As positive and negative controls, constructs with the E-box containing promotor sequences of the verified Myc target gene CG5033 (E-box-CG5033) and the corresponding E-box mutated version (ΔE-box-CG5033) fused to firefly luciferase were used (Hulf et *al.* 2005). S2 cells were transiently co-transfected with each reporter construct in combination with a plasmid constitutively expressing the *Renilla* luciferase and then analyzed under control, Myc knock-down, or Myc overexpression conditions (knock-down of Myc was done by dsRNA and overexpression of UAS-HA::Myc was driven by tub-Gal4 driver

plasmid). Relative luciferase activities were measured after 48 h of transfection and revealed that the E-box1-mbm construct was responding to up- and down-regulation of Myc (Figure 29 B), whereas in case of ΔE-box1-mbm and rev-E-box1-mbm responsiveness was abolished (Figure 29 B). Moreover, there was not apparent difference in Myc responsiveness between reporter constructs carrying only one or both E-box sequences suggesting that E-box1 in the *mbm*-promotor region is the major mediator for Myc-induced transcription.

In addition, Myc-dependent expression of Mbm was also checked *in vivo*. Because the null mutation in the X-chromosomal *Myc* gene ($dm^4$) is lethal in homo- or hemizygous state, a clonal system was used to look at Mbm expression in neuroblasts devoid of Myc function. For this purpose, a fly line additionally expressing a *tubulin (tub)* promotor driven *Myc* transgene flanked by FRT sites ($dm^4$, *tub<FRT>Myc<FRT>Gal4, hs-FLP; UAS-GFP*) was used in order to restore viability. Clonal removal of the *FRT-Myc-FRT* cassette by heat shock induced Flipase (Flp) expression results in cells devoid of Myc and expressing GFP under *tub-Gal4* control instead. Larval neuroblasts were analyzed using Mbm, GFP, aPKC and Nop5 antibodies. GFP expression marks the Myc-deficient neuroblast lineage and aPKC and Nop5 were used as markers for neuroblasts and nucleoli, respectively (Figure 30).

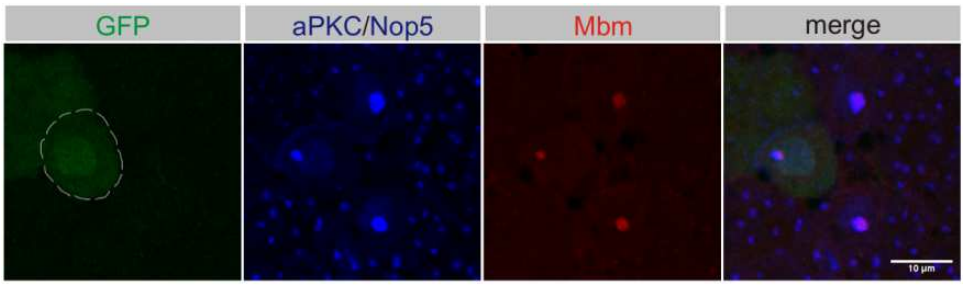


**Figure 30. Myc controls Mbm expression in neuroblasts.**
A single *Myc* ($dm^4$)-mutant neuroblast (encircled) and its associated cell lineage express GFP (green). In comparison with surrounding neuroblasts, expression of Nop5 (blue) and Mbm (red) are reduced. aPKC (blue) was used as a neuroblast marker. 293 wild-type and 81 *Myc*-mutant neuroblasts out of 15 brains were analyzed.

It is important to mention that Nop5 expression is also regulated by Myc, as many genes encoding nucleolar proteins (Hulf et *al.* 2005). As shown in Figure 30, Mbm and Nop5 expression are significantly down-regulated in GFP-positive neuroblasts in contrast to neighboring neuroblasts, which still express the *Myc* transgene. These results strongly suggest that *in vivo* expression of Mbm is controlled by Myc.

## 3.8 Function of Mbm is regulated by protein kinase CK2

### 3.8.1 CK2α is a nucleolar protein

One important aspect in regulation of protein function in a signal-dependent manner is phosphorylation or dephosphorylation processes. Excitingly, in the recently established comprehensive *Drosophila* protein interaction map (DPIM), the α-subunit of protein kinase CK2 was also indicated as an interaction partner of Mbm (Guruharsha et *al.* 2011). Furthermore, two phosphoproteomic studies in S2 cells and in *Drosophila* embryos identified Mbm as a phosphorylated protein suggesting that Mbm phosphorylation is mediated by CK2 (Bodenmiller et al. 2008, Zhai et al. 2007). CK2 kinase is a heterotetrameric holoenzyme composed of two catalytic α-subunits, which bind to a dimer of regulatory β-subunits. CK2 is ubiquitously expressed in a variety of cell types and tissues and considered to be constitutively active. Nevertheless, there are several mechanisms by which CK2 activity can be regulated, including localization, stability, phosphorylation and interaction of variety of proteins in different cellular compartments (Olsten and Litchfield 2004, Litchfield 2003, St-Denis & Litchfield 2009). In addition, it was previously shown that both subunits of CK2 can act separately (Bibby& Litchfield 2005).

In order to distinguish a functional regulation of Mbm by CK2, immunohistochemical analyses of 3$^{rd}$ instar larval interphase neuroblasts of wild-type and *mbm*$^{SH1819}$ were done. Neuroblasts were stained for CK2α and Mbm whereas Miranda and Fibrillarin were used as markers for neuroblas and nucleoli, respectively. Mbm and CK2α are co-localized in the nucleoli of wild-type neuroblasts (Figure 31 A). Interestingly, in *mbm*$^{SH1819}$ neuroblasts, nucleolar CK2α could still be detected, but expression levels were consistently weaker than in wild-type neuroblasts (Figure 31 B).

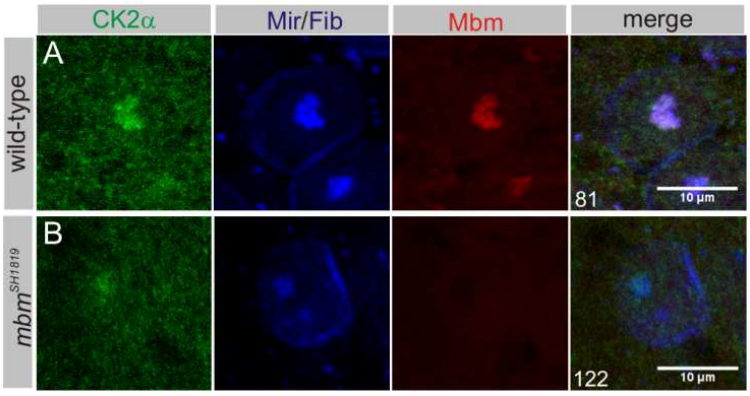

**Figure 31. Expression of CK2α in neuroblast.**
Interphase neuroblasts from wild-type and *mbm*$^{SH1819}$ were stained for CK2α (green), Fibrillarin (blue) and Mbm (red) as nucleolar markers and Miranda (blue) as a neuroblast marker. In comparison to wild-type (A), nucleolar expression of CK2α is greatly reduced in *mbm*$^{SH1819}$ (B).

### 3.8.2 Mbm is phosphorylated by CK2α

Relying on the co-purification and nucleolar co-localization results of Mbm and CK2α, possible phosphorylation of Mbm by CK2α was tested. CK2 kinase is an acidophilic kinase, which phosphorylates serine or threonine residues within a minimal consensus sequence S/T-X-X-acidic residue (+3 position). More recently it was found that an acidic residue at position +4 is also relevant for CK2-mediated phosphorylation (Zhai et al 2008). Mbm contains three clusters of acidic amino acids in its C-terminus each containing several serine and threonine residues which could be potential CK2 phosphorylation sites (amino acids 281-295, 327-338, 454-482, in the following referred to as acidic cluster AC-1, AC-2 and AC-3, respectively, Figure 32).

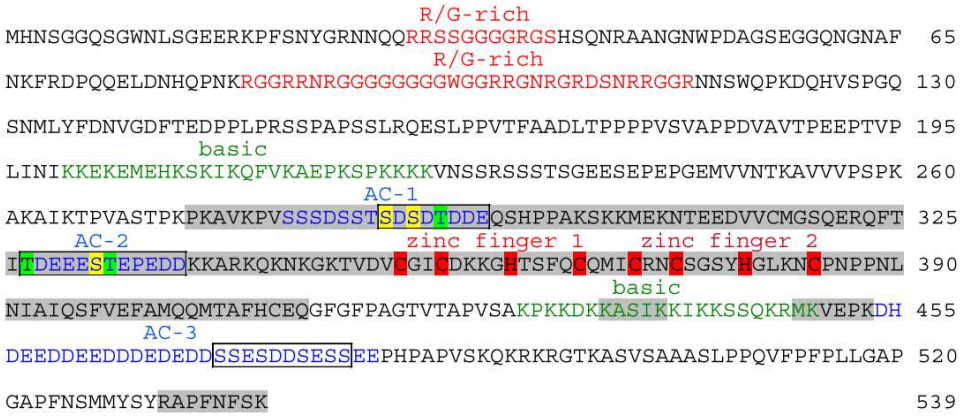


**Figure 32. Mbm protein sequence.**
Structural features include two zinc-finger motifs (CCHC, shaded in red), arginine/glycine rich regions (red), basic amino acid rich regions (green) and three acidic amino acid clusters named AC-1, AC-2 and AC-3 (blue). CK2 phosphorylation consensus sequences in the AC1-3 clusters are indicated by black boxes. Serine and threonine residues phosphorylated by CK2, which were identified by MS/MS analysis of GST::Mbm (amino acids 266-539) are highlighted in yellow and green, respectively. Mbm sequences covered by MS/MS analysis are highlighted in grey.

*In vitro* kinase assays were carried out with [γ-$^{32}$P] ATP together with bacterially expressed and purified GST::CK2α and two GST::Mbm fusion proteins as substrates (GST::Mbm1 amino acids 1-268 and GST::Mbm2 amino acids 266-539). Importantly, GST::Mbm2 includes all three acidic clusters. Both GST::Mbm proteins were

phosphorylated by CK2α, however, phosphorylation of GST::Mbm2 was much stronger compared to GST::Mbm1, which could be explained by the presence of all acidic clusters in GST::Mbm2 (Figure 33 A).

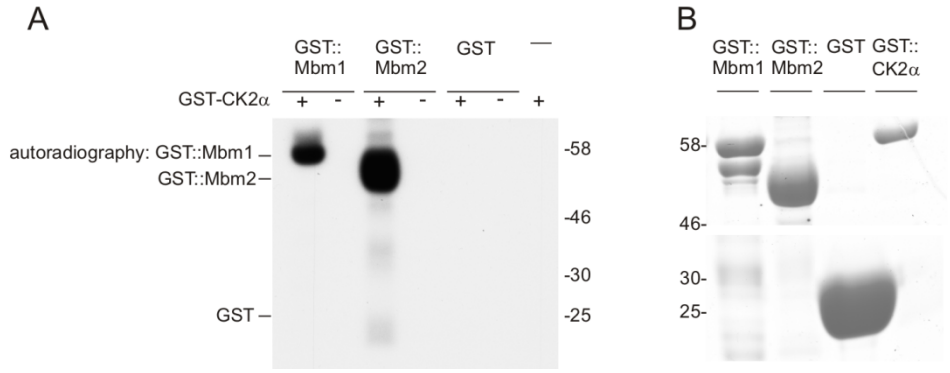


**Figure 33. Mbm becomes phosphorylated by CK2α.**
A) *In vitro* kinase assays of GST::Mbm1 and GST::Mbm2 in the presence (+) or absence (-) of GST::CK2α. Control reactions were performed with CK2α alone or in combination with GST. B) Coomassie staining of indicated Mbm, GST and GST::CK2α proteins in the reaction. Phosphorylation of Mbm proteins was detected by autoradiography. Molecular weight markers are indicated.

In order to define the exact phosphorylation sites of Mbm, *in vitro* kinase assays were repeated with non-radioactive labeled ATP and both fragments of GST::Mbm protein. Afterwards, the bands corresponding to the molecular weight of GST::Mbm1 and GST::Mbm2 fragments were cut out from the gel and sent for mass spectrometry analysis (Jens Pfannstiel, University of Hohenheim). Analyses identified five phosphorylated residues in GST::Mbm1; however none of them was surrounded by acidic amino acids, which is the prerequisite for phosphorylation by CK2. One explanation for this result could be unspecific phosphorylation due to excessive amounts of supplied CK2α and Mbm. In contrast, six identified phosphorylation sites in GST::Mbm2 are placed in acidic clusters; three in AC-1 (S288, S290, T292) and three in AC-2 (T327, S332, T333) (Figure 32). Moreover, the phosphorylation sites in AC-2 correspond to the results of the phosphoproteom analyses in S2 cells and embryos (Bodenmiller et al. 2008, Zhai et al. 2007). Thus, all further experiments were carried out only with GST::Mbm2 (in the following labeled as GST::Mbm). Based on the MS/MS data, Mbm becomes phosphorylated at multiple sites by CK2 at least *in vitro*, raising the question of their functional relevance. As a first step towards a functional characterization, all identified serine and threonine residues were substituted by alanine to abolish phosphorylation at these sites. Using the GST::Mbm (amino acids 266-539) expression vector as a template,

three constructs were assembled. In AC-1ΔP, S288, S290 and T292 were substituted by alanine. The same substitutions were done in AC-2 (T327A, S332A and T333A, labeled as AC-2ΔP) and in addition, a combination of both substitutions (AC-1+2ΔP) was introduced. Upon bacterial expression and purification of the corresponding GST fusion proteins, *in vitro* kinase assays were done. In neither case, CK2α -mediated phosphorylation was completely abolished, however, a strong reduction of phosphorylation was observed in case of GST::Mbm-AC-1ΔP and GST::Mbm-AC-1+2ΔP, whereas no or only a minor reduction was seen in case of GST::Mbm-AC-2ΔP (Figure 34).

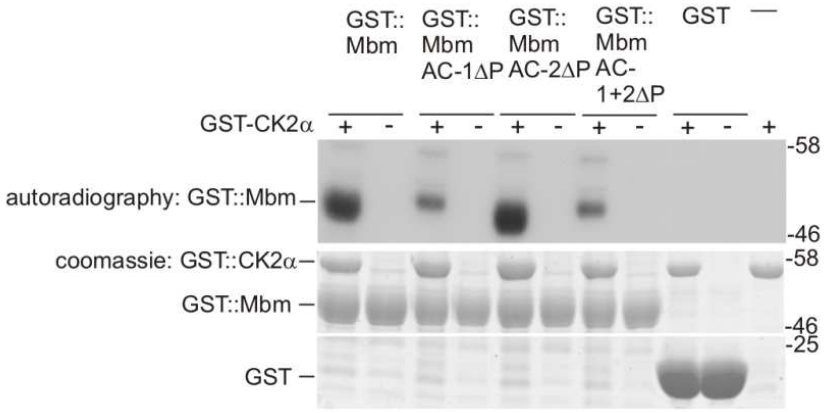


**Figure 34. CK2 phosphorylates Mbm.**
*In vitro* kinase assays of the indicated GST::Mbm fusion proteins in the presence (+) or absence (-) of GST::CK2α. Control reactions were performed with CK2α alone or in combination with GST. Coomassie staining proves the presence of equal amounts of indicated Mbm, GST and GST::CK2α proteins in each reaction. Phosphorylation of Mbm proteins was detected by autoradiography. Representative images of three independent experiments are shown. For uncropped images see Appendix 1.

This suggests that Mbm may contain additional CK2 phosphorylation sites in its C-terminus that escaped detection in the MS analysis. Indeed, the C-terminus contains a potential CK2 motif placed in the AC-3 cluster that was not covered by tryptic or chymotryptic peptides in the MS analysis. Although phosphorylation is not completely abolished neither in GST::Mbm-AC-1ΔP nor in GST::Mbm-AC-1+2ΔP, the results from the *in vitro* kinase assay allowed to conclude that S288, S290 and/or T292 are the primary CK2 phosphorylation sites.

### 3.8.3 *In vivo* regulation of Mbm by CK2α

The next step was to investigate whether CK2 affects Mbm *in vivo*. To test this, two experimental approaches were performed. On one hand, CK2α knock-down in neuroblasts was achieved by *worniu-Gal4* expression of two independently established *UAS-CK2α-RNAi* transgenes (gift from R. Jackson, Boston, USA, labeled as *CK2α-RNAi$_1$)*, Bloomington stock center #35136 (*CK2α-RNAi$_2$*). In the second approach, a dominant negative version of *CK2α* (*UAS-CK2α$^{Tik}$*) (Meissner et *al.* 2008) was expressed in neuroblasts. Neuroblasts were stained for CK2α and Mbm whereas Miranda and Fibrillarin were used as markers for neuroblast and nucleoli, respectively. Although CK2α expression was not completely abolished under knock-down conditions, its expression was strongly reduced compare to wild-type (Figure 35 B, C). Importantly, the reduction of CK2α leads to localization defects of Mbm. In addition to the nucleolar expression also cytoplasmic localization was observed (arrows in Figure 35 B, C).

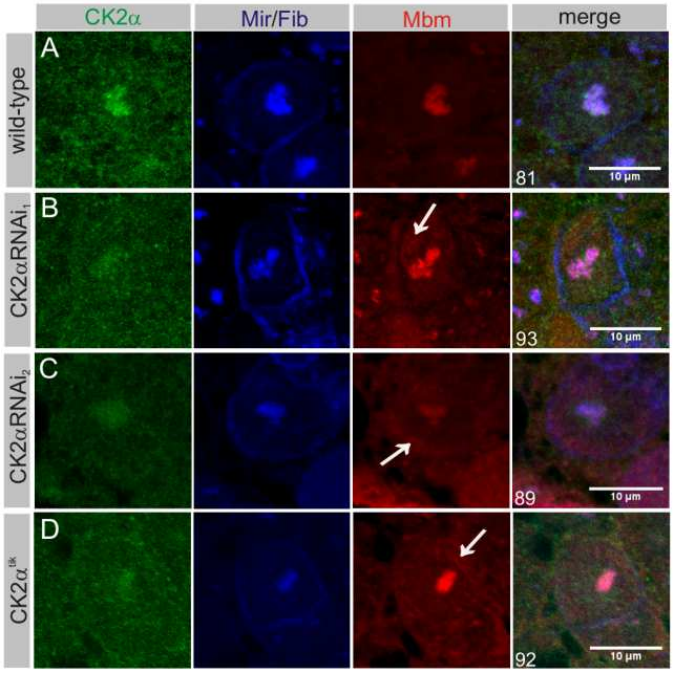


**Figure 35. CK2α affects Mbm localization.**
Interphase neuroblasts from wild-type and animals expressing one of two different *UAS-CK2α-RNAi* transgenes or a dominant negative version of *CK2α* (*UAS-CK2α$^{Tik}$*) with *wor-Gal4* in neuroblasts were stained for CK2α (green), Fibrillarin (blue) and Mbm (red) as nucleolar markers and Miranda (blue) as a neuroblast marker. In comparison to wild-type (A), nucleolar expression of CK2α is greatly reduced by under *CK2α* knock-down conditions (B, C) or by overexpression of *CK2α$^{Tik}$* (D). Under these conditions, Mbm shows partial localization in the cytoplasm (arrows), which is not seen in wild-type neuroblasts. $n_{wt}$: 8 brains, $n_{mbm}$: 12 brains, $n_{CK2α\text{-}RNAi}$: 10 brains.

Surprisingly, overexpression of the dominant negative CK2α$^{Tik}$ also resulted in reduced CK2α signal in the nucleolus. Yet, Mbm localization was changed similar to both *CK2α RNAi* lines with a clearly visible cytoplasmic signal (arrow in Figure 35 D).

In summary, these results suggested that Mbm phosphorylation by CK2α is required for localization or stability.

### 3.8.4 Effect of the CK2β regulatory subunit on Mbm

Since CK2α was found in a complex with Mbm, this raised the question whether the regulatory CK2β subunit also has a function in neuroblasts. Numerous works have indicated that CK2β subunit is essential for assembly of the tetrameric complex of CK2 and regulation of interactions between the catalytic subunit and certain substrates (Graham & Litchfield 2000, Canton et *al.* 2001, Niefind et *al.* 2009). Although CK2 predominantly shows nuclear localization, CK2β is also expressed at other subcellular sites where the catalytic subunit is not present (Krek et *al.* 1992, Filhol et *al.* 2003) indicating the possibility of CK2-independent functions of CK2β (Litchfield 2003, Bibby & Litchfield 2005). Moreover, several proteins were identified as independent CK2β interaction partners, which interact with CK2β at the same binding site important for CK2α binding (Liberman & Ruderman 2004, Bibby & Litchfield 2005).

An antibody against CK2β only gave unspecific signals and also coimmunoprecipitation experiments using a FLAG-tagged version of CK2β did not provide reliable results for an interaction of CK2β with Mbm. Therefore, immunostainings of a *CK2β* null mutant (*CK2β*$^{\Delta A26}$) were performed. These animals are lethal at larval stages and their brains are largely reduced in size. As a control, *CK2β*$^{\Delta A26}$ animals carrying a genomic rescue construct (*CK2β*$^{gDNA}$) were used (Jauch et *al*. 2002). Stainings were done using Mbm, aPKC, Miranda and Fibrillarin antibodies, where aPKC and Miranda were used as neuroblast and Fibrillarin as nucleolar markers. Interestingly, Mbm localization patterns in *CK2β*$^{\Delta A26}$ neuroblasts were similar to CK2α knock-down phenotype and showed not only nucleolar but also cytoplasmic staining of Mbm (arrow in Figure 36 B). Neuroblast size is strongly reduced in most cases, although few neuroblasts are also abnormal big in size. Introducing the genomic rescue construct *CK2β*$^{gDNA}$ in a *CK2β*$^{\Delta A26}$ background entirely reverted the mutant phenotypes (Figure 36 C).

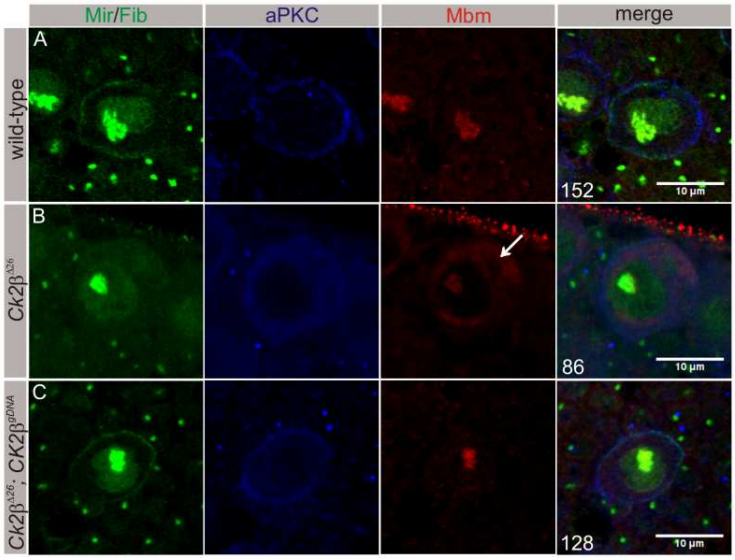


**Figure 36. Loss of CK2β causes a change in Mbm localization.**
Interphase neuroblasts from wild-type, *CK2β*$^{\Delta A26}$ and *CK2β*$^{\Delta A26}$; *CK2β* $^{gDNA}$ were stained for Mbm (red), the neuroblast markers aPKC (blue) and Miranda (green), and Fibrillarin (green) as a nucleolar marker. In comparison with wild-type (A), Mbm shows partial localization in the cytoplasm in the *CK2β* null mutant (arrow in B). The phenotype is completely reversed by introducing the genomic rescue construct. $n_{wt}$: 15 brains, $n_{CK2\beta}{}^{\Delta A26}$: 12 brains, $n_{CK2\beta}{}^{\Delta A26}{}_{;CK2\beta}{}^{gDNA}$: 15 brains.

Strikingly, not only Mbm, but also Miranda and aPKC were affected in *CK2β* null mutant neuroblasts. Particularly, Miranda staining was undetectable, whereas αPKC showed homogeneous cytoplasmic expression (Figure 36 B). However, further experiments to determine the role of CK2β in neuroblasts were not done, also because in *Drosophila* there are several protein isoforms of CK2β, which have redundant and non-redundant functions (Jauch et *al.* 2006).

### 3.8.5 CK2 phosphorylation sites of Mbm are required for correct localization

Relaying on the fact that CK2 is a multifunctional kinase, it is possible that the Mbm localization defect upon knock-down of CK2α might be an indirect effect. Thus, experiments were performed using the identified CK2 phosphorylation sites. For this purpose, corresponding transgenic lines were generated by introducing the triple alanine substitutions in AC-1, AC-2 or combination of both mutant in the genomic rescue construct *P[mbm*$^{wt}$*]*, which were correspondingly labeled as *P[mbm*$^{AC\text{-}1\Delta P}$*]*, *P[mbm*$^{AC\text{-}2\Delta P}$*]* and *P[mbm*$^{AC\text{-}1+2\Delta P}$*]*. All transgenes were integrated at the same chromosomal position by

site-specific recombination. Transgenic lines were first tested for their ability to rescue homozygous lethality of *mbm*$^{SH1819}$. This was the case in the presence for the wild-type transgene *P[mbm*$^{wt}$*]*. The *P[mbm*$^{AC\text{-}2\Delta P}$*]* transgene provided rescue to a much lower degree, whereas in the case of *P[mbm*$^{AC\text{-}1\Delta P}$*]* only very rarely rescued flies were observed. The *P[mbm*$^{AC\text{-}1+2\Delta P}$*]* transgene was unable to rescue lethality of *mbm*$^{SH1819}$. Afterwards, immunostainings of interphase neuroblasts of the different transgenes expressed in a *mbm*$^{SH1819}$ background were done. Stainings revealed that the wild-type transgene *P[mbm*$^{wt}$*]* compensated the loss of Mbm expression in *mbm*$^{SH1819}$ and the same nucleolar localization than the endogenous Mbm in wild-type neuroblasts was observed (Figure 37 A-C).

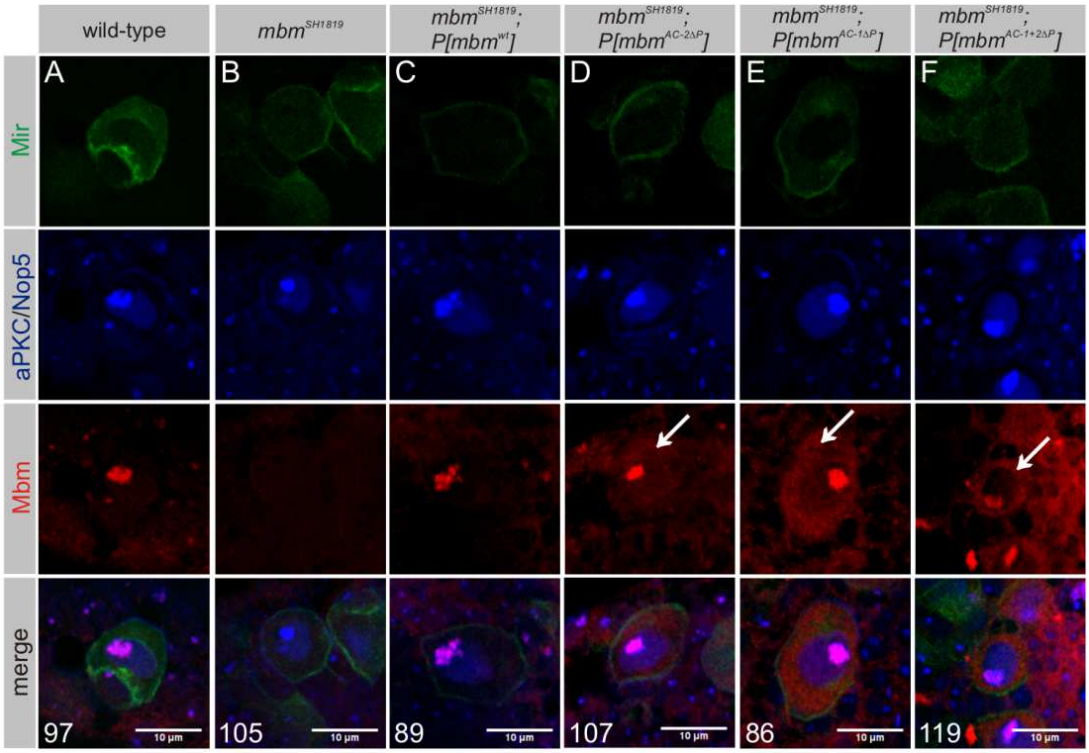


**Figure 37. Requirement of CK2 phosphorylation sites for Mbm localization.**
Neuroblasts of the indicated genotype were stained for the neuroblast markers Miranda (green) and aPKC (blue), Mbm (red) and Nop5 (blue) as an independent nucleolar marker. A-C) Lack of nucleolar Mbm expression in *mbm*$^{SH1819}$ is completely restored by the genomic rescue construct *P[mbm*$^{wt}$*]*. D-F) Alanine substitution of identified CK2 phosphorylation sites in the acidic cluster 2 (*P[mbm*$^{AC\text{-}2\Delta P}$*]*), acidic cluster 1 (*P[mbm*$^{AC\text{-}1\Delta P}$*])* or a combination of both (*P[mbm*$^{AC\text{-}1+2\Delta P}$*]*) resulted in partial delocalization of the mutated Mbm proteins in the cytoplasm (arrows). From each genotype at least 8 brains were analyzed.

The picture was different in case of all three mutated transgenes, which revealed nucleolar expression of Mbm but also prominent staining in the cytoplasm (Figure 37 D-F). These results were comparable but much more pronounced to the results obtained by

CK2α knock-down (Figure 35 C-E), which could be explained by residual amount of CK2α after knock-down (Figure 35).

Furthermore, to determine whether the relative expression levels of Mbm in the cytoplasma and nucleolus differ significantly between endogenous Mbm and the different transgenes, Mbm signal intensities in the cytoplasm and the nucleolus were quantified. Compared to wild-type Mbm and *P[mbm$^{wt}$]*, which exclusively localize in the nucleolus, Mbm proteins expressed from the *P[mbm$^{AC\text{-}2\Delta P}$]*, *P[mbm$^{AC\text{-}1\Delta P}$]* and (*P[mbm$^{AC\text{-}1+2\Delta P}$]* transgenes showed a significant increase in cytoplasmic Mbm expression levels (Figure 38).

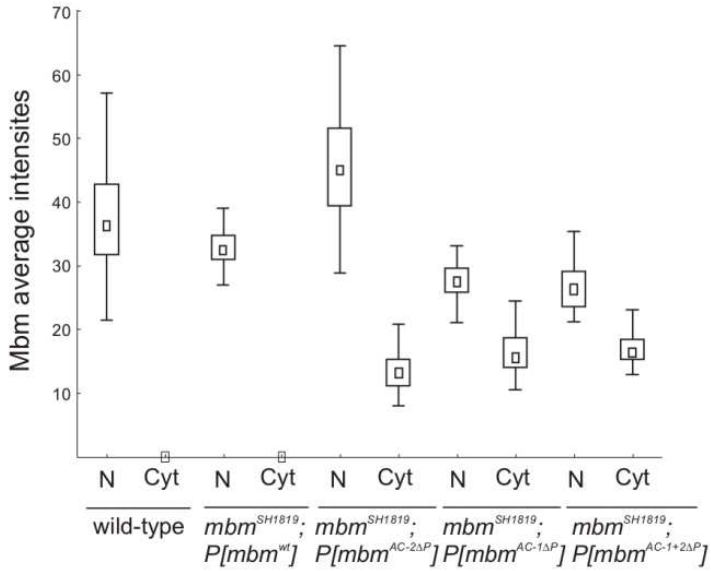


**Figure 38. Avarage intensity of Mbm expressed in different constructs.**
Box blot analysis of nucleolar (N) and cytoplasmic (Cyt) Mbm signal intensities for each genotype was calculated. Mbm expression levels either in cytoplasm or nucleolus between *P[mbm$^{AC\text{-}1\Delta P}$]*, *P[mbm$^{AC\text{-}2\Delta P}$]*, *P[mbm$^{AC\text{-}1+2\Delta P}$]* and wild-type and *P[mbm$^{wt}$]* are significantly different.

Even though the *in vitro* phosphorylation studies identified three residues in the AC-1 cluster as major phosphorylation sites, the transgenic analysis proved that both clusters of CK2 phosphorylation sites in AC-1 and AC-2 are necessary for proper function of Mbm *in vivo.*

# 4 Discussion

## 4.1 Mbm is a new nucleolar protein involved in *Drosophila* brain development

The results of this study have identified Mbm as a new nucleolar protein, which is involved in cell growth regulation of neural progenitor cells during brain development of *Drosophila*. It is known that the nucleolus is a multistructural organelle and has variable morphology based on growing conditions and cell cycle. Generally, the nucleolus consists of three subcompartments designated fibrillar center (FC), the dense fibrillar component (DFC) and the granular component (GC) (Hernandez-Verdun et *al.* 2010). However, the nucleolus of *Drosophila* displays a particular ultrastructural organization, which is different from the nucleoli of higher eukaryotes and characterized by absence of a fibrillar center (Knibiehler et al. 1982). It comprises only two components: a central fibrillo-granular structure called also the nucleolar core and referred to as fibrillar component (FC), since it features both characteristics of mammalian FC and DFC. The FC is surrounded by large granules of ribonucleoprotein material referred to as GC. The internal organization of *Drosophila* nucleoli is difficult to resolve, since all the components appear to be intermingled (Knibiehler et al. 1982). Nevertheless, co-localization of Mbm with Fibrillarin and Nop5 has proven that Mbm is expressed in neuroblast nucleoli of 3$^{rd}$ instar larval brains and displays cell cycle dependent localization. Particularly, Mbm is expressed in the nucleolus of interphase cells. During the cell cycle, starting from metaphase, cells show low expression level of Mbm in the cytoplasm. It is well known that both Fibrillarin and Nop5 are C/D small nucleolar RNPs (snoRNPs), which are essential for nascent rRNA processing (Matera et *al.* 2007, Taft et *al.* 2009), which takes place in DFC of the nucleolus. Thus, Fibrillarin is the most prominent marker to identify the dense fibrillar component of nucleoli. Therefore, co-localization of Mbm with Fibrillarin indicates that Mbm is a new component of fibrillar component of the nucleolus.

### 4.1.1 Mbm does not affect asymmetric cell division

Animals lacking Mbm are not surviving till adulthood; in addition they show developmental delay before they die around pupal formation. Particularly, the larval brain is apparently smaller compared to wild-type animals at the same age; in addition the

overall size of the larvae is also smaller. My experiments have shown that complete loss of Mbm function causes a general proliferation defect of central brain neuroblasts in 3rd instar larvae, which corresponds to the previous finding that mushroom body neuroblast proliferation is affected in the strong hypomorphic combination *mbm$^{1}$/Df(2)A1* (Raabe et *al.* 2004). Thus, my results provided evidence for the requirement of Mbm in the entire neuroblast population. However, a more careful analysis should be done to differentiate between type I, type II and optic lobe neuroblasts. Furthermore, a requirement of Mbm function at different developmental stages should be analyzed. These studies might also address the question, why in the hypomorphic *mbm$^{1}$* allele the phenotype is largely restricted to a reduction of the mushroom body neuropile. This emphasizes the need of a neuroblast lineage specific analysis.

The most prevalent explanation for the observed proliferation defect is disruption of asymmetric cell division. It is well known that progenitor cells, in this case neuroblasts, undergo a series of asymmetric divisions, each giving a raise to a new neuroblast and a ganglion mother cell, which divides one more time to give rise to a pair of neurons or glia cells. Asymmetric cell division is a well-organized process and based on differential segregation of the evolutionally conserved PAR cell polarity complex and intrinsic cell fate determinants (Yamashita & Fuller 2008, Neumüller & Knoblich 2009, Knoblich 2010). Moreover, malfunction of any step in asymmetric cell division leads to proliferation defects (Knoblich 2010, Sousa-Nunes & Somers 2013). However, stainings against different polarity and cell fate determinants provided no evidence that loss of Mbm affects this machinery; consequently the entire process of asymmetric cell division is apparently not disturbed. However, the analysis performed so far provides a static picture of a dynamic process. Thus live imaging experiments should be performed to follow *mbm* neuroblasts throughout mitosis in more detail and to measure cell cycle length.

### 4.1.2 Mbm is require for cell growth

It is well known that cell proliferation and growth are tightly coordinated. In *Drosophila*, the two waves of neurogenesis (embryonic and postembryonic) are separated by a quiescence state. After exit from quiescence, neuroblasts first enlarge size before they start to proliferate (Truman & Bate 1988, Colombani et *al.* 2003, Chell & Brand 2010). Re-entry to the cell cycle fails when neuroblasts are unable to enlarge due to the lack of nutrition (Britton and Edgar 1998). Moreover, during embryogenesis neuroblasts reduce in

size after each division and enter quiescence when they reach a critical minimal size (Hartenstein et *al.* 1987). In contrast, postembryonic neuroblasts grow and regain their size between rounds of divisions and only start to reduce growth at the end of neurogenesis before they undergo apoptosis or final differentiation (Ito & Hotta 1992, Maurange et *al.* 2008, Siegrist et *al.* 2010). Thus, all previous observations prove that cell size reduction of neuroblasts impairs proliferation. Comparison of wild-type and $mbm^{SH1819}$ 3rd instar larval neuroblasts sizes revealed that loss of Mbm leads to significant reduction of central brain neuroblast size, which correlates with a proliferation defect (Figure 23). Furthermore, it was distinguished that Mbm does not affect cell size in other tissues of *Drosophila*, as well as in tissue culture S2 cells suggesting its particular role in neuroblasts. However, it is still not clear whether neuroblasts lacking Mbm become consecutively smaller during development being unable to re-grow to normal size after each postembryonic cell division. Alternatively, there might be an initial failure to grow in response to nutrition after the quiescence phase. On the other hand, Mbm might have an effect already at early embryogenesis. To address these questions, further analyses of *mbm* neuroblast sizes should be done at different developmental stages.

For proper development organisms need proper supply of nutrients. The neuroblast proliferation depends on nutritional status of the organism (Britton and Edgar 1988). TOR and InR/PI3K/Akt pathways are regulators of nutrient-dependent growth of cells. Moreover, most of the genes regulated by TOR signaling pathway are involved in ribosome biogenesis (Guertin et *al.* 2006). The observed cell size phenotype caused by loss of Mbm raises the question, how Mbm might regulate cell growth and proliferation? And does it have a role in cell growth regulated by the TOR and InR/PI3K/Akt pathways?

## 4.2 Loss of Mbm inhibites small ribosomal subunit biogenesis or transport

The nucleolus is a major regulator of cell growth and proliferation, since it is the ribosome factory of a cell (Boisvert et *al.* 2007, Hernandes-Verdun et *al.* 2010). The efficient supply of ribosomes ensures sufficient levels of protein synthesis needed for proper cell growth and further proliferation. Therefore, it is not surprising that all steps of ribosome biogenesis, including rRNA modification, assembly and transport of ribosomal subunits are tightly regulated. However, beside ribosome biogenesis, the nucleolus is also regulating cell-cycle control and stress responses by inducing cell-cycle arrest or inhibiting

rDNA transcription as well as the processing and maturation of other RNAs, such as small RNAs transcribed by RNA pol III and also microRNAs (Boisvert et *al.* 2007, Gerbi et *al.* 2003). More than 200 proteins from plants and 700 from humans were identified by proteomic analysis from isolated nucleoli. Although 90% homology was observed between the yeast and human nucleolar proteome, the function of many of the proteins remains unknown (Pendle et *al.* 2005, Andersen et *al.* 2005, Boisvert et *al.* 2007).

Mbm is required for cell growth and proliferation and it co-localizes with Fibrillarin and Nop5, which are involved in rRNA processing in the nucleolus. These findings lead to the hypothesis that Mbm may contribute to cell growth by mediating ribosome processing or transport. To test this hypothesis, the functional relevance of Mbm in large and small ribosomal subunit biogenesis was analyzed by expression of GFP-tagged RpL11 and RFP-tagged RpS6 proteins as representative proteins for the large and small ribosomal subunit, respectively. Excitingly, the analyses revealed that Mbm indeed has a critical role in small ribosomal subunit biogenesis. Loss of Mbm caused retention of RpS6 in the nucleolus of neuroblasts, which might cause a lack of sufficient numbers functional ribosomes (Figure 27 D). A complementary result for the large ribosomal subunit was achieved by knock-down of Nucleostemin1 (NS1) (Rosby et *al.* 2009). It is important to mention that the RpS6 retention phenotype caused by *mbm* was observed only in neuroblasts, since the localization defect of RpS6 was not observed in GMCs and neurons (arrowhead in Figure 27 B). First evidence that retention of the small ribosomal subunit in the nucleolus indeed leads to impaired protein synthesis was provided by metabolic labeling experiments of neuroblasts (Figure 28), which could be the result of the cell being unable to build up sufficient numbers of mature ribosome. Nevertheless, 18% of analyzed *mbm* neuroblasts show also weak cytoplasmic expression of RpS6 indicating that protein synthesis in some neuroblasts is maintained at some degree. However, since *mbm* flies die around pupal stage, the amount of synthesized proteins is apparently not enough for animal survival.

Overall, all experiments suggest that Mbm functions as a new fibrillar component of the nucleolus, and loss of Mbm disturbs small ribosomal subunit maturation, its release to the nucleoplasm or the transport to the cytoplasm finally resulting in insufficient number of functional ribosomes. Therefore protein synthesis is impaired, which leads to reduced cell growth and proliferation. Moreover, relaying on results that Mbm has more pronounced expression in neuroblasts compared to surrounding cells and that the *mbm* phenotype is only observed in neuroblasts, it can be concluded that Mbm has a more neuroblast-specific function.

However, the exact function of Mbm in ribosome biogenesis is not clear yet. One of the complications to carry out further biochemical experiments is the lack of more accessible systems compared to neuroblasts, which are presenting only a minor fraction of the entire cell population of a brain. Tissue culture S2 cells are also impossible to use, since Mbm knock-down does not affect cell proliferation. However, some characteristic features of the Mbm protein, such as two zinc-finger motifs, which may bind to RNA or DNA, and also the arginine/glycine (RGG) rich clusters located in the N-terminal half of the protein may provide entry points for further investigations. As it was previously shown, RNA-binding proteins are characterized by the presence of several conserved motifs, which include also RGG box and zinc-finger motif (Burd & Dreyfuss 1994). In addition, RGG boxes containing proteins may associate with small nucleolar ribonucleoproteins, which participate in pre-rRNA processing (Godin & Varani 2007, Matera et *al.* 2007, Thandapani et *al*. 2013). Another entry point for further research might be eIF6 (eukaryotic translation initiation factor 6) and the CG8545 transcription unit, which are indicated in the *Drosophila* protein interaction map (DPIM) as interaction partners for Mbm. It is known, that eIF6 regulates association of 40S and 60S subunits, particularly, it prevents their premature association (Burwick et *al.* 2012, Gandin et *al.* 2008). In addition, Scd6 RGG box containing proteins may prevent the formation of 48S preinitiation complex due to the binding to eIF4G, resulting in inhibition of translation initiation (Thandapani et *al*. 2013). According to DPIM, the predicted CG8545 protein is involved in rRNA processing and also the String 9.0 database specifies Fibrillarin and Nop5 as interaction partners of CG8545 (Szklarszyk et *al.* 2010).

## 4.3 Mbm as a transcriptional target of dMyc

Regulation of cell growth, cell cycle progression, terminal differentiation and apoptosis are essential for normal development of an organism. The reason for developmental abnormalities could arise from regulatory defects in genes controlling these processes. The *myc* family of proto-oncogenes is one important group of such genes, which recognizes its downstream transcriptional targets through specific hexameric DNA sequences called E-boxes (Blackwell at al. 1993, Blackwood et al. 1992). Previously it was shown that appropriate levels of the single *Drosophila dmyc* gene is crucial to maintain normal cell and body size during development, which is mediated by regulation of cellular

growth (Johnson et *al*. 1999, Pierce et *al*. 2004). Moreover, Myc also regulates multiple processes in ribosome biogenesis. Myc activates pre 47S rRNA transcription from rDNA through interaction with cofactors that are required for RNA pol I recruitment, as well as RNA pol II dependent transcription of structural ribosomal protein genes. In addition, Myc activates transcription of 5S rRNA and tRNA through RNA pol III (Riggelen et *al*. 2010, Grandori et *al*. 2005, Arabi et *al*. 2005, Grewal et *al*. 2005, Tschocher and Hurt 2003). In spite of the fact that Myc expression correlates with induction or repression of number of genes, only few studies were done to systematically identify the sequence characteristics of Myc binding site. Hulf and coworkers (2005) identified 544 dMyc target genes that are characterized by the presence of an E-box, which is most often positioned within 100 nucleotides downstream of the transcriptional start site of the gene. On the other hand, it was shown that many of the dMyc target genes contain a second E-box in their promoter region, which could raise the responsiveness of a gene to dMyc (Hulf et al. 2005).

Mbm transcription might be controlled by two E-box motifs (E-box1 and E-box2) found in the vicinity of the transcription start site. E-box1 is located just downstream of the predicted transcriptional start site and thus also conforms to the positional bias of E-box sequences (Hulf et al. 2005), the degenerate E-box 2 is located further upstream. In order to verify functionality of both E-boxes for transcription of the *mbm* gene, luciferase reporter assays were done. The results suggested that E-box1 is the major mediator for Myc-induced transcription (Figure 29). Direct binding of Myc to E-box1 was verified by chromatin immunoprecipitation (ChIP) analyses (in collaboration with Peter Gallant and Eva Herter, Department of Biochemistry and Molecular Biology). In addition, the *in vivo* effect of Myc on Mbm expression was tested by complete removal of Myc function in single neuroblasts and revealed that both Mbm and Nop5 expression were reduced (Figure 30). This corresponds to the finding that *Drosophila* Myc regulates expression of many genes involved in ribosome biogenesis (Gallant 2013).

Investigations of Mbm as a transcriptional target of Myc raise the question how Mbm may regulate cell growth and correspondingly also proliferation. It is well established that Myc is placed downstream of the TOR and InR/PI3K/AKT pathways (Li et *al* 2010, Parisi et *al.* 2011). Myc has a key role in regulation of cell growth and metabolism as a mediator of InR/PI3K/AKT and TOR pathways in a tissue specific manner (Teleman et *al.* 2008). Myc transcription is regulated by InR/PI3K/AKT via direct binding of FoxO to Myc promotor sequences, whereas posttranslational activity is controlled by TOR via TORC1 (Teleman et *al.* 2008, Demontis & Perrimon 2009). One

possible model could be that nutrition sensing mediated by the TOR and InR/PI3K/AKT pathways ensures Myc expression and activity in neuroblasts, which in its turn regulates transcription of Mbm but also expression of other proteins involved in ribosome biogenesis. Despite the evidence that Myc is a downstream effector of TOR and InR/PI3K/AKT pathways in other tissues (Demontis & Perrimon 2009, Teleman et *al.* 2008), information for neuroblasts is largely missing. Thus, it would be interesting to analyze the behavior of *mbm* neuroblasts under nutrient restriction condition. However, one should keep in mind that at late larval stages, the CNS is highly spared under nutrient restriction by Jeb/Alk signaling (Cheng et *al.* 2011), which also acts on downstream effectors of the TOR and InR/PI3K/AKT pathways.

## 4.4 Posttranslational regulation of Mbm by protein kinase CK2

Relaying on the co-localization and co-purification results (Guruharsha et *al.* 2011) the question was addressed whether Mbm function is regulated by CK2 phosphorylation. Protein phosphorylation is crucial for basic cellular processes, such as cell proliferation and cell survival. Mbm posttranslational modification is regulated by protein kinase CK2, which is built up by two catalytic (α–) and two regulatory (β–) subunits. CK2 is a highly conserved protein kinase, which is crucial for a variety of cellular processes and correspondingly, mutations in either subunit result in lethality. Meggio and Pinna (2003) listed more than 300 protein substrates phosphorylated by CK2. Previously, several studies indicated that CK2 predominantly localizes in the nucleolus. In addition, it has minor expression in the cytoplasm (Krek et al. 1992, Penner et al. 1997, Yu et al. 1991). However, both subunits may also act independently and localize in different compartments of the cell. CK2 targets several components of the Pol I machinery and also activates Pol III transcription, suggesting that the mechanisms controlling the transcriptional output of Pol I and Pol III could be regulated in a CK2 phosphorylation dependent manner (Bierhoff et *al*. 2008, Hu et *al*. 2003). In addition, phosphorylation of nucleophosmin (B23) by CK2 ensures the mobility of the protein between nucleolus and nucleoplasm (Negi & Olson 2006). Results of this study demonstrated that CK2α co-localizes with Mbm in the nucleoli of neuroblasts (Figure 31).

The idea that Mbm stability or localization is regulated by CK2-mediated phosphorylation was supported by *in vitro* kinase assays, which verified CK2-dependent

phosphorylation of Mbm in its C-terminal half. The precise phosphosites of Mbm were identified by MS/MS analysis within two acidic clusters (AC-1 and AC-2) and correspond to the CK2 consensus sequence (Figure 32). One of the identified phosphosites in the AC-2 cluster was previously identified by phosphoproteomic analysis of S2 cells and in *Drosophila* embryos thus providing an independent confirmation (Bodenmiller et al. 2008, Zhai et al. 2007). Further investigations to reveal the importance of identified phosphorylation sites were done by substitution of phosphorylated residues by alanine. Although *in vitro* kinase assays with the mutated Mbm proteins indicated that the major phosphorylation sites are located in the AC-1 cluster, in neither case phosphorylation was completely abolished (Figure 34). This can be explained by the presence of another potential CK2 phosphorylation site in the AC-3 cluster, which was not covered by MS analyses (Figure 32).

The *in vitro* studies were complemented by functional studies in flies. RNAi-mediated knockdown of CK2α leads to apparent redistribution of Mbm from the nucleolus to the cytoplasm (Figure 35), which was also evident upon neuroblast-specific expression of a dominant-negative variant of CK2α (*UAS-CK2α$^{TIK}$*, Meissner et *al.* 2008). A similar redistribution of Mbm was observed in a *CK2β* null mutant background indicating the presence of the CK2 holoenzyme in the nucleolus. *CK2β* null mutants have extremely small brains (data not shown). Direct evidence for a function of CK2β in proliferation and size control of neuroblasts was provided by a recent comprehensive RNAi study (Neumüller et al., 2011). However, all attempts to coimmunoprecipitate either endogenous CK2β or a FLAG-tagged variant of CK2β together with Mbm failed so far.

*Drosophila* CK2β transcription unit encodes five CK2β isoforms that differ in their C-terminal tail (Jauch et *al.* 2006, Jauch et *al.* 2002). However, all isoforms include an acidic stretch, which might bind polyamines (see below) and zinc-fingers essential for CK2β diamerization (Jauch et *al.* 2002). All identified CK2β isoforms equally interact with the CK2α subunit; however they differ in their ability to rescue lethality of the *CK2β* null mutant and to promote mushroom body development (Jauch et *al.* 2006). This suggested that CK2β isoforms may differently regulate CK2α activity. It would be interesting to identify whether one or combination of several CK2β isoforms has a specific function in neuroblasts. For this purpose, isoform specific antibodies or generation of mutant flies lacking only a single form of CK2β isoforms will be very helpful.

Finally, the identification of several CK2α phosphorylation sites in Mbm allowed me to evaluate their functional relevance *in vivo*. Transgenes carrying combined mutations in all phosphorylation sites in either the AC-1 or the AC-2 cluster largely failed to complement the loss of endogenous Mbm function and the corresponding proteins showed a pronounced cytoplasmic localization in contrast to the solely nucleolar accumulation of the wild-type Mbm protein. This corresponded to the observed Mbm localization defect upon RNAi mediated knockdown of CK2α.

Yet, it is not clear how the regulation of Mbm phosphorylation by CK2 takes place. Recently it was shown that CK2 activity is regulated by polyamines, which are derived from amino acid catabolism. CK2 is an intrinsically regulated kinase, which involves autoinhibition of CKα by CK2β. This inhibition is mediated by binding of the negative charged polyamine binding region of CK2β to the positive charged catalytic site of CK2α (Leroy et *al.* 1997a, Leroy et *al.* 1997b). Binding of polyamines induces a conformational change in the CK2 complex and thereby opening access to many protein substrates (Leroy et *al.* 1997b). Polyamines are important to enhance or inhibit protein phosphorylation by CK2 in insects (Song et *al.* 1994). Putrescine, spermidine and spermine are polycations that are essential for cell proliferation, tissue growth and development (Nishioka 1996, Montenarh 2010). The initial step of polyamine biosynthesis is converting L-ornithin to putrescence, which is catalyzed by ornithine decarboxylase (ODC). Sequential addition of aminopropyl groups to putrescine generates long carbon-chain spermidine and spermine (Wallace et *al.* 2003). Impairment of polyamine biosynthesis affects neuroblast proliferation (Cayre et *al.* 1997). Particularly, putrescine stimulates mushroom body neuroblasts proliferation in house cricket (*Acheta domesticus*), whereas spermidine and spermine act on neuronal differentiation (Cayre et *al.* 2001). Finding out, whether regulation of CK2 catalytic activity by different polyamines is relevant to control Mbm function by phosphorylation will be a future challenge.

Taken together all results allowed me to assume that Mbm regulates cell growth and proliferation by regulation of ribosome biogenesis in neuroblasts (Figure 39).

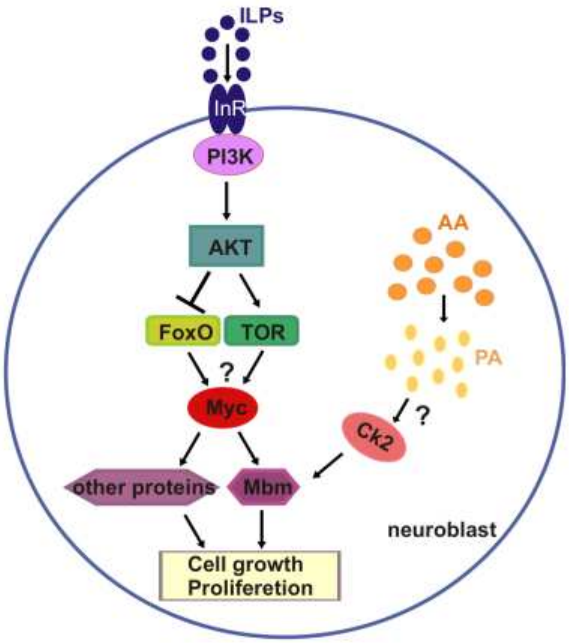


**Figure 39. A model for regulation of cell growth and proliferation by Mbm.**
ILPs activate TOR/PI3K pathways leading to expression of the transcription factor Myc. Myc regulates transcription of Mbm and other proteins required for ribosome biogenesis. Mbm posttranslational regulation is controlled by polyamine-modulated CK2 kinase activity.

Mbm transcription is regulated by Myc, which provides a potential link to systemic growth control mediated by the TOR/PI3K pathways. On the other hand, Mbm function requires phosphorylation by protein kinase CK2. Regulation of catalytic activity of CK2 might depend on differential binding of polyamines thereby providing a link to cellular growth signals (Figure 39). Further studies are required to validate this model.

# 5 Summary

Cell growth and cell division are two interconnected yet distinct processes. Initiation of proliferation of central brain progenitor cells (neuroblasts) after the late embryonic quiescence stage requires cell growth, and maintenance of proper cell size is an important prerequisite for continuous larval neuroblast proliferation. Beside extrinsic nutrition signals, cell growth requires constant supply with functional ribosomes to maintain protein synthesis.

Mutations in the *mushroom body miniature (mbm)* gene were previously identified in a screen for structural brain mutants. This study focused on the function of the Mbm protein as a new nucleolar protein, which is the site of ribosome biogenesis. The comparison of the relative expression levels of Mbm and other nucleolar proteins in different cell types showed a pronounced expression of Mbm in neuroblasts, particularly in the fibrillar component of the nucleolus, suggesting that in addition to nucleolar components generally required for ribosome biogenesis, more neuroblast specific nucleolar factors exist. Mutations in *mbm* cause neuroblast proliferation defects but do not interfere with cell polarity, spindle orientation or asymmetry of cell division of neuroblasts. Instead a reduction in cell size was observed, which correlates with an impairment of ribosome biogenesis. In particular, loss of Mbm leads to the retention of the small ribosomal subunit in the nucleolus resulting in decreased protein synthesis. Interestingly, the defect in ribosome biogenesis was only observed in neuroblasts. Moreover, Mbm is apparently not required for cell size and proliferation control in wing imaginal disc and S2 cells supporting the idea of a neuroblast-specific function of Mbm.

Furthermore, the transcriptional regulation of the *mbm* gene and the functional relevance of posttranslational modifications were analyzed. *Mbm* is a transcriptional target of dMyc. A common feature of dMyc target genes is the presence of a conserved E-box sequence in their promoter regions. Two E-box motifs are found in the vicinity of the transcriptional start site of *mbm*. Gene reporter assays verified that only one of them mediates dMyc-dependent transcription. Complementary studies in flies showed that removal of dMyc function in neuroblasts resulted in reduced Mbm expression levels.

At the posttranslational level, Mbm becomes phosphorylated by protein kinase CK2. Six serine and threonine residues located in two acidic amino acid rich clusters in the C-terminal half of the Mbm protein were identified as CK2 phosphorylation sites.

Mutational analysis of these sites verified their importance for Mbm function *in vivo* and indicated that Mbm localization is controlled by CK2-mediated phosphorylation.

Although the molecular function of Mbm in ribosome biogenesis remains to be determined, the results of this study emphasize the specific role of Mbm in neuroblast ribosome biogenesis to control cell growth and proliferation.

# 6 Zusammenfassung

Zellwachstum und Zellteilung stellen zwei miteinander verknüpfte Prozesse dar, die dennoch grundsätzlich voneinander zu unterscheiden sind. Die Wiederaufnahme der Proliferation von neuralen Vorläuferzellen (Neuroblasten) im Zentralhirn von *Drosophila* nach der spät-embryonalen Ruhephase erfordert zunächst Zellwachstum. Der Erhalt der regulären Zellgröße ist eine wichtige Voraussetzung für die kontinuierliche Proliferation der Neuroblasten über die gesamte larvale Entwicklungsphase. Neben extrinsischen Ernährungssignalen ist für das Zellwachstum eine kontinuierliche Versorgung mit funktionellen Ribosomen notwendig, damit die Proteinsynthese aufrechterhalten werden kann.

Mutationen im *mushroom body miniature (mbm)* Gen wurden über einen genetischen Screen nach strukturellen Gehirnmutanten identifiziert. Der Schwerpunkt dieser Arbeit lag in der funktionellen Charakterisierung des Mbm Proteins als neues nukleoläres Protein und damit seiner möglichen Beteiligung in der Ribosomenbiogenese. Der Vergleich der relativen Expressionslevel von Mbm und anderen nuklearen Proteinen in verschiedenen Zelltypen zeigte eine verstärkte Expression von Mbm in der fibrillären Komponente des Nukleolus von Neuroblasten. Diese Beobachtung legte die Vermutung nahe, dass in Neuroblasten neben generell benötigten Faktoren der Ribosomenbiogenese auch Zelltyp-spezifische Faktoren existieren. Mutationen in *mbm* verursachen Proliferationsdefekte von Neuroblasten, wirken sich jedoch nicht auf deren Zellpolarität, die Orientierung der mitotischen Spindel oder die Asymmetrie der Zellteilung aus. Stattdessen wurde eine Reduktion der Zellgröße beobachtet, was im Einklang mit einer Beeinträchtigung der Ribosomenbiogenese steht. Insbesondere führt der Verlust der Mbm Funktion zu einer Retention der kleinen ribosomalen Untereinheit im Nukleolus, was eine verminderte Proteinsynthese zur Folge hat. Interessanterweise wurden Störungen der Ribosomenbiogenese nur in den Neuroblasten beobachtet. Zudem ist Mbm offensichtlich nicht erforderlich, um Wachstum oder die Proliferation von Zellen der Flügelimginalscheibe und S2-Zellen zu steuern, was wiederum dafür spricht, dass Mbm eine Neuroblasten-spezifische Funktion erfüllt.

Darüber hinaus wurden die transkriptionelle Regulation des *mbm*-Gens und die funktionelle Bedeutung von posttranslationalen Modifikationen analysiert. *Mbm* Transkription wird von dMyc reguliert. Ein gemeinsames Merkmal von dMyc Zielgenen ist das Vorhandensein einer konservierten „E-Box“-Sequenz in deren Promotorregionen. In

der Umgebung der *mbm*-Transkriptionsstartstelle befinden sich zwei „E-Box“-Motive. Mit Hilfe von Genreporteranalysen konnte nachgewiesen werden, dass nur eine von ihnen die dMyc-abhängige Transkription vermittelt. Die dMyc-abhängige Expression von Mbm konnte auch in Neuroblasten verifiziert werden.

Auf posttranslationaler Ebene wird Mbm durch die Proteinkinase CK2 phosphoryliert. In der C-terminalen Hälfte des Mbm Proteins wurden in zwei Clustern mit einer Abfolge von sauren Aminosäuren sechs Serin- und Threoninreste als CK2-Phosphorylierungsstellen identifiziert. Eine Mutationsanalyse dieser Stellen bestätigte deren Bedeutung für die Mbm Funktion *in vivo*. Weiterhin ergaben sich Evidenzen, dass die Mbm-Lokalisierung durch die CK2-vermittelte Phosphorylierung gesteuert wird.

Obwohl die genaue molekulare Funktion von Mbm in der Ribosomenbiogenese noch im Unklaren ist, unterstreichen die Ergebnisse dieser Studie die besondere Rolle von Mbm in der Ribosomenbiogenese von Neuroblasten um Zellwachstum und Proliferation zu regulieren.

# 7 Acknowledgment

Completing my PhD degree is one of the most challenging activities of my life. The best and worst moments of my doctoral journey have been shared with many people. It has been a great pleasure to spend several years in the Institute of Medical Radiation and Cell Research of Würzburg University and its members will always remain dear to me.

Foremost, I would like sincerely to thank to my advisor, Prof. Dr. Thomas Raabe for the opportunity to carry out my Ph.D. project at the Institute of Medical Radiation and Cell Research, for the continuous support of my Ph.D study and research. He patiently provided the vision, encouragement and advises necessary for me to proceed through my research. Being a supportive adviser, he always gave me freedom to pursue independent work. Without his guidance and persistence this dissertation would not have been possible. In addition, I would like specially to thank him for his support and care about me since my arrival, which allowed me to have a feeling that I am at my home country.

I would like to express my gratitude to my Ph.D defense committee member Prof. Dr. Charlotte Förster for her strong interest and effort to support my project and giving the possibility to complete it, for reviewing and evaluating my work.

A special thank goes to Prof. Dr. Peter Gallant and Eva Herter from Institute for Biochemistry and Molecular Biology University of Würzburg. I was having a pleasant time working with them in their laboratory, where Eva Herter kindly was supporting me.

I am indebted to Dr. Jens Pfannstiel from Proteomics Core Facility of the Life Science Center University of Hohenheim for his great input to my work carrying out MS/MS analysis, which helped me a lot to complete my dissertation.

I would like also to thank Dr. Stefan Kircher and Dr. Friederike Berberich-Siebelt from Institute of Pathology giving me opportunity to use their radioactive laboratory and complete my experiments.

Of course I wish to thank Dr. Tanja Bedke from Department of Medical 2, Division of Hematology of University Hospital of Würzburg for helping me with FACS experiments and data analysis.

A special thank goes to my friend and my college Katherina Back. We shared not only the laboratory, the fruitful discussions and comments, but also nice evenings and chats. Her generous personality and support at the times of frustrations made my days brighter. She became my family in Germany. I enjoyed your company very much and hope to keep in touch always.

I would like to thank and share the credit of my work with my lab members: Dr. Benjamin Mentzel, Dr. Stephanie Pütz, Dr. Juliane Melzer, Dr. Felix Stark, Viera Albertova, Kirsten Langenbrink and Heike Wecklein. Their friendship and assistance has meant more to me than I could ever express and their support was helping me to go through several complications during my work. I would like to thank also Sebastian Bott for cooking the most delicious fly-food, which was making my flies to "work" better for me.

I would like to give a special thanks to Gunther Tietsch and Monika Wagenbrener. Without them our work in the institute and laboratory would have been stopped.

My friends, Dr. Zhasmine Mirzoyan, Lusine Ghazaryan and Vahan Serobyan, thanks a lot. I was always feeling you next to me and you were always giving me love and force to move forward.

Last, but not least, I wish to thank my husband Gevorg Hovhannisyan, whose love and encouragement allowed me to finish this journey. Thank you very much to my lovely parents and my brother wiht his wife Lilit and my amazing nephews and niece. These small pirates were always giving me the power and love to go through all difficulties and Lilit was always giving me unconditional support. Finally, I would like to dedicate this work to my daddy, he is not with us anymore, but all what I have achieved today was always encouraged and supported by him. I am very happy and proud to have a possibility with my work to give a small feedback to my parents for all the things what they have done and still doing for me.

# 8 Publications and conferences

## Publications

**Hovhanyan A.[a], Herter E.[b], Pfannstiel J.[c], Gallant P.[b], Raabe T.[a] (2014).** *Drosophila* Mbm is a nucleolar Myc and CK2 target required for ribosome biogenesis and cell growth of central brain neuroblasts. *Mol. And Cell. Biol.* (under revision)

**Hovhanyan A.[1] and Raabe T.[1†] (2009)**. Structural Brain Mutants: Mushroom Body Defect (Mud): A Case Study. *J. Neurogenetic*. Vol. 23, No. 1-2, 42-47 (doi:10.1080/01677060802471700)

## Poster presentation in conferences

**Hovhanyan A. and Raabe T. (2011).** Role of Mbm (Mushroom body minature) in brain development of Drosophila melanogaster. 22nd European *Drosophila* Research Conference 2011, Lissabon, Portugal.

**A.Hovhanyan[1], E.Herter[2], J.Pfannstiel[3], P.Gallant[2] and T. Raabe[1] (2013).** The new nucleolar protein Mbm is required for neuroblast cell growth. 23rd European *Drosophila* Research Conference 2013, Barcelona, Spain.

# 9 List of abbreviations

| | |
|---|---|
| 20E | Ecdysone |
| 40S | ribosomal small subunit |
| 4E-BP | initiation factor 4E binding protein |
| 60S | ribosomal large subunit |
| *abd-A* | *abdominal-A* |
| *ac* | *achaeta* |
| Alk | anaplastic lymphoma kinase |
| *ana* | *anachronism* |
| *Anp* | *Anntenopodia* |
| AP | anterior-posterior |
| aPKC | atypical protein kinase C |
| AS-C | *achaeta-scute-complex* |
| Ase | Asense |
| B23 | nucleophosmin |
| Brat | Brain tumor |
| BrdU | Bromodesoxyuridine |
| ca | calyx |
| Cas | Castor |
| ChIP | chromatin immunopercipitation |
| CNS | Central nervous system |
| D | Delta |
| DFC | dense fibrillar component |
| Dlg | Discs large |
| *dm* | *diminutive* |
| DPIM | *Drosophila* protein interaction map |
| Dpn | Deadpan |
| DV | dorso-ventral |
| *E(spl)* | *Enhancer of Split* |
| EdU | 5-ethynyl-2´-deoxyuridine |
| eIF6 | eukaryotic translation initiation factor 6 |
| F | fibrillar component |
| FACS | Fluorescence-activated cell sorting |
| FBDM | Fat body derived mitoge |
| FC | fibrillar center |
| FDS | fat body derived signal |
| FGF | Fibroblast growth factor |
| Flp | Flipase |
| FoxO | Forkhead box class O |
| GC | granular component |
| GMC | Ganglion mother cell |
| Grh | Grainyhead |

| | |
|---|---|
| Hb | Hunchback |
| Hh | Hedgehog |
| HPG | L-homopropargylglycine |
| IGF | insulin growth factor |
| ILP | insulin like peptide |
| INP | Intermediate neural progenitor |
| InR | insulin-like receptor |
| Insc | Inscutable |
| IPC | Inner Proliferation Center |
| Jeb | Jelly Belly |
| KCs | Kenyon cells |
| kd | knock-down |
| Khc73 | kinesin heavy chain 73 |
| Kr | Kruppel |
| *l'sc* | *lethal of scute* |
| Lgl | Lethal (2) giant larvae |
| MB | Mushroom body |
| *mbm* | *mushroom body miniature* |
| Mir | Miranda |
| Mud | Mushroom body defect |
| N | Notch |
| NB | Neuroblast |
| $N^{ICD}$ | Notch intracellular domain |
| NR | nutrient restriction |
| NS1 | nucleostemin 1 |
| ODC | ornithine decarboxylase |
| OL | Optic lobes |
| OPC | Outer Proliferation Center |
| ORF | open reading frame |
| ped | peduncle |
| pH3 | phospho-histone H3 |
| PI3K | phosphatidylinositol 3-kinase |
| Pins | Partner of Inscutable |
| Pon | Partner of Numb |
| pre-rRNA | preribosomal RNA |
| Pros | Prospero |
| R/G | arginine/glycine |
| rDNA | ribosomal DNA |
| *RHG* | *grim*, *hid* and *reaper* |
| RNA pol I | RNA polymerases I |
| RNA pol II | RNA polymerases II |
| RNA pol III | RNA polymerases III |
| RPs | ribosomal proteins |
| rRNAs | ribosomal RNAs |

| | |
|---|---|
| *sc* | *scute* |
| SDS-PAGE | sodium dodecyl sulfate Polyacrylamide gel electrophoresis |
| SLIF | Slimfast |
| snoRNAs | small nucleolar RNAs |
| SSU | small subunit processome |
| Su(H) | Suppressor of hairless |
| Svp | Seven-up |
| TIF-IA | transcription initiation factor IA |
| TOR | target of rapamycin |
| TORC1 | TOR complex 1 |
| TORC2 | TOR complex 2 |
| TPRs | tetratricopeptide repeats |
| *trol* | *terribly reduced optic lobe* |
| TTF | Temporal transcription-factor |
| UBF | upstream binding factor |
| *Ubx* | *Ultrabithorax* |
| VNC | Ventral nerve cord |
| wt | wild-type |

# 10 References

**Andersen, J.S., Lam, Y.W., Leung, A.K., Ong, S.E., Lyon, C.E., Lamond, A.I., Mann, M., 2005.** Nucleolar proteome dynamics. Nature 433, 77-83.

**Andlauer, T.F., Sigrist, S.J., 2012.** Quantitative analysis of Drosophila larval neuromuscular junction morphology. Cold Spring Harbor protocols 2012, 490-493.

**Arabi, A., Wu, S., Ridderstrale, K., Bierhoff, H., Shiue, C., Fatyol, K., Fahlen, S., Hydbring, P., Soderberg, O., Grummt, I., Larsson, L.G., Wright, A.P., 2005.** c-Myc associates with ribosomal DNA and activates RNA polymerase I transcription. Nature cell biology 7, 303-310.

**Aso, Y., Grubel, K., Busch, S., Friedrich, A.B., Siwanowicz, I., Tanimoto, H., 2009.** The mushroom body of adult Drosophila characterized by GAL4 drivers. Journal of neurogenetics 23, 156-172.

**Atwood, S.X., Prehoda, K.E., 2009.** aPKC phosphorylates Miranda to polarize fate determinants during neuroblast asymmetric cell division. Current biology : CB 19, 723-729.

**Bayraktar, O.A., Boone, J.Q., Drummond, M.L., Doe, C.Q., 2010.** Drosophila type II neuroblast lineages keep Prospero levels low to generate large clones that contribute to the adult brain central complex. Neural development 5, 26.

**Bayraktar, O.A., Doe, C.Q., 2013.** Combinatorial temporal patterning in progenitors expands neural diversity. Nature 498, 449-455.

**Bello, B., Reichert, H., Hirth, F., 2006.** The brain tumor gene negatively regulates neural progenitor cell proliferation in the larval central brain of Drosophila. Development (Cambridge, England) 133, 2639-2648.

**Bello, B.C., Hirth, F., Gould, A.P., 2003.** A pulse of the Drosophila Hox protein Abdominal-A schedules the end of neural proliferation via neuroblast apoptosis. Neuron 37, 209-219.

**Berdnik, D., Torok, T., Gonzalez-Gaitan, M., Knoblich, J.A., 2002.** The endocytic protein alpha-Adaptin is required for numb-mediated asymmetric cell division in Drosophila. Developmental cell 3, 221-231.

**Betschinger, J., Knoblich, J.A., 2004.** Dare to be different: asymmetric cell division in Drosophila, C. elegans and vertebrates. Current biology : CB 14, R674-685.

**Betschinger, J., Mechtler, K., Knoblich, J.A., 2003.** The Par complex directs asymmetric cell division by phosphorylating the cytoskeletal protein Lgl. Nature 422, 326-330.

**Bibby, A.C., Litchfield, D.W., 2005.** The multiple personalities of the regulatory subunit of protein kinase CK2: CK2 dependent and CK2 independent roles reveal a secret identity for CK2beta. International journal of biological sciences 1, 67-79.

**Bierhoff, H., Dundr, M., Michels, A.A., Grummt, I., 2008.** Phosphorylation by casein kinase 2 facilitates rRNA gene transcription by promoting dissociation of TIF-IA from elongating RNA polymerase I. Molecular and cellular biology 28, 4988-4998.

**Blackwell, T.K., Huang, J., Ma, A., Kretzner, L., Alt, F.W., Eisenman, R.N., Weintraub, H., 1993.** Binding of myc proteins to canonical and noncanonical DNA sequences. Molecular and cellular biology 13, 5216-5224.

**Blackwood, E.M., Luscher, B., Eisenman, R.N., 1992.** Myc and Max associate in vivo. Genes & development 6, 71-80.

**Bodenmiller, B., Campbell, D., Gerrits, B., Lam, H., Jovanovic, M., Picotti, P., Schlapbach, R., Aebersold, R., 2008.** PhosphoPep--a database of protein phosphorylation sites in model organisms. Nature biotechnology 26, 1339-1340.

**Boisvert, F.M., van Koningsbruggen, S., Navascues, J., Lamond, A.I., 2007.** The multifunctional nucleolus. Nature reviews. Molecular cell biology 8, 574-585.

**Bossing, T., Udolph, G., Doe, C.Q., Technau, G.M., 1996.** The embryonic central nervous system lineages of Drosophila melanogaster. I. Neuroblast lineages derived from the ventral half of the neuroectoderm. Developmental biology 179, 41-64.

**Britton, J.S., Edgar, B.A., 1998.** Environmental control of the cell cycle in Drosophila: nutrition activates mitotic and endoreplicative cells by distinct mechanisms. Development (Cambridge, England) 125, 2149-2158.

**Brody, T., Odenwald, W.F., 2000.** Programmed transformations in neuroblast gene expression during Drosophila CNS lineage development. Developmental biology 226, 34-44.

**Burd, C.G., Dreyfuss, G., 1994.** Conserved structures and diversity of functions of RNA-binding proteins. Science (New York, N.Y.) 265, 615-621.

**Burwick, N., Coats, S.A., Nakamura, T., Shimamura, A., 2012.** Impaired ribosomal subunit association in Shwachman-Diamond syndrome. Blood 120, 5143-5152.

**Caldwell, M.C., Datta, S., 1998.** Expression of cyclin E or DP/E2F rescues the G1 arrest of trol mutant neuroblasts in the Drosophila larval central nervous system. Mechanisms of development 79, 121-130.

**Campos-Ortega, J.A., 1993.** Mechanisms of early neurogenesis in Drosophila melanogaster. Journal of neurobiology 24, 1305-1327.

**Campos-Ortega, J.A., Hartenstein, V., 1985.** The Embryonic development of Drosophila melanogaster.

**Campos-Ortega, J.A., Knust, E., 1990.** Genetic and molecular mechanisms of neurogenesis in Drosophila melanogaster. Journal de physiologie 84, 1-10.

**Canton, D.A., Zhang, C., Litchfield, D.W., 2001.** Assembly of protein kinase CK2: investigation of complex formation between catalytic and regulatory subunits using a zinc-finger-deficient mutant of CK2beta. The Biochemical journal 358, 87-94.

**Bullock, Theodore Holmes, and G. Adrian Horridge 1966.** Structure and Function in the Nervous System of Invertebrates. 2 vol. San Francisco and London: W. H. Freeman a. Comp. Ltd. 1965. XXVIII + 1722 pp. $4 27.–. Internationale Revue der gesamten Hydrobiologie und Hydrographie 51, 544-544.

**Cayre, M., Malaterre, J., Strambi, C., Charpin, P., Ternaux, J.P., Strambi, A., 2001.** Short- and long-chain natural polyamines play specific roles in adult cricket neuroblast proliferation and neuron differentiation in vitro. Journal of neurobiology 48, 315-324.

**Cayre, M., Strambi, C., Charpin, P., Augier, R., Strambi, A., 1997.** Specific requirement of putrescine for the mitogenic action of juvenile hormone on adult insect neuroblasts. Proceedings of the National Academy of Sciences of the United States of America 94, 8238-8242.

**Cenci, C., Gould, A.P., 2005.** Drosophila Grainyhead specifies late programmes of neural proliferation by regulating the mitotic activity and Hox-dependent apoptosis of neuroblasts. Development (Cambridge, England) 132, 3835-3845.

**Chell, J.M., Brand, A.H., 2010.** Nutrition-responsive glia control exit of neural stem cells from quiescence. Cell 143, 1161-1173.

**Cheng, L.Y., Bailey, A.P., Leevers, S.J., Ragan, T.J., Driscoll, P.C., Gould, A.P., 2011.** Anaplastic lymphoma kinase spares organ growth during nutrient restriction in Drosophila. Cell 146, 435-447.

**Cheng, L.Y., Bailey, A.P., Leevers, S.J., Ragan, T.J., Driscoll, P.C., Gould, A.P., 2011.** Anaplastic lymphoma kinase spares organ growth during nutrient restriction in Drosophila. Cell 146, 435-447.

**Choksi, S.P., Southall, T.D., Bossing, T., Edoff, K., de Wit, E., Fischer, B.E., van Steensel, B., Micklem, G., Brand, A.H., 2006.** Prospero acts as a binary switch between self-renewal and differentiation in Drosophila neural stem cells. Developmental cell 11, 775-789.

**Colombani, J., Raisin, S., Pantalacci, S., Radimerski, T., Montagne, J., Leopold, P., 2003.** A nutrient sensor mechanism controls Drosophila growth. Cell 114, 739-749.

**Colombani, J., Raisin, S., Pantalacci, S., Radimerski, T., Montagne, J., Leopold, P., 2003.** A nutrient sensor mechanism controls Drosophila growth. Cell 114, 739-749.

**Dang, C.V., 1999.** c-Myc target genes involved in cell growth, apoptosis, and metabolism. Molecular and cellular biology 19, 1-11.

**Dang, C.V., 2013.** MYC, metabolism, cell growth, and tumorigenesis. Cold Spring Harbor perspectives in medicine 3.

**Datta, S., 1995.** Control of proliferation activation in quiescent neuroblasts of the Drosophila central nervous system. Development (Cambridge, England) 121, 1173-1182.

**Datta, S., 1999.** Activation of neuroblast proliferation in explant culture of the Drosophila larval CNS. Brain research 818, 77-83.

**de Belle, J.S., Heisenberg, M., 1996.** Expression of Drosophila mushroom body mutations in alternative genetic backgrounds: a case study of the mushroom body miniature gene (mbm). Proceedings of the National Academy of Sciences of the United States of America 93, 9875-9880.

**Demontis, F., Perrimon, N., 2009.** Integration of Insulin receptor/Foxo signaling and dMyc activity during muscle growth regulates body size in Drosophila. Development (Cambridge, England) 136, 983-993.

**Dragon, F., Gallagher, J.E., Compagnone-Post, P.A., Mitchell, B.M., Porwancher, K.A., Wehner, K.A., Wormsley, S., Settlage, R.E., Shabanowitz, J., Osheim, Y., Beyer, A.L., Hunt, D.F., Baserga, S.J., 2002.** A large nucleolar U3 ribonucleoprotein required for 18S ribosomal RNA biogenesis. Nature 417, 967-970.

**Dumstrei, K., Wang, F., Hartenstein, V., 2003.** Role of DE-cadherin in neuroblast proliferation, neural morphogenesis, and axon tract formation in Drosophila larval brain development. The Journal of neuroscience : the official journal of the Society for Neuroscience 23, 3325-3335.

**Ebens, A.J., Garren, H., Cheyette, B.N., Zipursky, S.L., 1993.** The Drosophila anachronism locus: a glycoprotein secreted by glia inhibits neuroblast proliferation. Cell 74, 15-27.

**Egger, B., Boone, J.Q., Stevens, N.R., Brand, A.H., Doe, C.Q., 2007.** Regulation of spindle orientation and neural stem cell fate in the Drosophila optic lobe. Neural development 2, 1.

**Egger, B., Chell, J.M., Brand, A.H., 2008.** Insights into neural stem cell biology from flies. Philosophical transactions of the Royal Society of London. Series B, Biological sciences 363, 39-56.

**Filhol, O., Nueda, A., Martel, V., Gerber-Scokaert, D., Benitez, M.J., Souchier, C., Saoudi, Y., Cochet, C., 2003.** Live-cell fluorescence imaging reveals the dynamics of protein kinase CK2 individual subunits. Molecular and cellular biology 23, 975-987.

**Foe, V.E., 1989.** Mitotic domains reveal early commitment of cells in Drosophila embryos. Development (Cambridge, England) 107, 1-22.

**Frank, D.J., Edgar, B.A., Roth, M.B., 2002.** The Drosophila melanogaster gene brain tumor negatively regulates cell growth and ribosomal RNA synthesis. Development (Cambridge, England) 129, 399-407.

**Furrer, M., Balbi, M., Albarca-Aguilera, M., Gallant, M., Herr, W., Gallant, P., 2010.** Drosophila Myc interacts with host cell factor (dHCF) to activate transcription and control growth. The Journal of biological chemistry 285, 39623-39636.

**Gallant, P., 2013.** Myc function in Drosophila. Cold Spring Harbor perspectives in medicine 3, a014324.

**Gandin, V., Miluzio, A., Barbieri, A.M., Beugnet, A., Kiyokawa, H., Marchisio, P.C., Biffo, S., 2008.** Eukaryotic initiation factor 6 is rate-limiting in translation, growth and transformation. Nature 455, 684-688.

**Gerbi, S.A., Borovjagin, A.V., Lange, T.S., 2003.** The nucleolus: a site of ribonucleoprotein maturation. Current opinion in cell biology 15, 318-325.

**Godin, K.S., Varani, G., 2007.** How arginine-rich domains coordinate mRNA maturation events. RNA biology 4, 69-75.

**Gomez-Roman, N., Grandori, C., Eisenman, R.N., White, R.J., 2003.** Direct activation of RNA polymerase III transcription by c-Myc. Nature 421, 290-294.

**Graham, K.C., Litchfield, D.W., 2000.** The regulatory beta subunit of protein kinase CK2 mediates formation of tetrameric CK2 complexes. The Journal of biological chemistry 275, 5003-5010.

**Grandi, P., Rybin, V., Bassler, J., Petfalski, E., Strauss, D., Marzioch, M., Schafer, T., Kuster, B., Tschochner, H., Tollervey, D., Gavin, A.C., Hurt, E., 2002.** 90S pre-ribosomes include the 35S pre-rRNA, the U3 snoRNP, and 40S subunit processing factors but predominantly lack 60S synthesis factors. Molecular cell 10, 105-115.

**Grandori, C., Gomez-Roman, N., Felton-Edkins, Z.A., Ngouenet, C., Galloway, D.A., Eisenman, R.N., White, R.J., 2005.** c-Myc binds to human ribosomal DNA and stimulates transcription of rRNA genes by RNA polymerase I. Nature cell biology 7, 311-318.

**Green, P., Hartenstein, A.Y., Hartenstein, V., 1993.** The embryonic development of the Drosophila visual system. Cell and tissue research 273, 583-598.

**Grewal, S.S., Li, L., Orian, A., Eisenman, R.N., Edgar, B.A., 2005.** Myc-dependent regulation of ribosomal RNA synthesis during Drosophila development. Nature cell biology 7, 295-302.

**Grosskortenhaus, R., Pearson, B.J., Marusich, A., Doe, C.Q., 2005.** Regulation of temporal identity transitions in Drosophila neuroblasts. Developmental cell 8, 193-202.

**Grosskortenhaus, R., Robinson, K.J., Doe, C.Q., 2006.** Pdm and Castor specify late-born motor neuron identity in the NB7-1 lineage. Genes & development 20, 2618-2627.

**Guertin, D.A., Stevens, D.M., Thoreen, C.C., Burds, A.A., Kalaany, N.Y., Moffat, J., Brown, M., Fitzgerald, K.J., Sabatini, D.M., 2006.** Ablation in mice of the mTORC

components raptor, rictor, or mLST8 reveals that mTORC2 is required for signaling to Akt-FOXO and PKCalpha, but not S6K1. Developmental cell 11, 859-871.

**Guruharsha, K.G., Rual, J.F., Zhai, B., Mintseris, J., Vaidya, P., Vaidya, N., Beekman, C., Wong, C., Rhee, D.Y., Cenaj, O., McKillip, E., Shah, S., Stapleton, M., Wan, K.H., Yu, C., Parsa, B., Carlson, J.W., Chen, X., Kapadia, B., VijayRaghavan, K., Gygi, S.P., Celniker, S.E., Obar, R.A., Artavanis-Tsakonas, S., 2011.** A protein complex network of Drosophila melanogaster. Cell 147, 690-703.

**Hartenstein, V., Rudloff, E., Campos -Ortega, J., 1987.** The pattern of proliferation of the neuroblasts in the wild-type embryo of Drosophila melanogaster. Roux's Arch Dev Biol 196, 473-485.

**Hartenstein, V., Wodarz, A., 2013.** Initial neurogenesis in Drosophila. Wiley Interdisciplinary Reviews: Developmental Biology 2, 701-721.

**Heisenberg, M., 2003.** Mushroom body memoir: from maps to models. Nature reviews. Neuroscience 4, 266-275.

**Heisenberg, M., Borst, A., Wagner, S., Byers, D., 1985.** Drosophila mushroom body mutants are deficient in olfactory learning. Journal of neurogenetics 2, 1-30.

**Heitzler, P., Bourouis, M., Ruel, L., Carteret, C., Simpson, P., 1996.** Genes of the Enhancer of split and achaete-scute complexes are required for a regulatory loop between Notch and Delta during lateral signalling in Drosophila. Development (Cambridge, England) 122, 161-171.

**Henras, A.K., Soudet, J., Gerus, M., Lebaron, S., Caizergues-Ferrer, M., Mougin, A., Henry, Y., 2008.** The post-transcriptional steps of eukaryotic ribosome biogenesis. Cellular and molecular life sciences : CMLS 65, 2334-2359.

**Hernandez-Verdun, D., Roussel, P., Thiry, M., Sirri, V., Lafontaine, D.L., 2010.** The nucleolus: structure/function relationship in RNA metabolism. Wiley interdisciplinary reviews. RNA 1, 415-431.

**Hietakangas, V., Cohen, S.M., 2009.** Regulation of tissue growth through nutrient sensing. Annual review of genetics 43, 389-410.

**Hirata, J., Nakagoshi, H., Nabeshima, Y., Matsuzaki, F., 1995.** Asymmetric segregation of the homeodomain protein Prospero during Drosophila development. Nature 377, 627-630.

**Homem, C.C., Knoblich, J.A., 2012.** Drosophila neuroblasts: a model for stem cell biology. Development (Cambridge, England) 139, 4297-4310.

**Horvitz, H.R., Herskowitz, I., 1992.** Mechanisms of asymmetric cell division: two Bs or not two Bs, that is the question. Cell 68, 237-255.

**Hu, P., Wu, S., Hernandez, N., 2003.** A minimal RNA polymerase III transcription system from human cells reveals positive and negative regulatory roles for CK2. Molecular cell 12, 699-709.

**Hulf, T., Bellosta, P., Furrer, M., Steiger, D., Svensson, D., Barbour, A., Gallant, P., 2005.** Whole-genome analysis reveals a strong positional bias of conserved dMyc-dependent E-boxes. Molecular and cellular biology 25, 3401-3410.

**Isshiki, T., Pearson, B., Holbrook, S., Doe, C.Q., 2001.** Drosophila neuroblasts sequentially express transcription factors which specify the temporal identity of their neuronal progeny. Cell 106, 511-521.

**Ito, K., Awano, W., Suzuki, K., Hiromi, Y., Yamamoto, D., 1997.** The Drosophila mushroom body is a quadruple structure of clonal units each of which contains a virtually identical set of neurones and glial cells. Development (Cambridge, England) 124, 761-771.

**Ito, K., Hotta, Y., 1992.** Proliferation pattern of postembryonic neuroblasts in the brain of Drosophila melanogaster. Developmental biology 149, 134-148.

**Jauch, E., Melzig, J., Brkulj, M., Raabe, T., 2002.** In vivo functional analysis of Drosophila protein kinase casein kinase 2 (CK2) beta-subunit. Gene 298, 29-39.

**Jauch, E., Wecklein, H., Stark, F., Jauch, M., Raabe, T., 2006.** The Drosophila melanogaster DmCK2beta transcription unit encodes for functionally non-redundant protein isoforms. Gene 374, 142-152.

**Jimenez, F., Campos-Ortega, J.A., 1990.** Defective neuroblast commitment in mutants of the achaete-scute complex and adjacent genes of D. melanogaster. Neuron 5, 81-89.

**Johnston, L.A., Prober, D.A., Edgar, B.A., Eisenman, R.N., Gallant, P., 1999.** Drosophila myc regulates cellular growth during development. Cell 98, 779-790.

**Kanai, M.I., Okabe, M., Hiromi, Y., 2005.** seven-up Controls switching of transcription factors that specify temporal identities of Drosophila neuroblasts. Developmental cell 8, 203-213.

**Kim, E., Goraksha-Hicks, P., Li, L., Neufeld, T.P., Guan, K.L., 2008.** Regulation of TORC1 by Rag GTPases in nutrient response. Nature cell biology 10, 935-945.

**Knibiehler, B., Mirre, C., Rosset, R., 1982.** Nucleolar organizer structure and activity in a nucleolus without fibrillar centres: the nucleolus in an established Drosophila cell line. Journal of cell science 57, 351-364.

**Knoblich, J.A., 2010.** Asymmetric cell division: recent developments and their implications for tumour biology. Nature reviews. Molecular cell biology 11, 849-860.

**Knoblich, J.A., Jan, L.Y., Jan, Y.N., 1995.** Asymmetric segregation of Numb and Prospero during cell division. Nature 377, 624-627.

**Knoblich, J.A., Jan, L.Y., Jan, Y.N., 1997.** The N terminus of the Drosophila Numb protein directs membrane association and actin-dependent asymmetric localization. Proceedings of the National Academy of Sciences of the United States of America 94, 13005-13010.

**Krek, W., Maridor, G., Nigg, E.A., 1992.** Casein kinase II is a predominantly nuclear enzyme. The Journal of cell biology 116, 43-55.

**Kressler, D., Hurt, E., Bassler, J., 2010.** Driving ribosome assembly. Biochimica et biophysica acta 1803, 673-683.

**Krishna, S.S., Majumdar, I., Grishin, N.V., 2003.** Structural classification of zinc fingers: survey and summary. Nucleic acids research 31, 532-550.

**Kunz, T., Kraft, K.F., Technau, G.M., Urbach, R., 2012.** Origin of Drosophila mushroom body neuroblasts and generation of divergent embryonic lineages. Development (Cambridge, England) 139, 2510-2522.

**Laity, J.H., Lee, B.M., Wright, P.E., 2001.** Zinc finger proteins: new insights into structural and functional diversity. Current opinion in structural biology 11, 39-46.

**Lee, C.Y., Andersen, R.O., Cabernard, C., Manning, L., Tran, K.D., Lanskey, M.J., Bashirullah, A., Doe, C.Q., 2006.** Drosophila Aurora-A kinase inhibits neuroblast self-renewal by regulating aPKC/Numb cortical polarity and spindle orientation. Genes & development 20, 3464-3474.

**Lee, C.Y., Wilkinson, B.D., Siegrist, S.E., Wharton, R.P., Doe, C.Q., 2006.** Brat is a Miranda cargo protein that promotes neuronal differentiation and inhibits neuroblast self-renewal. Developmental cell 10, 441-449.

**Lee, T., Lee, A., Luo, L., 1999.** Development of the Drosophila mushroom bodies: sequential generation of three distinct types of neurons from a neuroblast. Development (Cambridge, England) 126, 4065-4076.

**Lehmann, R., Dietrich, U., Jiménez, F., Campos-Ortega, J.A., 1981.** Mutations of early neurogenesis inDrosophila. Wilhelm Roux' Archiv 190, 226-229.

**Lehmann, R., Jiménez, F., Dietrich, U., Campos-Ortega, J., 1983.** On the phenotype and development of mutants of early neurogenesis inDrosophila melanogaster. Wilhelm Roux' Archiv 192, 62-74.

**Lempiainen, H., Shore, D., 2009.** Growth control and ribosome biogenesis. Current opinion in cell biology 21, 855-863.

**Leroy, D., Filhol, O., Delcros, J.G., Pares, S., Chambaz, E.M., Cochet, C., 1997.** Chemical features of the protein kinase CK2 polyamine binding site. Biochemistry 36, 1242-1250.

**Leroy, D., Heriche, J.K., Filhol, O., Chambaz, E.M., Cochet, C., 1997.** Binding of polyamines to an autonomous domain of the regulatory subunit of protein kinase CK2

induces a conformational change in the holoenzyme. A proposed role for the kinase stimulation. The Journal of biological chemistry 272, 20820-20827.

**Li, L., Edgar, B.A., Grewal, S.S., 2010.** Nutritional control of gene expression in Drosophila larvae via TOR, Myc and a novel cis-regulatory element. BMC cell biology 11, 7.

**Li, L., Xie, T., 2005.** Stem cell niche: structure and function. Annual review of cell and developmental biology 21, 605-631.

**Lieberman, S.L., Ruderman, J.V., 2004.** CK2 beta, which inhibits Mos function, binds to a discrete domain in the N-terminus of Mos. Developmental biology 268, 271-279.

**Litchfield, D.W., 2003.** Protein kinase CK2: structure, regulation and role in cellular decisions of life and death. The Biochemical journal 369, 1-15.

**Loewith, R., Jacinto, E., Wullschleger, S., Lorberg, A., Crespo, J.L., Bonenfant, D., Oppliger, W., Jenoe, P., Hall, M.N., 2002.** Two TOR complexes, only one of which is rapamycin sensitive, have distinct roles in cell growth control. Molecular cell 10, 457-468.

**Lu, B., Roegiers, F., Jan, L.Y., Jan, Y.N., 2001.** Adherens junctions inhibit asymmetric division in the Drosophila epithelium. Nature 409, 522-525.

**Maggi, L.B., Jr., Kuchenruether, M., Dadey, D.Y., Schwope, R.M., Grisendi, S., Townsend, R.R., Pandolfi, P.P., Weber, J.D., 2008.** Nucleophosmin serves as a rate-limiting nuclear export chaperone for the Mammalian ribosome. Molecular and cellular biology 28, 7050-7065.

**Marinho, J., Casares, F., Pereira, P.S., 2011.** The Drosophila Nol12 homologue viriato is a dMyc target that regulates nucleolar architecture and is required for dMyc-stimulated cell growth. Development (Cambridge, England) 138, 349-357.

**Matera, A.G., Terns, R.M., Terns, M.P., 2007.** Non-coding RNAs: lessons from the small nuclear and small nucleolar RNAs. Nature reviews. Molecular cell biology 8, 209-220.

**Matsuzaki, H., Daitoku, H., Hatta, M., Tanaka, K., Fukamizu, A., 2003.** Insulin-induced phosphorylation of FKHR (Foxo1) targets to proteasomal degradation. Proceedings of the National Academy of Sciences of the United States of America 100, 11285-11290.

**Maurange, C., Cheng, L., Gould, A.P., 2008.** Temporal transcription factors and their targets schedule the end of neural proliferation in Drosophila. Cell 133, 891-902.

**Mayer, C., Zhao, J., Yuan, X., Grummt, I., 2004.** mTOR-dependent activation of the transcription factor TIF-IA links rRNA synthesis to nutrient availability. Genes & development 18, 423-434.

**Meggio, F., Pinna, L.A., 2003.** One-thousand-and-one substrates of protein kinase CK2? FASEB journal : official publication of the Federation of American Societies for Experimental Biology 17, 349-368.

**Meissner, R.A., Kilman, V.L., Lin, J.M., Allada, R., 2008.** TIMELESS is an important mediator of CK2 effects on circadian clock function in vivo. The Journal of neuroscience : the official journal of the Society for Neuroscience 28, 9732-9740.

**Melese, T., Xue, Z., 1995.** The nucleolus: an organelle formed by the act of building a ribosome. Current opinion in cell biology 7, 319-324.

**Merdes, A., Heald, R., Samejima, K., Earnshaw, W.C., Cleveland, D.W., 2000.** Formation of spindle poles by dynein/dynactin-dependent transport of NuMA. The Journal of cell biology 149, 851-862.

**Montagne, J., Stewart, M.J., Stocker, H., Hafen, E., Kozma, S.C., Thomas, G., 1999.** Drosophila S6 kinase: a regulator of cell size. Science (New York, N.Y.) 285, 2126-2129.

**Montenarh, M., 2010.** Cellular regulators of protein kinase CK2. Cell and tissue research 342, 139-146.

**Morata, G., 1993.** Homeotic genes of Drosophila. Current opinion in genetics & development 3, 606-614.

**Negi, S.S., Olson, M.O., 2006.** Effects of interphase and mitotic phosphorylation on the mobility and location of nucleolar protein B23. Journal of cell science 119, 3676-3685.

**Neumuller, R.A., Knoblich, J.A., 2009.** Dividing cellular asymmetry: asymmetric cell division and its implications for stem cells and cancer. Genes & development 23, 2675-2699.

**Neumuller, R.A., Richter, C., Fischer, A., Novatchkova, M., Neumuller, K.G., Knoblich, J.A., 2011.** Genome-wide analysis of self-renewal in Drosophila neural stem cells by transgenic RNAi. Cell stem cell 8, 580-593.

**Nguyen-Ngoc, T., Afshar, K., Gonczy, P., 2007.** Coupling of cortical dynein and G alpha proteins mediates spindle positioning in Caenorhabditis elegans. Nature cell biology 9, 1294-1302.

**Niefind, K., Raaf, J., Issinger, O.G., 2009.** Protein kinase CK2 in health and disease: Protein kinase CK2: from structures to insights. Cellular and molecular life sciences : CMLS 66, 1800-1816.

**Nipper, R.W., Siller, K.H., Smith, N.R., Doe, C.Q., Prehoda, K.E., 2007.** Galphai generates multiple Pins activation states to link cortical polarity and spindle orientation in Drosophila neuroblasts. Proceedings of the National Academy of Sciences of the United States of America 104, 14306-14311.

**Olsten, M.E., Litchfield, D.W., 2004.** Order or chaos? An evaluation of the regulation of protein kinase CK2. Biochemistry and cell biology = Biochimie et biologie cellulaire 82, 681-693.

**Parisi, F., Riccardo, S., Daniel, M., Saqcena, M., Kundu, N., Pession, A., Grifoni, D., Stocker, H., Tabak, E., Bellosta, P., 2011.** Drosophila insulin and target of rapamycin (TOR) pathways regulate GSK3 beta activity to control Myc stability and determine Myc expression in vivo. BMC biology 9, 65.

**Parisi, F., Riccardo, S., Daniel, M., Saqcena, M., Kundu, N., Pession, A., Grifoni, D., Stocker, H., Tabak, E., Bellosta, P., 2011.** Drosophila insulin and target of rapamycin (TOR) pathways regulate GSK3 beta activity to control Myc stability and determine Myc expression in vivo. BMC biology 9, 65.

**Park, Y., Rangel, C., Reynolds, M.M., Caldwell, M.C., Johns, M., Nayak, M., Welsh, C.J., McDermott, S., Datta, S., 2003.** Drosophila perlecan modulates FGF and hedgehog signals to activate neural stem cell division. Developmental biology 253, 247-257.

**Pearson, B.J., Doe, C.Q., 2003.** Regulation of neuroblast competence in Drosophila. Nature 425, 624-628.

**Pearson, B.J., Doe, C.Q., 2004.** Specification of temporal identity in the developing nervous system. Annual review of cell and developmental biology 20, 619-647.

**Pendle, A.F., Clark, G.P., Boon, R., Lewandowska, D., Lam, Y.W., Andersen, J., Mann, M., Lamond, A.I., Brown, J.W., Shaw, P.J., 2005.** Proteomic analysis of the Arabidopsis nucleolus suggests novel nucleolar functions. Molecular biology of the cell 16, 260-269.

**Penner, C.G., Wang, Z., Litchfield, D.W., 1997.** Expression and localization of epitope-tagged protein kinase CK2. Journal of cellular biochemistry 64, 525-537.

**Peterson, C., Carney, G.E., Taylor, B.J., White, K., 2002.** reaper is required for neuroblast apoptosis during Drosophila development. Development (Cambridge, England) 129, 1467-1476.

**Pierce, S.B., Yost, C., Britton, J.S., Loo, L.W., Flynn, E.M., Edgar, B.A., Eisenman, R.N., 2004.** dMyc is required for larval growth and endoreplication in Drosophila. Development (Cambridge, England) 131, 2317-2327.

**Poortinga, G., Hannan, K.M., Snelling, H., Walkley, C.R., Jenkins, A., Sharkey, K., Wall, M., Brandenburger, Y., Palatsides, M., Pearson, R.B., McArthur, G.A., Hannan, R.D., 2004.** MAD1 and c-MYC regulate UBF and rDNA transcription during granulocyte differentiation. The EMBO journal 23, 3325-3335.

**Prokop, A., Bray, S., Harrison, E., Technau, G.M., 1998.** Homeotic regulation of segment-specific differences in neuroblast numbers and proliferation in the Drosophila central nervous system. Mechanisms of development 74, 99-110.

**Prokop, A., Technau, G.M., 1991.** The origin of postembryonic neuroblasts in the ventral nerve cord of Drosophila melanogaster. Development (Cambridge, England) 111, 79-88.

**Raabe, T., Clemens-Richter, S., Twardzik, T., Ebert, A., Gramlich, G., Heisenberg, M., 2004.** Identification of mushroom body miniature, a zinc-finger protein implicated in brain development of Drosophila. Proceedings of the National Academy of Sciences of the United States of America 101, 14276-14281.

**Rhyu, M.S., Jan, L.Y., Jan, Y.N., 1994.** Asymmetric distribution of numb protein during division of the sensory organ precursor cell confers distinct fates to daughter cells. Cell 76, 477-491.

**Rolls, M.M., Albertson, R., Shih, H.P., Lee, C.Y., Doe, C.Q., 2003.** Drosophila aPKC regulates cell polarity and cell proliferation in neuroblasts and epithelia. The Journal of cell biology 163, 1089-1098.

**Rosby, R., Cui, Z., Rogers, E., deLivron, M.A., Robinson, V.L., DiMario, P.J., 2009.** Knockdown of the Drosophila GTPase nucleostemin 1 impairs large ribosomal subunit biogenesis, cell growth, and midgut precursor cell maintenance. Molecular biology of the cell 20, 4424-4434.

**Schafer, T., Maco, B., Petfalski, E., Tollervey, D., Bottcher, B., Aebi, U., Hurt, E., 2006.** Hrr25-dependent phosphorylation state regulates organization of the pre-40S subunit. Nature 441, 651-655.

**Schlosser, I., Holzel, M., Murnseer, M., Burtscher, H., Weidle, U.H., Eick, D., 2003.** A role for c-Myc in the regulation of ribosomal RNA processing. Nucleic acids research 31, 6148-6156.

**Schmid, A., Chiba, A., Doe, C.Q., 1999.** Clonal analysis of Drosophila embryonic neuroblasts: neural cell types, axon projections and muscle targets. Development (Cambridge, England) 126, 4653-4689.

**Schmidt, H., Rickert, C., Bossing, T., Vef, O., Urban, J., Technau, G.M., 1997.** The embryonic central nervous system lineages of Drosophila melanogaster. II. Neuroblast lineages derived from the dorsal part of the neuroectoderm. Developmental biology 189, 186-204.

**Schmidt-Ott, U., González-Gaitán, M., Jäckle, H., Technau, G.M., 1994.** Number, identity, and sequence of the Drosophila head segments as revealed by neural elements and their deletion patterns in mutants. Proceedings of the National Academy of Sciences 91, 8363-8367.

**Schmidt-Ott, U., Technau, G.M., 1992.** Expression of en and wg in the embryonic head and brain of Drosophila indicates a refolded band of seven segment remnants. Development (Cambridge, England) 116, 111-125.

**Schweisguth, F., 2004.** Regulation of notch signaling activity. Current biology : CB 14, R129-138.

**Siegrist, S.E., Doe, C.Q., 2005.** Microtubule-induced Pins/Galphai cortical polarity in Drosophila neuroblasts. Cell 123, 1323-1335.

**Siegrist, S.E., Haque, N.S., Chen, C.H., Hay, B.A., Hariharan, I.K., 2010.** Inactivation of both Foxo and reaper promotes long-term adult neurogenesis in Drosophila. Current biology : CB 20, 643-648.

**Siller, K.H., Doe, C.Q., 2009.** Spindle orientation during asymmetric cell division. Nature cell biology 11, 365-374.

**Skeath, J.B., 1999.** At the nexus between pattern formation and cell-type specification: the generation of individual neuroblast fates in the Drosophila embryonic central nervous system. BioEssays : news and reviews in molecular, cellular and developmental biology 21, 922-931.

**Skeath, J.B., Thor, S., 2003.** Genetic control of *Drosophila* nerve cord development. Current opinion in neurobiology 13, 8-15.

**Song, Q., Combest, W.L., Gilbert, L.I., 1994.** Spermine and polylysine enhanced phosphorylation of calmodulin and tubulin in an insect endocrine gland. Molecular and cellular endocrinology 99, 1-10.

**Sousa-Nunes, R., Cheng, L.Y., Gould, A.P., 2010.** Regulating neural proliferation in the Drosophila CNS. Current opinion in neurobiology 20, 50-57.

**Sousa-Nunes, R., Somers, W.G., 2013.** Mechanisms of asymmetric progenitor divisions in the Drosophila central nervous system. Advances in experimental medicine and biology 786, 79-102.

**Sousa-Nunes, R., Yee, L.L., Gould, A.P., 2011.** Fat cells reactivate quiescent neuroblasts via TOR and glial insulin relays in Drosophila. Nature 471, 508-512.

**Spana, E.P., Kopczynski, C., Goodman, C.S., Doe, C.Q., 1995.** Asymmetric localization of numb autonomously determines sibling neuron identity in the Drosophila CNS. Development (Cambridge, England) 121, 3489-3494.

**Speicher, S., Fischer, A., Knoblich, J., Carmena, A., 2008.** The PDZ protein Canoe regulates the asymmetric division of Drosophila neuroblasts and muscle progenitors. Current biology : CB 18, 831-837.

**St-Denis, N.A., Litchfield, D.W., 2009.** Protein kinase CK2 in health and disease: From birth to death: the role of protein kinase CK2 in the regulation of cell proliferation and survival. Cellular and molecular life sciences : CMLS 66, 1817-1829.

**Steitz, J.A., Berg, C., Hendrick, J.P., La Branche-Chabot, H., Metspalu, A., Rinke, J., Yario, T., 1988.** A 5S rRNA/L5 complex is a precursor to ribosome assembly in mammalian cells. The Journal of cell biology 106, 545-556.

**Szklarczyk, D., Franceschini, A., Kuhn, M., Simonovic, M., Roth, A., Minguez, P., Doerks, T., Stark, M., Muller, J., Bork, P., Jensen, L.J., von Mering, C., 2011.** The

STRING database in 2011: functional interaction networks of proteins, globally integrated and scored. Nucleic acids research 39, D561-568.

**Taft, R.J., Glazov, E.A., Lassmann, T., Hayashizaki, Y., Carninci, P., Mattick, J.S., 2009.** Small RNAs derived from snoRNAs. RNA (New York, N.Y.) 15, 1233-1240.

**Technau, G., Heisenberg, M., 1982.** Neural reorganization during metamorphosis of the corpora pedunculata in Drosophila melanogaster. Nature 295, 405-407.

**Technau, G.M., Berger, C., Urbach, R., 2006.** Generation of cell diversity and segmental pattern in the embryonic central nervous system of Drosophila. Developmental dynamics : an official publication of the American Association of Anatomists 235, 861-869.

**Teleman, A.A., Hietakangas, V., Sayadian, A.C., Cohen, S.M., 2008.** Nutritional control of protein biosynthetic capacity by insulin via Myc in Drosophila. Cell metabolism 7, 21-32.

**Tettweiler, G., Miron, M., Jenkins, M., Sonenberg, N., Lasko, P.F., 2005.** Starvation and oxidative stress resistance in Drosophila are mediated through the eIF4E-binding protein, d4E-BP. Genes & development 19, 1840-1843.

**Thandapani, P., O'Connor, T.R., Bailey, T.L., Richard, S., 2013.** Defining the RGG/RG motif. Molecular cell 50, 613-623.

**Thor, S., 2003.** Genetic control of *Drosophila* nerve corde development. *Curr. Opin. Neurobiol.* 13, 8-15.

**Trapman, J., Retel, J., Planta, R.J., 1975.** Ribosomal precursor particles from yeast. Experimental cell research 90, 95-104.

**Truman, J.W., Bate, M., 1988.** Spatial and temporal patterns of neurogenesis in the central nervous system of Drosophila melanogaster. Developmental biology 125, 145-157.

**Truman, J.W., Talbot, W.S., Fahrbach, S.E., Hogness, D.S., 1994.** Ecdysone receptor expression in the CNS correlates with stage-specific responses to ecdysteroids during Drosophila and Manduca development. Development (Cambridge, England) 120, 219-234.

**Tschochner, H., Hurt, E., 2003.** Pre-ribosomes on the road from the nucleolus to the cytoplasm. Trends in cell biology 13, 255-263.

**Urbach, R., Schnabel, R., Technau, G.M., 2003.** The pattern of neuroblast formation, mitotic domains and proneural gene expression during early brain development in Drosophila. Development (Cambridge, England) 130, 3589-3606.

**Urbach, R., Technau, G.M., 2003.** Molecular markers for identified neuroblasts in the developing brain of Drosophila. Development (Cambridge, England) 130, 3621-3637.

**Urbach, R., Technau, G.M., 2003.** Segment polarity and DV patterning gene expression reveals segmental organization of the Drosophila brain. Development (Cambridge, England) 130, 3607-3620.

**Urbach, R., Technau, G.M., 2004.** Neuroblast formation and patterning during early brain development in Drosophila. BioEssays : news and reviews in molecular, cellular and developmental biology 26, 739-751.

**van Riggelen, J., Yetil, A., Felsher, D.W., 2010.** MYC as a regulator of ribosome biogenesis and protein synthesis. Nature reviews. Cancer 10, 301-309.

**Voigt, A., Pflanz, R., Schafer, U., Jackle, H., 2002.** Perlecan participates in proliferation activation of quiescent Drosophila neuroblasts. Developmental dynamics : an official publication of the American Association of Anatomists 224, 403-412.

**Wallace, H.M., Fraser, A.V., Hughes, A., 2003.** A perspective of polyamine metabolism. The Biochemical journal 376, 1-14.

**Wallace, K., Liu, T.H., Vaessin, H., 2000.** The pan-neural bHLH proteins DEADPAN and ASENSE regulate mitotic activity and cdk inhibitor dacapo expression in the Drosophila larval optic lobes. Genesis (New York, N.Y. : 2000) 26, 77-85.

**Wang, C., Li, S., Januschke, J., Rossi, F., Izumi, Y., Garcia-Alvarez, G., Gwee, S.S., Soon, S.B., Sidhu, H.K., Yu, F., Matsuzaki, F., Gonzalez, C., Wang, H., 2011.** An ana2/ctp/mud complex regulates spindle orientation in Drosophila neuroblasts. Developmental cell 21, 520-533.

**Wang, H., Ouyang, Y., Somers, W.G., Chia, W., Lu, B., 2007.** Polo inhibits progenitor self-renewal and regulates Numb asymmetry by phosphorylating Pon. Nature 449, 96-100.

**Wang, H., Somers, G.W., Bashirullah, A., Heberlein, U., Yu, F., Chia, W., 2006.** Aurora-A acts as a tumor suppressor and regulates self-renewal of Drosophila neuroblasts. Genes & development 20, 3453-3463.

**White, K., Grether, M.E., Abrams, J.M., Young, L., Farrell, K., Steller, H., 1994.** Genetic control of programmed cell death in Drosophila. Science (New York, N.Y.) 264, 677-683.

**Wirtz-Peitz, F., Nishimura, T., Knoblich, J.A., 2008.** Linking cell cycle to asymmetric division: Aurora-A phosphorylates the Par complex to regulate Numb localization. Cell 135, 161-173.

**Wodarz, A., Ramrath, A., Grimm, A., Knust, E., 2000.** Drosophila atypical protein kinase C associates with Bazooka and controls polarity of epithelia and neuroblasts. The Journal of cell biology 150, 1361-1374.

**Yamashita, Y.M., Fuller, M.T., 2008.** Asymmetric centrosome behavior and the mechanisms of stem cell division. The Journal of cell biology 180, 261-266.

**Younossi-Hartenstein, A., Nassif, C., Green, P., Hartenstein, V., 1996.** Early neurogenesis of the Drosophila brain. The Journal of comparative neurology 370, 313-329.

**Yu, F., Kuo, C.T., Jan, Y.N., 2006.** Drosophila neuroblast asymmetric cell division: recent advances and implications for stem cell biology. Neuron 51, 13-20.

**Yu, I.J., Spector, D.L., Bae, Y.S., Marshak, D.R., 1991.** Immunocytochemical localization of casein kinase II during interphase and mitosis. The Journal of cell biology 114, 1217-1232.

**Zeller, K.I., Haggerty, T.J., Barrett, J.F., Guo, Q., Wonsey, D.R., Dang, C.V., 2001.** Characterization of nucleophosmin (B23) as a Myc target by scanning chromatin immunoprecipitation. The Journal of biological chemistry 276, 48285-48291.

**Zemp, I., Kutay, U., 2007.** Nuclear export and cytoplasmic maturation of ribosomal subunits. FEBS letters 581, 2783-2793.

**Zhai, B., Villen, J., Beausoleil, S.A., Mintseris, J., Gygi, S.P., 2008.** Phosphoproteome analysis of Drosophila melanogaster embryos. Journal of proteome research 7, 1675-1682.

**Zhong, W., Chia, W., 2008.** Neurogenesis and asymmetric cell division. Current opinion in neurobiology 18, 4-11.